Endocytosis Controlled by Monolayer Area Asymmetry

D I S S E R T A T I O N

zur Erlangung des akademischen Grades

doctor rerum naturalium
(Dr. rer. nat.)
im Fach Biophysik

eingereicht an der
Mathematisch-Naturwissenschaftlichen Fakultät I
Humboldt-Universität zu Berlin

von
Diplom-Biophysikerin Nina Ohlwein

Präsident der Humboldt-Universität zu Berlin:
Professor Dr. Jan-Hendrik Olbertz

Dekan der Mathematisch-Naturwissenschaftlichen Fakultät I:
Professor Dr. Andreas Herrmann

Gutachter:
1. Professor Dr. Sophie Cribier
2. Professor Dr. Thomas Günther-Pomorski
3. Professor Dr. Andreas Herrmann

eingereicht am: 10. Mai 2011
Tag der mündlichen Prüfung: 5. Oktober 2011

„. . . Geheimnisvoll am lichten Tag
Lässt sich Natur des Schleiers nicht berauben,
Und was sie deinem Geist nicht offenbaren mag,
Das zwingst du ihr nicht ab mit Hebeln und mit Schrauben. . . . “

Johann Wolfgang von Goethe

Abstract

Endocytic engulfment requires high local membrane curvature and causes significant area changes of the membrane leaflets with respect to each other. Beside individual proteins this can be initiated by differences between the surface areas of the two monolayers related to leaflet specific modulation of lipid composition. Thus, it was proposed that ATP-dependent lipid translocators, pumping phospholipids from one membrane leaflet to the opposite leaflet, account for generation of altered area relation between both leaflets as an early step in endocytosis.

To elucidate the influence of differences in the monolayer area asymmetry of the plasma membrane on endocytosis, surface area relation was altered by adding exogenous phospholipids to living cells and changes in endocytic activity were distinctly quantified. Depending on the lipid species, exogenous lipids were only incorporated into the outer layer or subsequently translocated across the plasma membrane thereby increasing either the outer or inner surface area.

Addition of different analogues of aminophospholipids, which are translocated to the inner leaflet, led to an enhancement of bulk flow endocytosis in K562 cells. Moreover, our data indicate that clathrin-mediated endocytosis of Hep2 cells was stimulated as well. Inversely, addition of analogues of phosphatidylcholine, which are not recognised by lipid translocators, reduced bulk flow or clathrin-mediated endocytosis in various cell lines. Notably, also clathrin-mediated endocytosis was influenced by the addition of lipids, although many proteins noted for their ability to induce membrane curvature are known to be implicated in this pathway.

This corroborates a recent model how aminophospholipid translocases are implicated in endocytosis. Upon translocating lipids from the exo- to the cytoplasmic leaflet and additionally interacting with endocytic accessory proteins, aminophospholipid translocases could integrate two processes to generate curvature: membrane bending based on area asymmetry of membrane monolayers and protein-based mechanisms to induce and stabilise curvature. Collectively, findings in the present study and in recent publications suggest that monolayer area asymmetry induced by the translocation of lipids is not the only but one of the mechanisms leading to curvature generation necessary for endocytic events.

Zusammenfassung

Endozytotische Einstülpungen erfordern eine hohe lokale Membrankrümmung und führen zu erheblichen Flächenänderungen der Membranhälften, die gegenseitig voneinander abhängen. Neben bestimmten Proteinen kann dies durch eine Oberflächendifferenz zwischen den Schichten initiiert werden, die durch die spezifische Anpassung der Lipidzusammensetzung einer Membranhälfte hervorgerufen werden kann. Daher wurde die Hypothese aufgestellt, dass ATP-abhängige Lipid-Transporter, die Phospholipide von der einen auf die gegenüberliegende Membranseite pumpen, in der Anfangsphase der Endozytose für veränderte Flächenverhältnisse zwischen den Membranschichten verantwortlich sind.

Um den Einfluss veränderter Flächenasymmetrien der Plasmamembranschichten auf Endozytose zu untersuchen, wurden in lebenden Zellen die Oberflächenverhältnisse der Membranhälften durch die Zugabe von exogenen Phospholipiden verändert und Unterschiede der endozytotischen Aktivität bestimmt. Abhängig von der Sorte wurden die exogenen Lipide nur in die äußere Membranschicht eingebaut oder anschließend auch auf die innere Membranseite transportiert, wodurch entweder die äußere oder innere Oberfläche vergrößert wurde. Die Zugabe verschiedener Aminophospholipid-Analoga, die auf die innere Membranseite transportiert werden, führte zu gesteigerter *bulk flow*-Endocytose in K562-Zellen. Darüber hinaus deuten die Ergebnisse darauf hin, dass Clathrin-vermittelte Endozytose von Hep2-Zellen ebenfalls stimuliert wurde. Umgekehrt hatte die Zugabe von Phosphatidylcholin-Analoga, die nicht von Lipid-Transportern erkannt werden, reduzierte *bulk flow*- oder Clathrin-vermittelte Endozytose in verschiedenen Zelllinien zur Folge. Bemerkenswert ist, dass auch Clathrin-vermittelte Endozytose durch die Lipidzugabe beeinflusst wurde, obwohl gerade in diesem Endozytoseweg viele Proteine involviert sind, die Membrankrümmungen induzieren können.

Dies passt zu einem neuen Modell wie Aminophospholipid-Transporter in Endozytose involviert sind. Durch den Lipidtransport von der exo- auf die zytoplasmatische Membranhälfte und die zusätzliche Interaktion mit endozytotischen Hilfsproteinen, könnten diese Transporter zwei Mechanismen zur Erzeugung von Krümmung miteinander verbinden: Membrankrümmung induziert durch eine Flächenasymmetrie zwischen den Membranhälften und durch Wechselwirkung mit Proteinen, die Krümmung sowohl generieren als auch stabilisieren können. Zusammen genommen deuten die Ergebnisse dieser Arbeit so wie neuere Veröffentlichungen darauf hin, dass die durch Lipidtransport induzierte Flächenasymmetrie der Membranschichten nicht der einzige aber einer der Mechanismen ist, der die für Endozytose notwendige Membrankrümmung erzeugt.

Contents

Abbreviations

A488	Alexa 488
AB	acid buffer
ABC	ATP-binding cassette
AP-2	adaptor protein 2
APLT	aminophospholipid translocase
Arf	ADP-ribosylation factor
Arf-GEF	guanine nucleotide exchange factors for ADP-ribosylation factor GTPases
asc	clathrin heavy chain antisense RNA
BAR	Bin, Amphiphysin, Rvs
BB	basic buffer
BFEA	bulk flow endocytic activity
$BHKasc^-$	BHKasc cells with expression of asc
$BHKasc^+$	BHKasc cells without expression of asc
BSA	bovine serum albumin
C_6-	lipids with six carbons at the sn-2 position
Cdc42	cell division control protein 42
Cer	ceramide
CM	clathrin-mediated
CMEA	clathrin-mediated endocytic activity
CI	clathrin-independent
CI-BFEA	clathrin-independent bulk flow endocytic activity
CPE	carboxypeptidase E

CPZ	chlorpromazine
DRM	detergent resistent membrane
dialkyl-	dialkyl lipids
DLPS	dilauroyl-phosphatidylserine
DPBS	Dulbecco's modified phosphate buffered saline
DMEM	Dulbecco's modified Eagle medium
EDTA	ethylene diamine tetra-acetic acid
EGF	epidermal growth factor
F/EFC-	Fes/CIP4 homology- or EFC for Extended FCH Homology-
FACS	flourescence activated cell sorting
FBS	fetal bovine serum
FCS	forward scatter
FITC	fluorescein isothiocyanate
GEF	guanine nucleotide exchange factors
GPI	glycosyl-phosphatidylinositol
GUV	giant unilamellar vesicles
HBSS	Hanks' balanced salt solution
Hepes	4-(2-hydroxyethyl)-1-piperazine-ethanesulfonic acid
IB	internalisation buffer
IL2Rβ	β-chain of the interleukin-2 receptor
IQR	interquartile range
L-15	Leibovitz L-15 medium
LDL	low density lipoprotein
MLV	multilamellar vesicle
n	number of independent experiments
NBD-	(7-nitro-2-1,3-benzoxadiazol-4-yl)amino-
PC	phosphatidylcholine
PE	phosphatidylethanolamine
PS	phosphatidylserine
PI	phosphatidylinositol
PI(4)P	phosphatidylinositol-4-phosphate
PI(4,5)P_2	phosphatidylinositol-(4,5)-bis-phosphate

R^2	coefficient of determination
RhoA	ras homolog gene family member A
RPMI	Roswell Park Memorial Institute medium 1640
SEM	standard error of the mean
SM	sphingomyelin
SSC	side scatter
sulfo-NHS-LC-biotin	succinimidyl-6-(biotinamido)-hexanoate
TET	tetracycline
Tf	transferrin from human serum
TIR-FM	total internal reflection fluorescence microscopy
TMR	tetramethyl-6-rhodamine

CHAPTER 1

Introduction

The first steps during all endocytic events necessarily take place at the plasma membrane of cells. Among other processes, this includes the generation of high local curvature for the formation of endocytic vesicles out of a comparably flat plasma membrane. Several mechanisms are known to be able to induce this required curvature, but it is still not completely established which of these mechanisms are involved in the various endocytic pathways. Thus, the present study focuses on the influence of a specific mechanism to induce membrane curvature, the monolayer area asymmetry, on the activity of different endocytic pathways. Therefore, the following introduction describes first of all the composition and properties of the plasma membrane relevant for this study. Then, endocytosis and selected endocytic pathways will be introduced with particular emphasis on the first steps of the respective pathway. Finally, various mechanisms leading to membrane bending are shortly reviewed and it is subsequently summarised how membrane curvature can be induced in particular by the transversal lipid asymmetry of the plasma membrane. Furthermore, the studies supporting an involvement of lipid translocators in endocytosis and two models, how lipid translocators could be connected with the generation of endocytic invaginations, will be introduced.

1.1 Plasma Membrane

Even though the origin of cell membranes is still a major unresolved issue of evolution, the invention of selective permeable barriers was certainly a pivotal moment in the evolution of life. By surrounding a cell and intracellular compartments with an amphiphilic lipid membrane, the membrane barrier physically separates the cytoplasm from the extracellular environment and reaction compartments within a cell from each other. Moreover, via this barrier vital chemical gradients can be maintained against the environment and between intracellular compartments. Due to the amphiphilic properties of lipids composing the barrier, the membrane spontaneously forms a bilayer structure with a hydrophobic inner core, constituted by the lipid acyl chains, and a polar outer layer on both surfaces, composed of the hydrophilic lipid headgroups. Thereby, the aqueous environment entropically drives the hydrophobic fatty acid chains to self assemble and the hydrophilic headgroups have a propensity to interact with each other and with the polar environment.

Besides the lipids, a biological membrane consists of proteins, that are embedded in the bilayer, and a low percentage of either protein- or lipid-associated carbohydrates. Their organisation in the membrane was primarily described by the fluid mosaic model introduced by Singer and Nicolson (1972), which considered the restrictions imposed by thermodynamics. Here, both proteins and lipids are thought to freely diffuse in the lateral direction of the membrane. Currently, this model was amended, because the protein density in native membranes is in general much higher than in most artificial membranes that have been studied in the last decades. The high protein density as well as the formation of lateral microdomains most likely limits the lateral mobility of membrane components (Rajendran and Simons, 2005; Jacobson et al., 2007). An updated model is given in Engelman (2005) and the lateral distribution of lipids and their formation into microdomains is described more detailed in 1.1.2. The membrane proteins either partially or completely traverse the lipid bilayer, integral membrane proteins, or are loosely associated with it, peripheral membrane proteins. The protein to lipid ratio of biological membranes can range between 0.2 and 0.8 (Gennis, 1989). While the proteins fulfil a number of specialised functions in the membrane, for example as enzymes, transporters, structural elements, or receptors, lipids supply a strong yet flexible matrix for the membrane. Despite the huge diversity of different lipid species in biological membranes, the basic formation with the hydrophilic headgroups on either side and the

hydrophobic chains oriented towards the interior of the membrane is conserved in every membrane.

However, lipids have far more functions than forming the backbone of the membrane barrier. Particular lipid species and mixtures provide membranes with the ability to bud, tubulate, and fuse, processes that are essential for cell division, biological reproduction, and intracellular membrane trafficking (van Meer et al., 2008). Moreover, they are involved in the regulation of protein activity, enzymatic reactions, as well as cell-cell interactions, and can act as first and second messengers in signal transduction and molecular recognition processes (Zachowski, 1993; van Meer et al., 2008). The following clauses describe the major lipid species composing the plasma membrane and their implication in mechanisms relevant for endocytosis.

1.1.1 Lipid Composition

The three major classes of lipids found in the plasma membrane of eukaryotic cells are glycerophospholipids, sphingolipids, and sterols. Glycerophospholipids, in general referred to as phospholipids, are made up of a glycerol backbone esterified with two acyl chains at position sn-1 and sn-2, and at least a phosphate ester at position sn-3. Distinct lipid species are discerned by different functional groups bound to the phosphate yielding a phosphoric acid diester. The most abundant headgroups are choline, ethanolamine, and serine forming the glycerophospholipids phosphatidylcholine (PC), phosphatidylethanolamine (PE), and phosphatidylserine (PS), respectively. The hydrolytic cleavage of one of the two acyl chains of glycerophospholipids leads to lyso-glycerophospholipids. Thus, lyso-phospholipids have a free alcohol in either the sn-1 or sn-2 position. Length and degree of saturation of the fatty acid chains as well as size, charge, and chemical nature of the headgroups define the properties of glycerophospholipids, which are also determining the properties of membranes. Dependent upon the lipid composition the thickness, permeability, and fluidity of a membrane, to mention but a few, differs a lot. Additionally, the size of fatty acid chains relative to the headgroup defines the molecular shape of a lipid, which can influence the curvature of a membrane (see clause 1.3). Another native headgroup is inositol, giving phosphatidylinositols (PI), which are a minor lipid species in the cytoplasmic leaflet of the plasma membrane. PI with a phosphorylated inositol ring are called phosphoinositides and play important roles in signalling as well as membrane trafficking. For instance, phosphatidylinositol-(4,5)-

bis-phosphate ($PI(4,5)P_2$) is enriched in the plasma membrane where it is an important substrate for a number of important signalling proteins (Toker, 1998) and has an essential role in many endocytic pathways (see clause 1.2).

Although very similar to glycerophospholipids in many physicochemical properties, sphingolipids do not originate from glycerol, but from the aliphatic amino alcohol sphingosine. Ceramide (Cer), the basic structural unit in all sphingolipids, consists of a fatty acid chain linked through an amide bond to sphingosine. The replacement of the 1-hydroxyl group by phosphocholine leads to sphingomyelin (SM), which is the major phosphosphingolipid of mammals and in comparison to intracellular membranes enriched in the plasma membrane (Fahy et al., 2005). Glycosphingolipids are achieved by the linkage of either a single sugar residue yielding cerebrosides, which can be sulfated, called sulfatides, or at minimum three sugars with at least one sialic acid, namely gangliosides.

Sterols, a subgroup of steroids, are tetracyclic molecules which vary in their side chains and localisation of double bonds. Along with the glycerophospholipids PC, PS, PE, and PI as well as the sphingolipid SM, the sterol cholesterol constitutes the major components of membrane lipids in the plasma membrane of mammalian cells (Fahy et al., 2005). The cholesterol content of mammalian membranes increases along the secretory pathway from the endoplasmic reticulum, over the Golgi to the plasma membrane, where it gains about 0.8 related to the phospholipid concentration. Cholesterol consists of a rigid sterol ring system, a short hydrocarbon chain, and a small polar headgroup comprised by a hydroxyl group, which is responsible for an amphiphilic structure character of the molecule. Figure 1.1 illustrates the structure of the major lipid species in the plasma membrane of eukaryotic cells that are mentioned above.

How the enrichment of SM and cholesterol in the plasma membrane is generated is not well understood. Recent studies indicate that the trans-Golgi network, which is the major sorting station in the secretory pathway, is responsible for the sorting of membrane lipids by addressing specific secretory vesicles to the plasma membrane (Klemm et al., 2009). However, it is the particular composition that characterises biological membranes in different cell types as well as certain cell organelles. While the basic structure of membranes is strongly retained, the composition of lipids and proteins is adapted to comply with the individual requirements. For instance, the plasma membrane of Schwann cells, electrically insulating neuronal axons, has a protein content of only about 20 % and is rich in the otherwise rare sphingolipid class of gangliosides (Devaux and Seigneuret, 1985). Another interesting example is the membrane of hyperthermophilic archaea in

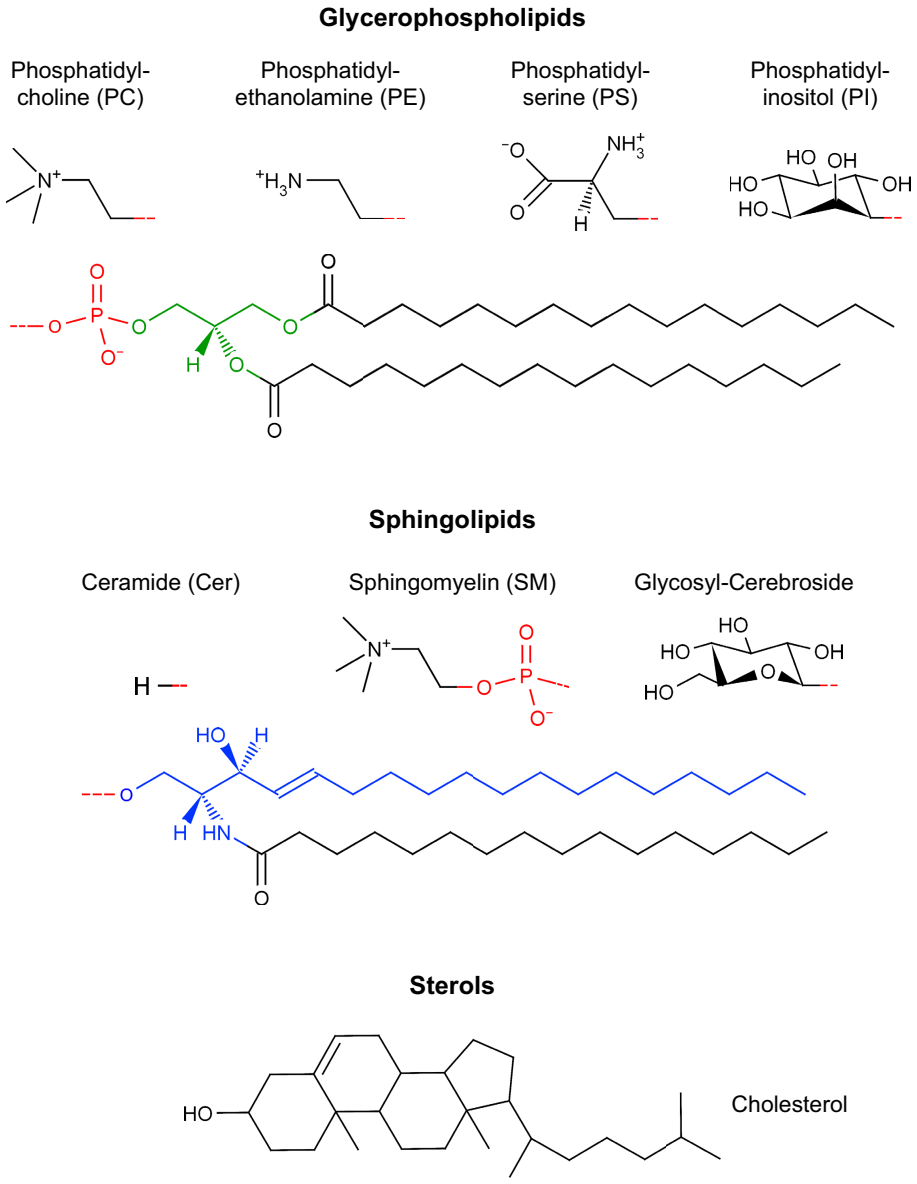

Figure 1.1: Major lipid classes in the plasma membrane of eukaryotic cells. The common feature of the heterogeneous group of lipids is their good solubility in organic solvents, and a limited solubility in water. The main eukaryotic membrane lipids are glycerophospholipids, sphingolipids and the sterol cholesterol. Apart from the lipids occurring in membranes, triacylglycerols, which serve as energy stores, and steroids, which include many vitamins and hormones, are lipids of biological importance.

which phospholipids comprises isoprene linked to the glycerol by ether bonds instead of ester bonds (Lai et al., 2008). This provides the membranes with a high stability against extreme temperatures and prevents hydrolysis of the lipids. Beyond this specific lipid composition of the plasma membrane, the lipids are not equally distributed across the two leaflets of the bilayer, which is important for diverse cellular functions. In the following, the lateral and transversal lipid distribution will be explained more detailed, since this asymmetry of lipids in the plasma membrane is thought to be involved in endocytic mechanisms.

1.1.2 Lateral Heterogenous Organisation of Lipids

Even within one membrane the lipid composition was found to be different between separated domains, for instance in the plasma membrane of polarised cells, in which basolateral and apical domains are separated by tight junctions, as well as in lateral microdomains, so called *rafts*. The latter ones are defined as follows: "Membrane rafts are small (10-200 nm), heterogeneous, highly dynamic, sterol- and sphingolipid-enriched domains that compartmentalize cellular processes. Small rafts can sometimes be stabilized to form larger platforms through protein-protein and protein-lipid interactions." (Pike, 2006). Lateral microdomains were already mentioned more than 30 years ago (Petit and Edidin, 1974) and since then many studies have focused on the revelation of their size, formation, and function in cellular processes (Simons and Ikonen, 1997; Ikonen, 2001; Rajendran and Simons, 2005). Despite these strong efforts the exact nature of rafts and even their nomenclature remains surprisingly controversial (Hancock, 2006). However, independently on their nomenclature, it has convincingly been shown that lateral nanoscale domains indeed exist in biological membranes (Silvius and Nabi, 2006; Sengupta et al., 2007) and that they are implicated in endocytic events, especially in clathrin-independent endocytosis (Sharma et al., 2004, and see 1.2.2).

1.1.3 Transbilayer Lipid Asymmetry

Furthermore, the plasma membrane of eukaryotic cells displays differences in the lipid composition between its two leaflets, a transversal asymmetry. Whereas in the membrane of the endoplasmic reticulum all lipids are transversal symmetrically distributed within the bilayer, the membranes of the Golgi, endosomal membranes, and the plasma membrane show a transmembrane lipid asymmetry (Zachowski, 1993; van Meer et al.,

2008). In the plasma membrane of eukaryotic cells the aminophospholipids PS and PE as well as less abundant lipids, such as PI and phosphatidic acid, are predominantly located in the cytoplasmic leaflet, while the exoplasmic leaflet comprises the majority of the choline containing lipids PC and SM as well as glycosphingolipids (Devaux and Morris, 2004). In this process, the distribution of PC and PE in the respective layer appears to be less strictly limited than the restricted localisation of SM and PS to the outer and inner leaflet, respectively. For cholesterol, an asymmetric distribution across the leaflets of the plasma membrane is not conclusively established. Some studies suggest an asymmetric distribution with cholesterol either preferentially present in the exoplasmic (Pomorski et al., 2001; de Almeida et al., 2003) or cytoplasmic leaflet (Schroeder et al., 1991), whereas in other studies the distribution is proposed to be symmetrical (e.g. Lange and Slayton, 1982). Several data obtained with cholesterol analogues indicate a rapid diffusion of cholesterol from one layer to the other (e.g. Muller and Herrmann, 2002). However, the transmembrane distribution of cholesterol will most likely be determined not only by the exchange rate between bilayers, but also by the affinity of cholesterol for the other lipid and protein components of the membrane. The number of fatty acid double bonds and the properties of the headgroup play a major role in the interactions of cholesterol with other membrane lipids (Aittoniemi et al., 2007). Since the other membrane components are not symmetrically distributed in the plasma membrane, it seems to be rather likely that cholesterol is also not equally distributed across the bilayer (Devaux and Morris, 2004; van Meer et al., 2008).

The transversal asymmetry of membrane lipids has important functional consequences for various cellular mechanisms and is associated with many patho- and physiological processes (Balasubramanian and Schroit, 2003). For instance, increased amounts of PS appear on the exoplasmic leaflet of the plasma membrane of tumorigenic cell lines (Utsugi et al., 1991) and the asymmetry of PS is largely lost in apoptotic cells (Fadok et al., 1992). Although the lipid asymmetry was first thought to be a static characteristic of membranes (Bretscher, 1972), it is now evident that this asymmetry results from continuous translocation of lipids across the bilayer, which is called *flip-flop*. Multiple factors are involved in the maintenance of the transmembrane lipid asymmetry: biophysical properties that limit amphiphilic lipids to spontaneously cross the hydrophobic core of a membrane, retentive mechanisms that attract lipids in one of the two leaflets, such as charged lipids favouring different pH values, and specific proteins that translocate lipids from one layer to the other (Daleke, 2007; van Meer et al., 2008).

The spontaneous transversal movement of lipids carrying a polar headgroup across a pure lipid membrane is very rare with a typical half time of hours to days. This time depends on the size, polarity, and charge of the headgroups, the hydrophobicity of the fatty acid chains, and the composition of the lipid bilayer (Sprong et al., 2001). In addition to the difficulties of polar moieties to penetrate the hydrophobic core of a lipid membrane, the very low lateral elasticity of lipid layers, as demonstrated in Langmuir-Blodgett troughs, hampers the spontaneous flip-flop of membrane lipids. To maintain the asymmetric distribution of specific lipids in the plasma membrane, proteins translocate lipids more rapidly from one leaflet to the other. Such translocator proteins have been already postulated by Bretscher (1974) and the activity of an aminophospholipid translocase (APLT) was first observed in human erythrocytes by Seigneuret and Devaux (1984). By now, much is known about translocated lipid species (e.g. Daleke, 2007), but the exact identity and biological function of lipid translocator proteins remain elusive. However, relevant for this thesis is mainly the fact that a lipid asymmetry of the plasma membrane exists and that specific lipids are translocated to either of the two leaflets. Therefore, the following clause will only give a brief introduction into the subject of lipid translocators and the reader is referred to more extensive descriptions in the following excellent reviews: Pohl et al. (2005); Devaux et al. (2006); Pomorski and Menon (2006); Daleke (2007).

1.1.4 Lipid Translocators

The proteins involved in lipid translocation can be divided into four classes based on their direction of transport, requirement for energy, sensitivity to Ca^{2+} concentrations, and substrate specificity. Proteins that translocate lipids from the exoplasmic or luminal to the cytoplasmic side of membranes are commonly called *flippases* and translocators that move lipids in the opposite direction are named *floppases*. Energy-independent translocators unspecifically allow lipids to traverse the membrane in both directions, whereas energy-dependent translocators mediate a net transfer of lipids to one leaflet of the membrane against a concentration gradient with a differing substrate selectivity. Candidates for the former translocators are proteins called *scramblases*, which are ATP-independent and activated by elevated Ca^{2+} concentrations. Activity of scramblases as well as energy-dependent flippases and floppases can be found in the plasma membrane of eukaryotic cells, where the latter ones regulate the nonrandom transbilayer

lipid distribution. The activation of scramblases leads to the randomisation of lipid distribution, which is thought to occur for example during apoptosis. The fourth class of translocators, energy-independent flippases, mediate rapid and rather unspecific lipid translocation in the endoplasmic reticulum membrane.

Several members of the P_4 subfamily of P-type ATPases are believed to be responsible for the ATP-dependent inward translocation of aminophospholipids in the plasma membrane. After the discovery of APLT activity in human erythrocytes (Seigneuret and Devaux, 1984), subsequent studies defined the biochemical properties of these flippases, such as vanadate and Ca^{2+} sensitivity as well as a high selectivity for PS (Daleke and Lyles, 2000). Based on these biochemical properties, further potential enzymes were defined. Purification of the bovine adrenal chromaffin granule-associated APLT activity (ATPase II) led to the cloning of a gene currently referred to as Atp8a1 (Tang et al., 1996). This enzyme was found to be homologous to proteins in the P-type ATPase superfamily and most closely homologous to Drs2p, a yeast ATPase that is resident in the trans-Golgi network. Both, Atp8a1 and Drs2p, are constituent members of a conserved subfamily of P-type ATPases, namely P_4-ATPases, that are divided into five subclasses by particular sequence characteristics. Many of the P_4-ATPases have been linked to the maintenance of membrane structure, transport of amphiphilic molecules, and vesicle trafficking and at least two of them are thought to be involved in human diseases (Paulusma and Oude Elferink, 2006). In this regard, it has been shown recently that Atp8b1 deficiency causes a severe liver disease and loss of hearing, that is associated with progressive degeneration of cochlear hair cells (Folmer et al., 2009; Stapelbroek et al., 2009). The P_4-ATPase subclasses include five yeast proteins Drs2p, Dnf1p, Dnf2p, Dnf3p, and Neo1p (Hua et al., 2002), six members in *Caenorhabditis elegans* (Ruaud et al., 2009), 12 members in *Arabidopsis thaliana* (Poulsen et al., 2008) and 14 human enzymes Atp8a1-Atp11c (Paulusma and Oude Elferink, 2005). There is accumulating evidence that P_4-ATPases actively translocate phospholipids, thereby maintaining the transbilayer lipid asymmetry in the plasma membrane. For instance, yeast cells lacking Dnf1p and Dnf2p were shown to have an abolished inward translocation of fluorescently labelled analogues of PC, PS, and PE (Pomorski et al., 2003). Recent studies could show the translocation of the native phospholipids lyso-PC and lyso-PE across the plasma membrane of yeast by the same enzymes (Riekhof et al., 2007). To unequivocally demonstrate the lipid translocation by P_4-ATPases the current work of many groups focuses on the reconstitution of purified proteins into model mem-

branes to show P_4-ATPase specific lipid translocation. Recently, two different groups successfully reconstituted P_4-ATPases and provided direct biochemical evidence that P_4-ATPases translocate phospholipids.Zhou and Graham (2009) purified and reconstituted Drs2p along with the noncatalytic subunit Cdc50p into proteoliposomes. It could be shown that fluorescently labelled analogues of PS were actively translocated across the liposome bilayer, whereas the respective analogues of PC and SM were not translocated. Although the obtained effects were relatively small and further experiments need to be performed to identify the amount of active Drs2p reconstituted in liposomes, this study confirmed the active and probably selective translocation of phospholipids by P_4-ATPases. This finding is underlined by the results of Coleman et al. (2009) who purified and reconstituted Atp8a2 into liposomes containing fluorescently labelled analogues of PS resulting in an ATP-dependent translocation of PS across the bilayer.

A second member of ATP-dependent lipid translocators, the ATP-binding cassette (ABC) transporter family, was identified in studies originally related to multidrug resistance in cancer cells and is apparently responsible for an active outward translocation of lipids. ABC transporters are members of a large family of highly conserved, multispan transmembrane proteins that translocate a wide variety of substrates, such as ions, sugars, drugs, and peptides, across different cell membranes. Several ABC proteins were found to be mutated in lipid linked diseases, therefore suggesting their involvement in lipid translocation. In contrast to P_4-ATPases, ABC transporters move lipids from the cytoplasmic to the exoplasmic leaflet of the plasma membrane and, moreover, even expel a given lipid out of the membrane (van Meer et al., 2006). As for flippases, an increasing number of lipids was shown to be translocated, but the mechanisms of translocation remain unsolved. For instance, the multidrug transporter ABCC1 translocates fluorescently labelled short chain PC, PS, SM, and glucosylceramide analogues and has been suggested to maintain the outward orientation of natural choline phospholipids to the plasma membrane (Pomorski and Menon, 2006). A comprehensive review of Pohl et al. (2005) provides the implication of ABC proteins in lipid translocation and an overview of the actual known main ABC transporters for lipids in humans and their presumed substrates can be found in Box 2 of van Meer et al. (2008).

The potential implication of these lipid translocators, primarily of flippases translocating lipids from the outer to the inner leaflet of the plasma membrane, in the generation of membrane invaginations and therefore in endocytic events is outlined in 1.3.2. Based on

the general features and composition of the plasma membrane, the following clauses now introduce the processes of endocytosis with special focus on the first steps of endocytic events in which the plasma membrane is the pivotal point.

1.2 Endocytosis

Endocytosis is a collective term for processes by which cells ingest selected cargoes from the cell surface by engulfing them with regions of their plasma membrane. Typically, endocytic pathways start with recruiting the cargo at the cell surface. Subsequently, an invagination of the plasma membrane is generated that becomes a closed vesicle and must be detached from the parent membrane into the cell. In the cytoplasm, this vesicle must fuse with the first compartment of its itinerary, a highly complex system resulting in the eventual sorting or degradation of the vesicle contents. This allows the cell to internalise extracellular components and fluids as well as plasma membrane lipids and integral membrane proteins. The morphological contrary process, called exocytosis, delivers specific compounds to the extracellular space as well as lipids and proteins to the plasma membrane by fusing internal vesicles with it. Via these processes of membrane traffic the composition of the plasma membrane can precisely be regulated, which is essential for responding to, or affecting, the extracellular environment or other cells. Hence, endocytosis is required for diverse and disparate cellular functions such as immune surveillance, cellular and organismal homeostasis, mitosis, antigen presentation, and cell migration and plays a key role in the positive regulation of intracellular signalling cascades (Doherty and McMahon, 2009).

There are several mechanisms of endocytosis which can be separated into two broad categories (Conner and Schmid, 2003): in phagocytosis, the uptake of large particles (from Greek $\phi\alpha\gamma\epsilon\iota\nu$ [phagein] - *to eat* and Latin [cyta] - *cell*), and in pinocytosis, in which the cell ingests fluid and solutes (from Greek $\pi\iota\nu\epsilon\iota\nu$ [pinein] - *to drink*). Phagocytosis can be observed only in protozoa and specialised mammalian cells, e.g. macrophages or mastocytes. Pinocytosis exists in all eukaryotic cells and includes macropinocytosis, clathrin-mediated (CM), caveolae-mediated, and clathrin-independent (CI) endocytosis (Conner and Schmid, 2003). Further distinctions are made between constitutive endocytosis, which occurs continuously, and induced pathways of endocytosis, in which the activity is stimulated by ligand binding and downstream events (Benmerah and Lamaze, 2007). In the latter process, specific molecules are taken up by receptor-mediated en-

docytosis, such as clathrin- or caveolae-mediated endocytosis. Here, cells specifically internalise solutes by vesicles containing proteins with receptor sites specific to the ligands being endocytosed. In contrast to this, the nonspecific uptake of fluid and solutes takes place by a process often referred to as bulk flow endocytosis. Here, external material is internalised into inner cell compartments without binding to specific receptors.

The existence and regulation of the multiple mechanisms and pathways of endocytosis are becoming of increasing interest in relation to the huge variety of fundamental cellular functions. Although much is known about the cargoes, the specific mechanisms for the recruitment of these cargoes to the plasma membrane, the subsequent sorting into specific vesicles of the different endocytic pathways, and the regulation of these pathways are less clear. For instance, epidermal growth factor (EGF) receptor is hyperactive in many cancers and is endocytosed by CM as well as CI pathways. In CI endocytosis the receptor appears to be degraded, while in CM endocytosis it is recycled and can continue to participate in signalling (Sigismund et al., 2008). Further investigations could provide tools to direct this receptor to CI mechanisms and thereby enhance degradation of the receptor as means of affecting cancer cell proliferation (Doherty and McMahon, 2009).

Initially, CM endocytosis was thought to be responsible for everything endocytosed (Doxsey et al., 1987). Even though it has been shown that cells still undergo endocytosis when the clathrin-dependent pathway is inhibited, it took time to accept the existence of CI pathways. Since it was published that CI endocytosis not only exists but is also regulated (Damke et al., 1995), it became apparent that an expanding fraction of cargoes is taken up by CI pathways (Sandvig et al., 2008). CI endocytic pathways are further categorised into dynamin-dependent or -independent as well as caveolae-mediated, cell division control protein 42 homolog (Cdc42)-, ras homolog gene family member A (RhoA)-, or ADP-ribosylation factor (Arf)-6-regulated pathways, based on the use of the dynamin-mediated scission mechanism and the involvement of small GTPases (Mayor and Pagano, 2007). Statements on relative proportions of the different pathways diverge in the literature. Doherty and McMahon (2009) refer to roughly equiprevalent modes of clathrin-dependent and -independent endocytosis in fibroblastic cells, whereas Ungewickell and Hinrichsen (2007) quote the CM pathway to be the major route in fibroblasts in which cells take up the equivalent of the cell's total plasma membrane within one hour. This demonstrates the difficulties to quantify endocytosis examined with different techniques. It has to be assumed that proportions of endocytic activity most likely vary in different cell types due to their adaptations and specific functions

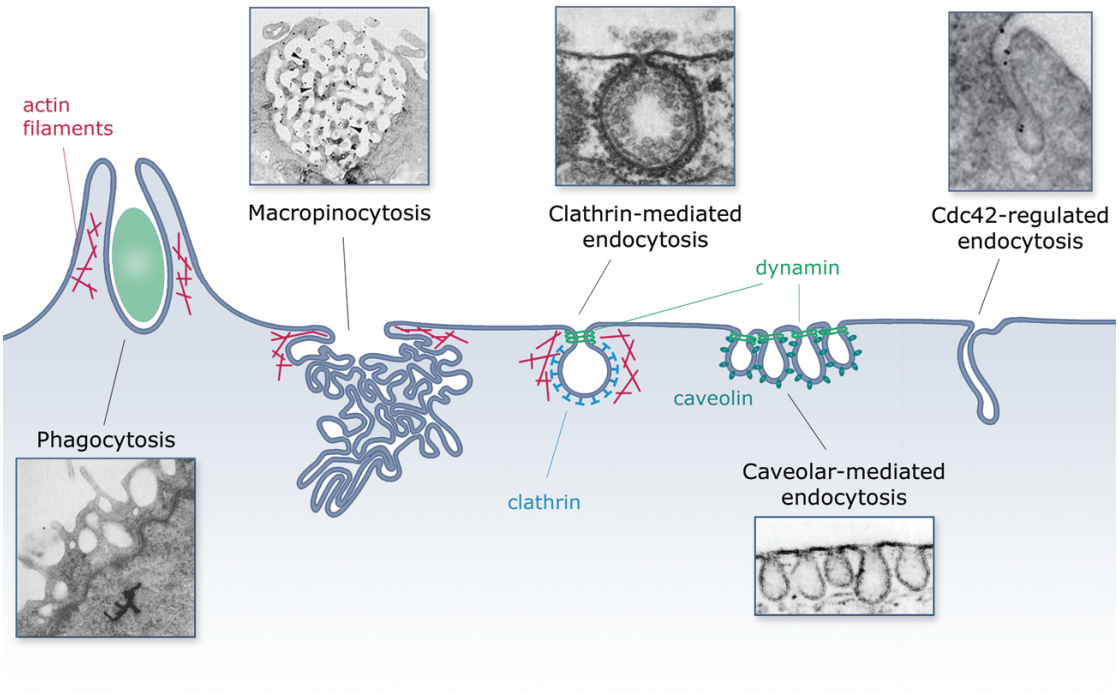

Figure 1.2: Morphological structures of selected endocytic pathways. The variability of morphologies ranges from enveloping membrane extensions during phagocytosis (North, 1969), over highly ruffled regions in macropinocytosis (Shao et al., 2002), spherical and coated buds of clathrin-mediated endocytosis (Perry and Gilbert, 1979), flask shaped caveolae (Rothberg et al., 1992), to tubular structures in Cdc42-regulated endocytosis (Sabharanjak et al., 2002). Membrane invaginations of clathrin- and caveolae-mediated endocytosis are coated by clathrin and caveolin, respectively, and the membrane scission protein dynamin was shown to be involved in both pathways. Actin filaments most likely support the formation of membrane structures during phago- and macropinocytosis and are associated in the fission of clathrin-coated vesicles. Figure based on Mayor and Pagano (2007, Fig. 1) and Doherty and McMahon (2009, Fig. 1).

(Sato et al., 1996). A specific endocytic pathway already differs within a single cell line when cells are apicobasally polarised (Sandvig et al., 2008), such as epithelial cells and hepatocytes. For instance, epithelial Madin-Darby canine kidney cells form caveolae only at the basolateral but not at the apical surface (Verkade et al., 2000). Moreover, special treatments of cells or the inhibition of specific proteins in order to investigate single pathways may functionally alter the activity of a route that is more silent or even not existent under normal conditions.

All these different pathways comprise different proteins that are associated and exhibit a high morphological variability (Fig. 1.2). It is becoming increasingly proven that budding structures do not only form spherical vesicles but also tubular and more complex formations. The endocytic morphologies range from spherical clathrin-coated pits (Roth and Porter, 1964) over tubular structures in Cdc42-regulated endocytosis (Kirkham and Parton, 2005; Mayor and Pagano, 2007) to highly ruffled regions of the plasma membrane in macropinocytosis (Shao et al., 2002). A summary of membrane morphology, involved cargoes, small G-protein dependence, dynamin implication, and other implicated proteins is given in Mayor and Pagano (2007, Table 1) and Doherty and McMahon (2009, Table 1). It gives an impression of the complex interrelations and high variability of the involved cargoes and regulating proteins. However, besides this diversity all internalisation processes have one scene in common: the formation of budding structures which requires bending of the plasma membrane. The present study focuses on the implication of plasma membrane properties in the generation of membrane curvature in emerging endocytic invaginations. Thus, the following introduction to selected endocytic pathways will concentrate on the first steps of the respective pathway, on associated proteins that are known to induce membrane bending or fission, and on possible interactions with plasma membrane lipids.

1.2.1 Clathrin-Mediated Endocytosis

The primarily discovered clathrin-mediated pathway has extensively been studied since many years and is well characterised. For example, essential nutrients, such as iron loaded transferrin and low density lipoprotein (LDL), are endocytosed by this route. Also several enveloped viruses, for instance Influenza and Ebola virus, exploit this pathway to mediate their internalisation into cells. The molecular mechanisms behind the recruitment of cargoes into emerging clathrin-coated pits and the subsequent fission of coated vesicles become progressively decoded and are reviewed in numerous publications, e.g. Benmerah and Lamaze (2007); Ungewickell and Hinrichsen (2007); Rappoport (2008). Here, the high diversity of implicated cargoes, adaptors, and accessory proteins will be summarised to give an overview on the general functionality of this highly complex pathway.

As a first step of this pathway, upon binding of an extracellular ligand to specific receptors on the cell surface, such as transferrin, clathrin together with adaptors and

endocytic accessory proteins is recruited to the plasma membrane to eventually assemble in polyhedral lattices. These predominantly flat structures are coating membrane buds in patches with diameters from 10 nm to more than 500 nm. The coat proteins, with clathrin as primary structural unit, simultaneously sense the transmembrane cargo and PI(4,5)P_2, the most abundant phosphoinositide in the plasma membrane. This assures that a productive coat formation only occurs in the presence of both, a transmembrane cargo and a specific lipid environment. Indeed, the depletion of PI(4,5)P_2 inhibited the uptake of transferrin receptors and caused an increase in the concentration of transferrin receptors in the plasma membrane (Abe et al., 2008). The regulation and the functional role of PI(4,5)P_2 in clathrin-mediated endocytosis has been reviewed in detail by Haucke (2005). Different receptors use diverse mechanisms for their entry into clathrin-coated vesicles. Four types of internalisation signals at the cytoplasmic tails of transmembrane proteins have been identified that are recognised by different endocytic adaptor proteins. For example, the tetrameric adaptor protein 2 (AP-2) complex interacts with a tyrosine based sorting motif, that is included in the cytoplasmic tail of the transferrin receptor. The LDL receptor uses another sorting motif: FXNPXY that associates with the monomeric adaptor Dab2 which binds AP-2. The leucine based motif [DE]XXXL[LI] serves as an internalisation signal in many single- and multi-spanning transmembrane proteins (Sorkin, 2004).

At the same time, the binding of adaptor proteins to PI(4,5)P_2 is mediated by protein intrinsic domains. The adaptor protein AP-2, with its potential to associate with a lot of proteins of the endocytic machinery, has two binding sites for inositol lipids. Due to a conformational change after cooperative binding to the first lipid, the affinity of AP-2 to associate with the plasma membrane highly increases (Honing et al., 2005). Additionally, AP-2 stimulates the local concentration of PI(4,5)P_2 in two ways: by binding to a phosphoinositide-kinase its activity is increased and by interacting with the small GTP-binding Arf-6, which also amplifies the activity of the phosphoinositide-kinase. Alongside, to the interaction of Arf6 with AP-2, Arf6 can also bind to the heavy chain of clathrin, which results in a complex formation of AP-2, clathrin, and Arf6 (Poupart et al., 2007). Thus, AP-2 is thought to hold a central position among the other proteins and regulates the recruitment of more adaptors to the plasma membrane by creating a positive feedback loop (Bairstow et al., 2006). With the exception of only one monomeric adaptor protein, Eps15/Eps15R, all adaptors are capable of binding to clathrin. The clathrin-coat basically consist of a triskelion that is composed of the

tight association of three clathrin heavy chains with three clathrin light chains. The heavy chains provide the structural backbone, whereas the light chains are thought to regulate the formation and disassembly. In addition to clathrin, the coat network contains assembly proteins, for instance the adaptor proteins AP-180 and AP-1, and gathers into a lattice of hexagons and pentagons. By interacting with AP-2, the clathrin lattice is targeted to the plasma membrane for the formation of clathrin-coated pits (Motley et al., 2003).

How the flat hexagonal lattices contribute to the subsequent bending of the plasma membrane is not exactly known yet. Indeed, clathrin was shown to be essential for the invagination of coated membrane patches, but theoretical considerations suggest that the energetics of clathrin assembly are not sufficient for the generation of membrane curvature in relatively rigid membranes, such as the plasma membrane or membranes of the trans-Golgi network (Nossal, 2001). However, the transformation of the clathrin network from hexagonal structures into pentagonal ones gives the lattice an inherent tendency to form a bent coat. The wide range of clathrin lattice formations and a potential dependence of the vesicle position within the lattice on the polarity of assembly, from initiation of coat formation to membrane pinching, are excellently shown in electron microscopical studies in Cheng et al. (2007). Additionally, clathrin and other implicated adaptor proteins interact with proteins that are noted for their ability to induce membrane curvature. Epsin and proteins comprising domains of the BAR (Bin, Amphiphysin, Rvs) superfamily, including "classical" BAR domains, N-BAR and F-BAR (Fes/CIP4 homology-BAR or EFC for Extended FCH Homology) domains, are well known exemplars of proteins that are involved in the formation of clathrin-coated pits and can generate, sense, and stabilise membrane bending (Ford et al., 2002; Lundmark and Carlsson, 2003; Hinrichsen et al., 2006). The amphipathic helix of epsin inserts into the proximal leaflet of a lipid bilayer which causes a displacement of lipid headgroups and a reorientation of acyl chains. Upon binding directly to inositol lipids and the simultaneous insertion of the helix, epsin generates membrane curvature by increasing the protein proximal monolayer area relatively to the other layer (Horvath et al., 2007). In this process, formation of the amphipathic helix in epsin is thought to be coupled to inositol lipid binding (Ford et al., 2002; Yoon et al., 2009). Proteins containing a concavely shaped BAR domain bind to negatively charged membrane surfaces mainly due to electrostatic interactions (Gallop and McMahon, 2005; Frost et al., 2009). In addition to a BAR domain, some proteins contain an amino-terminal amphipathic helix

preceding the BAR domain, called N-BAR domain, that inserts into the membrane like the helix of epsin (Fernandes et al., 2008; Campelo et al., 2010). F-BAR proteins have a more shallow curvature than BAR proteins and seem to deform membranes into structures with a wider diameter. Several F-BAR proteins have an established role in binding phospholipids and are known to be involved in actin dynamics at the plasma membrane. In this way, the actin polymerisation apparatus and the machinery regulating membrane dynamics is linked by these proteins (Aspenstrom, 2009). Only these joint contributions of clathrin network forming and curvature generating proteins can most likely account for an effective bending of the coated membrane patches.

The subsequent fission of the coated invagination and its release into the cytoplasm is mediated by dynamin and its interactions with actin filaments. The membrane scission protein dynamin, a large, modular GTPase, is recruited by curvature sensing proteins and has domains that support binding to PI(4,5)P_2. By creating a GTP-dependent conformational change into helical rings, it induces fission by tracing the small neck of the coated bud like a scaffold and ties up the membrane into tubular structures (Chen et al., 2004; McMahon and Gallop, 2005). In this process, the insertion of the pleckstrin homology domain into the membrane was shown to be essential for fission and subsequent vesicle release (Ramachandran et al., 2009). The activity of dynamin is thought to be regulated by transferrin receptor trafficking protein (Tosoni et al., 2005). By interacting simultaneously with the transferrin receptor and dynamin it can negatively regulate the rate of GTP hydrolysis by dynamin, which provides a mechanism to accumulate a sufficient amount of cargoes before vesicles are pinched off. The last step of coated vesicle fission is the dissociation from the plasma membrane into the cytoplasm. There is more and more evidence that this happens in an actin dependent manner (Merrifield et al., 2002; Brett et al., 2006) and currently there are two models how actin is thought to be involved. In the first model, the clathrin coat is suggested to be connected to actin filaments via an accessory protein and the vesicle is thereby carried more deeply into the cytoplasm. This would increase the forces on the thin neck, which is scaffolded by dynamin, until the stretched neck snaps. The second model is an extension of the first, but not yet well established (Ungewickell and Hinrichsen, 2007). Here, it is proposed that two different actin motor proteins bind through accessory proteins to the clathrin coat and dynamin, respectively. This would pull the vesicle in two directions, the dynamin ring towards the surface of the cell and the coated bud deeper into the cytoplasm (see Fig. 1.3). Additionally, the scission of the coated vesicle

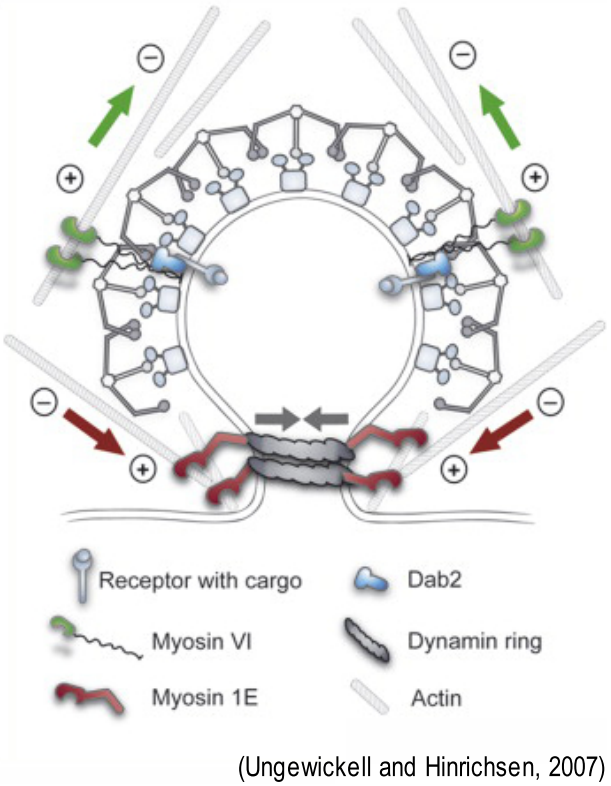

Figure 1.3: A model of clathrin-coated vesicle fission introduced by Ungewickell and Hinrichsen (2007). There is cumulative evidence that the fission of vesicles during clathrin-mediated endocytosis is not only mediated by dynamin but also in an actin dependent manner. Dynamin traces the small neck of the bud with helical rings like a scaffold and ties up the membrane into tubular structures. Additional pulling forces, provided by myosin motor proteins, are thought to stretch the vesicle neck in two directions: the dynamin ring towards the surface of the cell and the coated vesicle into the cytoplasm. Subsequently, this leads to the severance of the vesicle at the predetermined breaking point, that is induced by the dynamin constriction (see the text for references).

could be supported by a redistribution of membrane lipids. Boundary forces at model membranes were shown to result in a phase separation of lipids creating a breaking point that serves when longitudinal forces are applied (Roux et al., 2005; Liu et al., 2006).

After the dissociation from the plasma membrane into the cell, the clathrin basket is released from the vesicle by auxilin and hsc70. When the coat proteins are disassembled they are ready to be reused for another circuit of budding. The uncoated vesicle undergoes further trafficking before appropriate delivery of its cargoes through fusion with a destination compartment. Subsequent sorting depends on the cargo adaptors that are manifold and only related by the participation of the clathrin network (Benmerah and Lamaze, 2007). Additionally, the central role of AP-2 as well as the implication of actin in all clathrin-related pathways is not yet evident. In order to distinguish possible subtypes of CM endocytosis and the associated proteins, studies will have to focus on the participation of these proteins and other distinct adaptor and accessory proteins.

1.2.2 Clathrin-Independent Endocytosis

The number of revealed clathrin-independent endocytic pathways is continuously expanding and knowledge of these pathways was gained in studies when the CM pathway was blocked, for instance a clathrin- and dynamin-independent pathway in HeLa cells expressing a mutant of dynamin-1 (Damke et al., 1995), or by studies of specific cargoes, e.g. the uptake of the β-chain of the interleukin 2 receptor (Lamaze et al., 2001). In contrast to the well characterised CM pathway, only very little is known about the selection of cargoes in CI pathways. Many cargoes for CI endocytosis lack any known cytoplasmic signal suggesting that other mechanisms are responsible for the regulation of cargo recruitment. Although it was proposed that all cargoes endocytosed by CI mechanisms are linked to microdomains in the plasma membrane, the association with detergent resistant membranes (DRM) did not necessarily cause the uptake via a CI pathway (Abrami et al., 2003). Initially, DRM were defined on the basis of their resistance to extraction by detergents and were associated with microdomains in biological membranes, so called rafts (see 1.1.2). Meanwhile the method of in vitro separation of membrane domains by detergent extraction is thought to artificially induce the redistribution of lipids and proteins into such domains (Munro, 2003; Lichtenberg et al., 2005). However, it was shown that multiple endocytic pathways are sensitive to cholesterol and sphingolipids, which are supposed to be enriched in rafts of the plasma membrane. For instance, the depletion of cholesterol or glycosphingolipids inhibited caveolae-mediated endocytosis (Cheng et al., 2006). This suggests the importance of endogenous lipids in the regulation of endocytic pathways and could give a hint that specific microdomains in the plasma membrane are endocytosed by specific pathways.

The mechanisms for cargo selection can generally be divided into protein-, lipid-, and combined protein-lipid-based processes. An example for a protein-based cargo selection is the uptake of EGF. It was shown to be ingested by both, CM as well as CI pathways. However, when EGF was highly concentrated, EGF receptors were ubiquitylated, linked to DRM and endocytosed by a cholesterol sensitive CI mechanism (Sigismund et al., 2005). In lipid based processes the formation of cargoes or receptors in lipid tethered clusters is crucial for the direction into specific CI pathways. For example, cholera toxin B can be endocytosed via clathrin-, caveolae-, as well as Cdc42-regulated routes and its clustering and the distribution of its receptor is thought to give the direction to one of these specific pathways (Mayor and Pagano, 2007). How these domains are

assembled and subsequently recognised by cytoplasmic and pathway related adaptor proteins remains to be elucidated.

The individual role of proteins that are noted for their ability to induce and stabilise membrane bending and curvature is only beginning to be known (Hansen and Nichols, 2009). The membrane scission protein dynamin was shown to be involved in caveolae- and RhoA-regulated pathways, but is not crucial for Cdc42- and Arf6-regulated endocytosis. In most cases, this has been determined by overexpression of individual dynamin-1 or dynamin-2 mutants. Other methods are needed to assess and confirm the effects of the various dynamin isoforms on clathrin-independent internalisation, such as the use of more specific inhibitors of dynamin (Macia et al., 2006). Thus, it could turn out in future studies that the implication of dynamin has to be reconsidered. Likewise, the GTPase-regulated CI pathways were suggested to depend on actin. Theses GTPases are known to interact with the actin machinery and it seems likely that further investigations will show the implication of actin for all CI pathways (Girao et al., 2008; Sandvig et al., 2008). Furthermore, the activation of the Arf family GTP-binding proteins Arf1 and Arf6, which is the key regulator for a clathrin-independent endocytic pathway, was suggested to be dependent on membrane curvature (Lundmark et al., 2008b). Arf family GTP-binding proteins serve as regulatory proteins for numerous cellular processes, such as membrane-trafficking events and maintenance of organelle structure. Thus, these proteins are recruited to curved membranes and feed back to further enhance this curvature, thereby linking sensing and generation of membrane curvature as well as initiating curvature that is further enhanced by endocytic coat proteins during vesicle formation (Donaldson, 2008). Apart from this role of membrane bending proteins, it was proposed that chiral and tilted membrane lipid molecules alone are sufficient to generate membrane curvature (Sarasij et al., 2007). Microdomains seemed to be involved in most, probably even all, CI pathways and the molecular chirality and tilt of the raft forming constituents could favour a bended formation of the membrane. This induction of curvature could then allow the recruitment of proteins that sense and stabilise curvature, such as BAR domain containing proteins (see 1.2.1 for description).

Based on the participation of dynamin and the regulation by small GTPases, members of the Arf and Rho subfamilies, the CI pathways were classified as outlined in Figure 1.4 (modified from Mayor and Pagano, 2007, Fig. 3). However, other mechanisms have already been reported that do not fit into this proposed classification scheme. For example, the uptake of Herpes Simplex Protein VP22 is clathrin-independent and dependent on

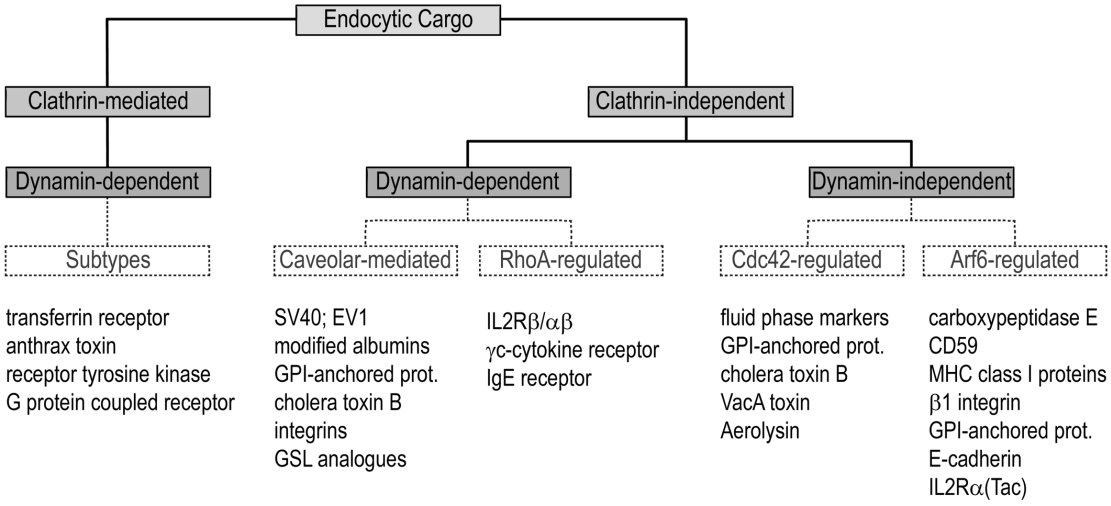

Figure 1.4: Classification scheme for receptor-mediated endocytosis and respective cargoes known or suggested to be endocytosed. Cargoes can be internalised by either clathrin-mediated or clathrin-independent mechanisms. The clathrin-mediated pathway was classified by the participation of the clathrin network and was shown to depend on dynamin. Potential subtypes remain to be addressed. Clathrin-independent pathways can be divided into dynamin-dependent and -independent and furthermore into the dependence on particular GTPases. So far, four different pathways have been discovered that are affected by the modification of one specific GTPase. There are probably other, not yet identified clathrin-independent mechanisms. Figure modified from Mayor and Pagano (2007, Fig. 3).

dynamin and Arf6 (Nishi and Saigo, 2007). However, the following paragraphs describe the four, as yet identified CI pathways and their connected proteins including the mechanisms for membrane bending, when already known. This classification is not meant to rule out other pathways that are not uncovered yet, but to give an overview of the actual knowledge about the routes determined to date.

Caveolae-Mediated Endocytosis (Dynamin-Dependent)

Caveolae-mediated endocytosis is probably the best characterised CI pathway (Mayor and Pagano, 2007) and under normal conditions caveolin-coated invaginations are quite stable structures at the plasma membrane that are not involved in endocytosis to a significant degree (Sandvig et al., 2008). Early electron microscopical examinations led to the assumption that these coated buds are the most abundant CI endocytic structures and the main CI entry route in cells. In some tissues the caveolin-coated invaginations can constitute approximately one third of the plasma membrane area, but only 2 %

of the coated vesicles become detached from the membrane per minute (Kirkham and Parton, 2005). For comparison, it takes only 50-150 seconds for a clathrin-coated vesicle to assemble and to become detached from the membrane (Ungewickell and Hinrichsen, 2007).

The flask shaped, small invaginations are called caveolae (from Latin [caveola] - *little cave*), have a diameter of 50-80 nm, and are named by caveolin-1, a member of the caveolin protein family. Caveolin-1 is enriched in caveolae with about 100-200 molecules per caveolae (Pelkmans and Zerial, 2005) and is able to form oligomers and to bind cholesterol and fatty acids, which stabilises oligomer formation (Monier et al., 1996). Consistently, caveolae were shown to be enriched in signalling proteins, sphingolipids, cholesterol, and clustered glycosyl-phosphatidylinositol (GPI)-anchored proteins. It was proposed that the coated buds serve as fixed containers and their internalisation can be stimulated under certain conditions or in the presence of specific adaptors (Tagawa et al., 2005). For instance, it is exploited by bacterial toxins and by viruses, such as Simian virus 40 and Echo 1 (Marsh and Helenius, 2006). However, no cell physiological cargo has been definitely identified yet. Indeed, albumin is taken up by this route in endothelial cells (Minshall et al., 2002), whereas in Chinese hamster ovary cells it is internalised by the RhoA-regulated pathway (Cheng et al., 2006), which is another CI and dynamin-dependent pathway and described in the following clause.

Possibly, the uptake of EGF receptors can be related to caveolae-mediated endocytosis. The receptors are recruited by a protein based mechanism via three proteins with ubiquitin interacting motifs: EPS15-related, EPS15, and epsin. An inhibition was only observed when all three proteins were knocked out in small interfering RNA-studies. Therefore, the proteins are suggested to be redundant in their functions for the recruitment of EGF receptors (Sigismund et al., 2005). Great care should be taken to interpret these results, because the three proteins are also heavily implicated in clathrin-mediated endocytosis (Doherty and McMahon, 2009) and a modulation of these proteins will most likely influence both pathways. Another interesting example is the uptake of glycosphingolipids. Only fluorescent analogues with a specific stereochemistry are endocytosed by the caveolae-mediated pathway, whereas analogues with a different chirality and non-natural analogues are internalised by other routes (Singh et al., 2006).

Up to now, two mechanism has been proposed to likely play a role in the generation of membrane curvature. First, the insertion of caveolin-1 into the invaginating membranes. Caveolin-1 forms a hairpin structure, that is embedded into the membrane, and

complexes composed of 14-16 monomers (Sargiacomo et al., 1995). Membrane bending is thought to be supported through this structure, which could reach through the inner leaflet into the outer monolayer, and the oligomerisation (Parton et al., 2006). By stretching through the two membrane layers it could also contribute to the necessary cross talk across the membrane (Doherty and McMahon, 2009). The second hypothesis was suggested by Sarasij et al. (2007). Due to the enrichment of raft constituents in caveolae and their specific chirality as well as intrinsic tilt, the membrane properties alone could be sufficient to induce membrane curvature. This suggestion is supported by the findings of Singh et al. (2006) that only fluorescent glycosphingolipids with a specific chirality are endocytosed by the caveolae-mediated pathway.

Other possible functions of caveolae, such as regulation of fatty acids and mechanosensing, are reviewed by Parton and Simons (2007), who suggest that the high ability of caveolae to respond to changes of the plasma membrane is due to their specialised lipid composition and biophysical properties. In addition to these functions, caveolae are proposed to have another putative role: the storage of excess surface area (Doherty and McMahon, 2009). As caveolae can undergo *kiss-and-run* fusion and fission with and from the plasma membrane (Pelkmans and Zerial, 2005), the flattening of caveolae invaginations would rapidly alter the surface area of monolayers and could thereby compensate temporary lateral tensions and/or contribute to the lateral elasticity of the plasma membrane, which is very limited (see clause 1.1). Consistent with this proposal, caveolae are enriched in cell types that are most exposed to physiological stretch and shear.

RhoA-Regulated Endocytosis (Dynamin-Dependent)

Dynamin-dependent RhoA-regulated endocytosis was identified as a specific CI pathway when the β-chain uptake of the interleukin 2 receptor (IL2Rβ) was investigated (Lamaze et al., 2001). The IL2Rβ receptor was found in DRM that are associated with CI endocytic processes and its uptake was inhibited in cells expressing mutants of dynamin and RhoA. Here, γc-cytokine is known to be a particular cargo. Its receptor is suggested to have a specific internalisation sequence at the cytoplasmic tail (Birkle et al., 2003), which would relate the recruitment to the protein based mechanisms. On the other hand, SM seems to be necessary for the recruitment of RhoA to the plasma membrane (Cheng et al., 2006), which suggests a combined mechanism. The small GTPase RhoA holds a central role in the regulation of actin cytoskeleton dynamics and could therefore

be required to recruit the actin machinery to this CI route. However, other accessory proteins and adaptors are not known yet and remain to be discovered.

Cdc42- and Arf6-Regulated Endocytosis (Dynamin-Independent)

The two as yet identified CI and dynamin-independent endocytic pathways share as common feature the participation of small GTPases, either the Rho family member Cdc42 or the Arf family member Arf6.

Cdc42-regulated endocytosis is the main route for the clathrin- and caveolae-independent uptake of cholera toxin B and the plant protein ricin and has been shown to be responsible for the major part of fluid phase internalisation in cells (Kalia et al., 2006). In contrast to the small and spherical budding structures in clathrin- and caveolae-mediated pathways, the budding morphologies of this route show comparably long and wide membrane invaginations with a tubular diameter around 40 nm (see Fig. 1.2). Compared to other pathways, along with the endocytic cargoes, a relatively large volume of fluid phase is therefore taken up in a single budding event. Here, the selection of cargoes is proposed to be an example for lipid based mechanisms. Native, nanoscale clustering of GPI-anchored proteins with cholesterol led to the internalisation of these domains by the Cdc42-regulated route, whereas artificial crosslinking directs the GPI-anchored proteins to other CI endocytic pathways (Sharma et al., 2004). Chadda et al. (2007) have shown that the activation of Cdc42 is sensitive to cholesterol and coupled to the actin polymerisation machinery, which suggests the implication of actin in the formation of the budding structures or the final fission of vesicles. Recently, an implication of the BAR domain containing protein Graf1 was suggested (Lundmark et al., 2008a). Upon localising PI(4,5)P_2-enriched, tubular, and punctate lipid structures, it sculpts the tubular membranes of the long invaginations and could thereby support membrane curvature or fission of the invaginations.

The role of the GTP-binding Arf family member Arf6 in CI endocytic events is not yet established, but **Arf6-regulated endocytosis** has been suggested to be responsible for the uptake of several proteins, such as β1-integrin, carboxypeptidase E (CPE), and also GPI-anchored proteins. The cytoplasmic tail sequence of CPE enables binding to Arf6, which would categorise the cargo recruitment of this pathway into protein based mechanisms. This can be supported by the studies of Gong et al. (2007), who found a new class of trafficking motifs. Membrane proteins containing these motifs are suggested

to prevent their uptake and/or facilitate their recycling via Arf6-regulated endocytosis by enhancing their association with the Arf6-specific guanine nucleotide exchange factor Efa6. Furthermore, Arf6 is known to be involved in the remodelling of actin, in the activation of phosphoinositide-kinases which stimulates the local concentration of $PI(4,5)P_2$ (see 1.2.1), in the complex formation with AP-2 and the heavy chain of clathrin (Poupart et al., 2007), and even in the regulation of clathrin-mediated endocytosis in certain cell types (Houndolo et al., 2005). Recently, it was also suggested that the GTP-loaded Arf6, which is the active form, can generate membrane curvature by the insertion of an amphiphatic helix into the proximal lipid monolayer, such as epsin (Lundmark et al., 2008b).

Since GPI-anchored proteins are endocytosed by both, the Cdc42- and the Arf6-regulated route, and actin appears to be involved in both routes, it remains to be determined whether these pathways are distinct mechanisms of CI endocytosis or related and the two GTPases have distinct roles in the same pathway. Probably, the multiple roles of Arf6 in endocytic mechanisms demonstrate a complex role of this small GTPase in the regulation of various endocytic pathways.

In conclusion, generation of bended plasma membranes, which is essential for endocytic processes, is most likely achieved by an interplay of different mechanisms to induce membrane curvature (Graham and Kozlov, 2010). Notably, all the different endocytic pathways that are described above seem to have at least one mechanism of curvature generation in common: formation of curvature by an increase of monolayer surface area. As outlined in the description of the different endocytic pathways, this surface area increase of one of the two monolayers composing the plasma membrane is gained by the insertion of helices or other special protein structures into the plasma membrane leaflet. Upon incorporation of these structures into the plasma membrane, the protein-proximal monolayer is increased relatively to the other leaflet. For instance, clathrin and other adaptor proteins of clathrin-mediated endocytosis interact with epsin and N-BAR domain containing proteins which have the ability to induce curvature by inserting amphipathic helices (e.g. Ford et al., 2002). For caveolae-mediated endocytosis it was proposed that the incorporation of hairpin structures of caveolin-1 plays a role in the generation of curvature (Parton et al., 2006). Moreover, the active form of Arf6 was suggested to mediate membrane bending in the Arf6-regulated pathway by the insertion of an amphipathic helix into the membrane (Lundmark et al., 2008b). In other words,

proteins were already shown to generate membrane bending in endocytosis by causing a difference between the surface areas of the two monolayers. Theoretically, differences between the surface areas leading to membrane curvature could also be achieved by the incorporation of other membrane constituents, for instance membrane lipids. The investigation of this hypothesis and the potential influence of differences in the monolayer surfaces areas related to leaflet specific modulations of lipid composition is the subject of the present study. The following clauses therefore describe various mechanisms leading to membrane bending with particular emphasis laid on the formation of curvature by the transversal lipid asymmetry of the plasma membrane.

1.3 Bending a Membrane

A crucial moment in the initial phase of endocytosis is the bending of a comparatively flat plasma membrane to generate the high curvature necessary for endocytic invaginations. There are several mechanisms to induce temporary high curvature that can be divided principally into two categories: curvature is either achieved by the interplay between proteins and lipids or by leaflet specific changes in the lipid composition of the membrane (Kozlov, 2010). Proteins can interact in various ways with membranes to generate curvature, such as scaffolding by peripheral membrane proteins, e.g. dynamin (see 1.2.1), or active helix insertion into membranes, e.g. epsin (see 1.2.1). These mechanisms are extensively reviewed in McMahon and Gallop (2005) as well as in Zimmerberg and Kozlov (2006) and a very nice summary of the actual knowledge can be found in Powell (2009). For the later mechanism of active helix insertion, the effectiveness of spontaneous membrane curvature caused by hydrophobic insertion of different helices was characterised in theoretical predictions and it was evaluated that inclusions shaped like shallow rods are very efficacious in membrane shaping (Campelo et al., 2008). The interaction of proteins bending membranes by insertion of their amphipathic helices is dependent on the lipid composition of the respective membrane area (Drin and Antonny, 2009). Thus, particular curvature generating proteins can be recruited to specific endocytic pathways due to different lipid compositions of endocytic buds or vesicles. Curvature generating or sensing proteins, that are known to be involved in endocytic pathways, are reviewed in Lundmark and Carlsson (2010) and are summarised in the respective clause of the present study (see 1.2.1 and 1.2.2). Here, the description will focus on curvature generation of membranes induced by alterations of the lipid composition.

As mentioned in 1.1.1, the size of fatty acid chains relative to the headgroup determines the molecular shape of a specific lipid. In cone shaped lipids, the fatty acid chains dominate in size over the headgroup, which is the case for PE (Cullis and de Kruijff, 1979). The headgroup is similar in size to the fatty acid chains in cylindrical lipids, such as in PC and PS, while the headgroup is larger than the fatty acid chains in inverted cone shaped lipids, for instance in lysolipids and, to some extent, in SM. Due to this molecular shape of lipids, curvature can be generated when cone shaped lipids, such as PE, dominate the convex side and inverted cone shaped lipids, such as lysolipids, govern the concave side of a curved bilayer.

In addition, membrane curvature can be induced by a difference between the surface areas of the two monolayers caused by leaflet specific changes of lipid composition, which will be referred to as monolayer area asymmetry (Devaux, 2000). This constitutes the mechanism of the well established bilayer couple model introduced by Sheetz and Singer (1974). Upon insertion of additional molecules in one of the bilayer leaflets, spectacular shape changes in membranes of red blood cells were observed. Further experimental verification of this model was performed in biological as well as in model systems. Sune and Bienvenue (1988) showed that addition of phospholipids led to a considerable change in the initial shape of platelets from a discoid form to a smaller body with very long pseudopods. In giant unilamellar vesicles (GUV) of pure lipid membranes the creation of small area differences between the vesicle monolayers was sufficient to drive vesicle shape changes, which had a character of budding invaginations (Farge and Devaux, 1992; Lopez-Montero et al., 2005; Papadopulos et al., 2007). The structural difference of the resulting shape changes can be explained by the existence of intracellular structures, such as the cytoskeleton, which provide an increase of the bilayer lateral tension (Devaux et al., 2008).

1.3.1 Shape Changes of GUV Induced by Lipid Asymmetry

Theoretical foundations for shape changes in vesicles or cells were already suggested in 1970 by Canham, who demonstrated that the biconcave shape of human red blood cells coincides with a minimum value of membrane bending energy (Canham, 1970). Correspondingly, two different models for the generation of curvature were proposed: the bilayer couple model introduced by Sheetz and Singer (1974) as mentioned above, and later on the spontaneous curvature model introduced by Deuling and Helfrich (1976). In

1991 these two models were compared by Udo Seifert and coworkers, who theoretically predicted the shape transformations of pure lipid bilayers by determining the phase diagram for each of the two models. For the bilayer couple model, they found an extreme sensitivity to an asymmetry in the monolayer area. This sensitivity could be supported in various experimental studies by using different ways to alter the monolayer area in giant liposomes. For instance, Sackmann et al. (1986) varied the temperature and observed a sequence of shape changes, which were explained by a small asymmetry in the thermal expansivities of the two monolayers. Alternatively, area differences between the two leaflets can be achieved by the manipulation of phospholipids in each monolayer. Farge and Devaux (1992) used two different procedures for this purpose: either a small quantity of egg phosphatidylglycerol was redistributed through the bilayer by means of a pH gradient or lyso-phosphatidylcholine was added or removed from the external leaflet of GUV. The experiments confirmed the general nature of the bilayer couple model by generating important shape changes of nonspherical GUV due to a redistribution of lipids as well as an addition or depletion of lipids from one monolayer.

In another study the external monolayer area of GUV was altered by the addition of ceramides comprising different acyl chains, which triggered shape changes from prolate to pear shape vesicles (Lopez-Montero et al., 2005). Additionally to the generation of curvature by the creation of area differences between vesicle monolayers, it could be shown by Papadopulos et al. (2007) that triggered shape transitions are reversible in the presence of translocator proteins that allow lipids to redistribute between the two membrane leaflets. In this study, the formation of a bud-like structure, which was induced by a very small excess of lipid in the outer monolayer, was stable under conditions of negligible flip-flop. Upon reconstitution of the energy independent flippase activity of the yeast endoplasmic reticulum into GUV, the initial bud formation was shown to be reversible, and the prolate shape was recovered. This was ascribed to a rapid flip-flop leading to relaxation of the monolayer area difference.

These studies with artificial systems, in which the generation of monolayer area asymmetry in unilamellar vesicles is controllable, are very helpful in understanding the physical properties of a membrane necessary for effective membrane bending. However, the size and number of the obtained budding invaginations in GUV is rather different to vesicles in living cells, for instance endocytic vesicles. In all of the above mentioned studies only one bud per liposome could be obtained and the bud size was not more than one order of magnitude smaller than the size of the initial vesicle. Recently, it was

shown in a theoretical consideration that lateral tension is required to cause vesiculation comparable to the building of intracellular transport vesicles (Devaux et al., 2008). Considering a closed membrane subjected to lateral tension and a difference in the monolayer spontaneous areas, the results of the analysis predicted the existence of three different vesiculation regimes: one regime with no vesicle formation, a single vesicle regime, and a multiple vesicle regime. The respective phase diagram demonstrated that the larger the tension, the larger monolayer area asymmetry is needed to generate a vesicle. The model also predicted that in the absence of lateral tension the monolayer area asymmetry can only generate a single vesicle, while application of sufficient asymmetry in the presence of a low lateral tension results practically always in the generation of multiple vesicles. Thus, this theory supports the hypothesis that a difference between the two monolayer areas composing a membrane, which is under lateral tension as it is the case for biological membranes, is sufficient for the formation of multiple, small vesicles.

1.3.2 How Endocytosis is Linked to Lipid Asymmetry

On the basis of the above described mechanism to induce membrane curvature, it was proposed that APLT account for monolayer area asymmetry as an early step in endocytosis. Upon the translocation of lipids from the exoplasmic leaflet to the cytoplasmic layer of the plasma membrane, APLT can mediate an increase of the inner surface area and thereby support the generation of membrane curvature during endocytosis. First mentioned by Devaux (1991), this hypothesis was supported in several studies and by now it seems commonly accepted that APLT are involved in endocytosis (Pomorski and Menon, 2006; Puts and Holthuis, 2009; Muthusamy et al., 2009; Graham and Kozlov, 2010). Studies supporting this hypothesis will be discussed in the following.

Already in 1994, it was shown that the incorporation of phospholipid analogues into the plasma membrane of human erythrocyte ghosts affected the ATP-induced vesiculation (Muller et al., 1994). Erythrocyte ghosts were incubated in the presence of ATP at 37 °C and the percentage of the total membrane taken in as vesicles was quantified by determining the loss of acetyl-cholinesterase activity after definite times. The addition of spin labelled PC or SM, which remain preferentially in the outer leaflet of the membrane, to ATP containing erythrocyte ghosts inhibited the formation of so called endocytic vesiculation immediately after the addition and vesiculation remained reduced in further incubation for about 40 minutes at 37 °C. Interestingly, the addition of spin

labelled PS, a substrate of APLT, also reduced the vesiculation directly after addition, but subsequent incubation for about 20 minutes at 37 °C abolished suppression of vesiculation reaching approximately the extend of the control after 60 minutes. The decrease of vesiculation immediately after the addition as well as the increasing kinetics after further incubations were dependent on the amount of analogue added. Further investigations of kinetics of redistribution of phospholipid analogues in the plasma membrane by using a back exchange assay showed that the enhancement of vesiculation after the addition of spin labelled PS was comparable to the kinetics of inward translocation of spin labelled PS mediated by APLT. Approximately 40 % of the analogue was translocated to the inner layer within 30 minutes at 37 °C. Thus, it was obtained that the incorporation of phospholipids in the outer layer of the plasma membrane inhibited endocytic-like processes while the redistribution of phospholipid analogues from the outer to the inner leaflet restored the activity of vesiculation, which supports the hypothesis of the implication of APLT in endocytosis. More recently, it was shown in several studies that APLT are required for vesicle formation in yeast cells. Yeast lacking the plasma membrane associated P_4-ATPases Dnf1p and Dnf2p displayed an abolished ATP-dependent transport of fluorescently labelled phospholipids from the outer to the inner plasma membrane leaflet (Pomorski et al., 2003). The loss of Dnf1p and Dnf2p also caused an exposure of endogenous PE to the outer leaflet which was twofold higher than in wild type cells. Furthermore, activity of bulk flow and receptor-mediated endocytosis in yeast cells with genomic deletions of Dnf1p, Dnf2p, and Drs2p (ATPase II homolog in the yeast Golgi) was investigated in this study. When cells were stained with a marker for bulk flow endocytosis, the internalisation and delivery to the vacuole of the marker was essentially inhibited in the triple mutant. Likewise, the uptake of a specific factor to follow receptor-mediated endocytosis was greatly reduced in cells lacking all three translocators. Collectively, these results were indicating that a loss of Dnf1p, Dnf2p, and Drs2p caused a general defect in the internalisation step of endocytosis.

In agreement with these findings, other studies of lipid translocators in yeast cells determined that inactivation of P_4-ATPase Drs2p rapidly inhibited translocation of fluorescently labelled PS and lowered the formation of vesicles (Graham, 2004), and the loss of the P_4-ATPases Drs2p and Dnf3p disrupted aminophospholipid translocation and asymmetry in post-Golgi secretory vesicles (Alder-Baerens et al., 2006). Furthermore, crucial roles for P_4-ATPases in vesicular transport have also been found recently in *Arabidopsis thaliana*, *Caenorhabditis elegans* and cultured mammalian cells. The P_4-

ATPase subfamily member ALA3 in *Arabidopsis thaliana* was shown to be required for the characteristic trans-Golgi proliferation of slime vesicles containing polysaccharides and enzymes for secretion (Poulsen et al., 2008), the *Caenorhabditis elegans* Drs2p homologue TAT-1 is required for yolk uptake in oocytes and an early step of fluid phase endocytosis in the intestine (Ruaud et al., 2009), and the novel murine P_4-ATPase FetA was shown to participate in the formation of acrosomes that involves intracellular vesicle formation and fusion (Xu et al., 2009).

In addition to this, endocytosis of eukaryotic cells was shown to be influenced by area changes of the membrane leaflets which were achieved with modifications of the lipid compositions. By treating macrophages and CHO cells with exogenous sphingomyelinase, endocytosis was shown to be activated and this was suggested to be on account of the reduction of crowding of SM in the outer leaflet and flipping of the produced ceramide across the bilayer (Zha et al., 1998). This prediction is supported by a later study which implies that the asymmetric formation of ceramide on the cytosolic leaflet of endosomes mediates the generation of membrane curvature (Trajkovic et al., 2008). Moreover, endocytic activity of a different cell line was shown to be accelerated by the addition of exogenous lipids actively transported from the exoplasmic to the cytoplasmic leaflet (Farge et al., 1999). Erythroleukemia K562 cells are derived from human erythroblasts, a precursor of erythrocytes, and have a high activity of APLT (Cribier et al., 1993). To study the influence of altered area relation of the plasma membrane on endocytic activity, Farge and collaborators added various exogenous lipids to K562 cells. By the direct addition of short chain lipids, which have a sufficient water solubility, to the cells in suspension, the lipids were incorporated into and, depending on the lipid species, subsequently translocated across the plasma membrane. When K562 cells were incubated with C_6-PS or C_6-PE, aminophospholipids with six carbons at the second chain which are translocated by APLT, an enhancement of endocytic activity was obtained. For C_6-PS, it was found that this stimulation increased with the amount of added lipids. In contrast, the addition of lyso-PS or poly(ethylene)$_{50}$-glycol-cholesterol, lipids that are known to remain on the outer layer, caused a partial inhibition of endocytic activity. These results were explained by the changes of surface area relation in the plasma membrane due to the addition of exogenous lipids.

Currently, two models have been suggested to explain the implication of APLT in endocytosis (Puts and Holthuis, 2009). In the first model P_4-ATPases are thought to support the recruitment of the vesicle budding machinery to the plasma membrane through

protein-protein interactions and/or by increasing the concentration of specific lipids in the cytoplasmic leaflet. The hypothesis of recruitment by protein-protein interactions is supported by the observation of Chantalat et al. (2004): the yeast P_4-ATPase Drs2p directly interacts with Gea2p, an Arf activator, that regulates recruitment of Arf, adaptor protein-1, and clathrin network proteins to trans-Golgi membranes. More recently, it was shown that Drs2p acts independently of coat recruitment to facilitate clathrin-dependent vesicle budding from the trans-Golgi network (Liu et al., 2008). However, these data indicate that, in absence of Drs2p, the recruitment of accessory proteins to the membrane would not result in the formation of clathrin-coated vesicles. This underlines the general assumption of interaction of P_4-ATPases with endocytic regulators.

The second model is based on a more direct and mechanical role in the formation of invaginations: the generation of membrane area asymmetry as outlined above. Upon translocating lipids from the exoplasmic to the cytoplasmic leaflet of the plasma membrane, the translocators create an imbalance in the surface areas of the two monolayers which leads to bending of the membrane (see above for examples). The specific activation or boost of activation of APLT in membrane areas, where endocytic invaginations need to be induced, could be provided by protein-protein interactions of APLT with regulatory proteins as part of endocytic pathways. For instance, it was shown that RhoA, a small GTPase holding a central role in the clathrin-independent RhoA-regulated endocytic pathway (cf. 1.2.2), is involved in the regulation of the localisation of Na^+/K^+-ATPase in the plasma membrane of epithelial cells (Maeda et al., 2002). By microinjection of the constitutively active mutant of RhoA, the Na^+/K^+-ATPase was translocated to the spike-like protrusions over the apical surfaces. Supporting these findings, in a later study it was determined that activation of RhoA is necessary for the endocytosis of Na^+/K^+-ATPases in cells exposed to hypoxia (Dada et al., 2007). Similar to Na^+/K^+-ATPases, P_4-ATPases are activated by specific subunits (Puts and Holthuis, 2009). Interestingly, Cdc50 proteins, chaperones of P_4-ATPases, are strikingly reminiscent of the β-subunit of the Na^+/K^+-ATPase. Therefore, it is conceivable that P_4-ATPases interact in a comparable way with regulatory proteins of endocytic pathways. This hypothesis is supported by the recent findings that Cdc50p is required for the APLT activity of purified and reconstituted Drs2p (Zhou and Graham, 2009) and that three potential binding partners of Drs2p are involved in phosphoinositide metabolism (Puts et al., 2010). Thus, interaction between Drs2p and a phosphatidylinositol-4-phosphatase, that is required for efficient recruitment of the vesicle budding machinery, could link APLT activity to

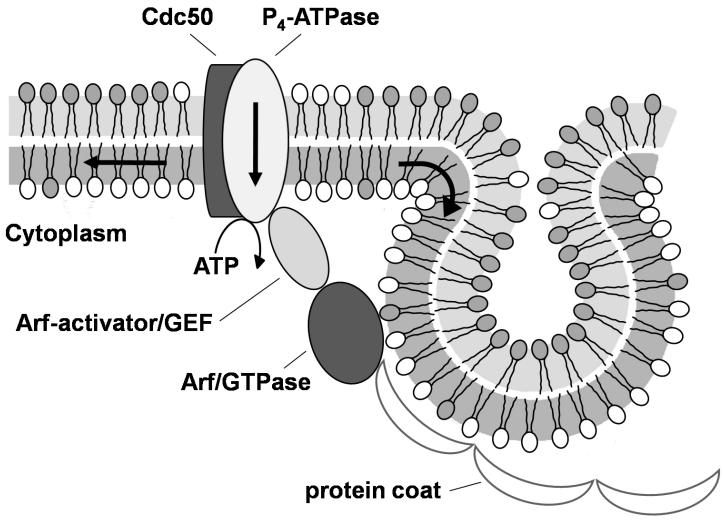

Figure 1.5: Suggested role of P_4-ATPases in the formation of endocytic invaginations. The model is based on the mechanical role of P_4-ATPases in the formation of vesicles. Upon translocating lipids from the exoplasmic to the cytoplasmic leaflet of the plasma membrane, the proteins generate a difference of the monolayer area asymmetry which induces membrane curvature. Additionally or alternatively P_4-ATPases are thought to support the recruitment of the vesicle budding machinery to the plasma membrane by interacting directly and/or in an indirect way via subunits with endocytic regulators. Figure based on Puts and Holthuis (2009, Fig. 3).

coat recruitment for the formation of secretory vesicles. Furthermore, family members of the P_4-ATPases were found to interact with cytoplasmic proteins, such as guanine nucleotide exchange factors (GEF) and small GTPases (Chen et al., 1999; Wicky et al., 2004), that are crucial for the recruitment of coat proteins in endocytic pathways (see 1.2.1 and 1.2.2). This may lead to the recruitment of endocytic accessory proteins to sites of ATPase-dependent phospholipid translocation. Figure 1.5 illustrates the potential role of P_4-ATPases in the formation of endocytic invaginations as suggested by the two models.

Summarising the role of lipid asymmetry in the generation of membrane invaginations during endocytosis, it can be concluded that monolayer area asymmetry can induce spectacular shape changes in biological as well as in pure lipid membranes. Furthermore, ATP-dependent specific flippases can alter the monolayer area difference of the plasma membrane and use ATP for this purpose. Additionally, there are several studies that support the hypothesis of an involvement of flippases in endocytosis, but this awaits further experimental confirmation.

CHAPTER 2

Aim

To date, the most efforts to elucidate endocytic mechanisms have focused on proteins and also the generation of membrane curvature, necessary for endocytic invaginations, has mainly been explained by proteins that can induce and stabilise curvature. The role of lipids and the properties of the membrane, which needs to be bended, has been largely pursued with less attention. In this regard, role of lipids may have been underestimated. Transversal lipid asymmetry of the plasma membrane seems to play an important role in endocytosis as stimulation of the aminophospholipid translocase, responsible for the inward transport of aminophospholipids, provokes endocytic like vesicles in erythrocytes and enhances endocytosis in K562 cells.

Therefore, the present study aimes at investigating the influence of plasma membrane structural properties on endocytosis. The transversal asymmetry of the plasma membrane and the insertion of exogenous lipids provide an easy tool to induce differences in the monolayer area asymmetry of the plasma membrane, which can generate membrane curvature. Lipids with a relatively high solubility in water, for example phospholipids with one long and one short chain, e.g. six carbons, insert spontaneously into a membrane because such amphiphiles nevertheless prefer the hydrophobic environment constituted by a membrane. Changes in the endocytic activity of cells can be distinctly quantified with a spectrofluorometric assay as presented by Farge et al. (1999). This assay monitors the activity of bulk flow endocytosis due to the pH sensitivity of a specific fluorophor linked to surface proteins of cells and the acidification of early endosomes. Farge and

collaborators could qualitatively show the stimulation of bulk flow endocytosis in K562 cells by the addition of exogenous short chain PS and PE as well as the partial inhibition by the application of lyso-PS and cholesterol derivatives.

As a first step in this thesis, the experiments of Farge et al. (1999) are repeated with various exogenous lipids intending to distinctly quantify the change of bulk flow endocytic activity by the percentage of added lipids, thereby also improving the used assay. In addition, the influence of various exogenous lipids on specific receptor-mediated pathways of endocytosis in K562 cells as well as in other cell lines has been investigated. A very feasible technique to quantify receptor-mediated endocytosis is flow cytometry, because properties of single cells can be analysed.

As a variety of cell lines and not only bulk flow but also receptor-mediated endocytosis is examined, the investigations of this study can confirm the proposed influence of lipid asymmetry on endocytosis and reveal new insights of this influence on specific endocytic pathways.

CHAPTER 3

Material and Methods

3.1 Material

3.1.1 Chemical Material

The unlabelled short chain diacyl glycerophospholipids 1-stearoyl-2-hexanoyl-sn-glycero-3-phosphocholine (C_6-PC), -L-serine (C_6-PS), and -ethanolamine (C_6-PE) as well as the unlabelled short chain di-alkyl glycerophospholipid 1-O-octadecyl-2-hexanoyl-sn-glycero-3-phospho-L-serine (dialkyl-C_6-PS) were kindly synthesised by Fabrice Giusti (Institut de Biologie Physico-Chimique, Paris, France) following previously described protocols (Joseph et al., 1991; Fellmann et al., 1994, 2000). 1,2-dilauroyl-sn-glycero-3-phospho-L-serine (DLPS), glycerophospholipids with a (7-nitro-2-1,3-benzoxadiazol-4-yl)amino (NBD)-group on the C_6-chain (C_6-NBD-PC, -PS, and -PE), and 1-palmitoyl-2-hydroxy-sn-glycero-3-phosphocholine (lyso-PC) were obtained from Avanti Polar Lipids (Alabaster, AL, USA). Succinimidyl-6-(biotinamido)-hexanoate (sulfo-NHS-LC-biotin) and streptavidin linked to fluorescein isothiocyanate (streptavidin-FITC) were purchased from Perbio Science (Frankfurt, Germany), Hepes and chlorpromazine (CPZ) were from Sigma-Aldrich (Taufkirchen, Germany). Transferrin from human serum conjugated to tetramethyl-6-rhodamine (Tf-TMR), FITC (Tf-FITC), or Alexa 488 (Tf-A488) was obtained from Invitrogen (Karlsruhe, Germany). Dulbecco's modified phosphate buffered saline with or without Mg^{2+} and Ca^{2+} (DPBS / DPBS$^-$), Hanks' balanced salt solution (HBSS), Leibovitz L-15 medium (L-15), Roswell Park Memorial Institute medium 1640

with or without phenolred (RPMI 1640 / RPMI 1640$^-$), and Dulbecco's modified Eagle medium with or without phenolred (DMEM / DMEM$^-$) came by PAN Biotech (Aidenbach, Germany), foetal bovine serum (FBS) was ordered from Invitrogen (Karlsruhe, Germany).

3.1.2 Cell Lines

K562 cells, a human erythroleukemia cell line with a high activity of aminophospholipid translocases (Cribier et al., 1993), were propagated in suspension in RPMI 1640 decomplemented with 10 % FBS and 2 mM L-glutamine. The Baby hamster kidney cell line derivative BHK-21-tTA clathrin heavy chain/antisense (BHKasc), kindly provided by Kirsten Sandvig (Institute for Cancer Research at the Norwegian Radium Hospital, Montebello), was grown as adherent monolayer culture in DMEM mixed one to one with L-15 supplemented with 10 % FBS, 2 mM L-glutamine, 20 μg/ml tetracycline (TET), 0.5 μg/ml puromycin, and 200 μg/ml geneticin. For induction of clathrin heavy chain antisense RNA expression, TET was removed from the medium (Iversen et al., 2001, 2003). The human negroid cervix carcinoma cell line Hep2, a HeLa cell derivative, was a kind donation from Nathalie Sauvonnet (Pasteur Institute, Paris, France) and cultured in DMEM supplemented with 10 % FBS, and 2 mM L-glutamine. All cell lines were maintained in 25 cm^2 or 75 cm^2 plastic cell culture flasks at 37 °C and 5 % CO_2 and routinely passaged every three to four days. By dilution, cell density was kept below 80 % confluency for the adherent cell lines and below 1×10^6 cells/ml for the suspension cell line.

3.2 Spectrofluorometry of Bulk Flow Endocytosis

The activity of bulk flow endocytosis of cells can precisely be investigated with a spectrofluorometric assay, that is based on the pH sensitivity of fluorescein isothiocyanate (FITC) and more quantitative than e.g. microscopic assays. In other words, bulk flow endocytic activity examined with this assay reflects activity of all endocytic events leading from the plasma membrane to acidified inner cell compartments. First measurements were mainly done as described by Farge et al. (1999). For the improvement of this assay, the order of cell incubation with exogenous lipids and FITC labelling of cells was modified as explicitly described in the following clauses.

3.2.1 Preparation of Cells

K562 cells were cultured in suspension to a density of 1×10^6 cells/ml. The desired volume of cell suspension was withdrawn, centrifuged (200×g, 5 min, 37 °C) and washed with DPBS. When BHKasc cells still undergoing clathrin-mediated endocytosis were analysed, all media and buffers were supplemented with 20 μg/ml TET (BHKasc$^+$). For induction of clathrin heavy chain antisense RNA expression TET was removed from growth medium 18 to 20 h before the experiment was started and all ensuing media and buffers were lacking TET (BHKasc$^-$). Adherent BHKasc cells were grown to 80 % confluency, washed with DPBS and harvested with DPBS$^-$ supplemented with 2 mM EDTA followed by a washing step with DPBS (200×g, 5 min, 37 °C). When cells were first incubated with exogenous lipids and afterwards labelled with FITC as originally designed by Farge et al. (1999), the resulting cell pellet was resuspended in HBSS to a final cell concentration of 1×10^5 cells/ml. The incubation of cells with various exogenous lipids was performed as described in the following clause. For the improvement of this assay the sequence was inverted: the cell pellet was resuspended in cold HBSS to a final concentration of 4×10^7 cells/ml and cell surface proteins were directly labelled with FITC as defined in 3.2.3.

3.2.2 Incubation with Exogenous Lipids

Stock solutions of phospholipids were stored at -20 °C in chloroform/methanol (1/1) or chloroform. Aliquots of the desired lipids were transferred into glass tubes and dried under a stream of nitrogen. The dried lipids were solubilised by a small quantity of ethanol. Subsequently, HBSS was added, yielding a maximum final ethanol concentration of 1 % and a total lipid concentration of 2 μM. To obtain multilamellar vesicles (MLV), lipid suspensions were vortexed vigorously for at least 30 s. In case of short chain lipids, MLV were then sonicated using a bath sonicator Sonorex Super (BANDELIN electronic, Berlin, Germany) for 10 min to completely solubilise the lipids. At the used concentrations, short chain phospholipids incorporate spontaneously into the outer layer of the plasma membrane bilayer (Cribier et al., 1993). To incorporate long chain lipids into the plasma membrane, a previously described protocol was followed (Daleke and Huestis, 1989). Briefly, small unilamellar vesicles were prepared by sonification of MLV with a Branson sonifier 250 (Danbury, CT, USA; duty cycle 70 %, output control 4) until suspensions became opalescent, usually for 20 min. During this process lipid samples

were tempered to 30 °C using a waterbath to keep suspensions above the transition temperature of gel-to-liquid crystalline phase. The percentage of added lipids was related to the total phospholipid amount of the plasma membrane of cells: 1×10^6 cells contain about 150 nmol phospholipids and about 10 % of this amount is distributed in the plasma membrane. This corresponds to the percentage evaluated by measuring the line width broadening due to spin-spin interactions (Marsh and Smith, 1973). In the original order of the assay this lipid solution was then added to the cell suspension (1×10^5 cells/ml) followed by an incubation for either 15 min or 30 min at 37 °C. This incubation allowed the lipids to be incorporated into and, depending on the lipid species, translocated across the plasma membrane. Upon halting endocytosis by cooling the cells to 4 °C the cell surface proteins were then unspecifically labelled with FITC as outlined in 3.2.3. When cells were first labelled with FITC before incubating with exogenous lipids, the prepared lipid solution was cooled down on ice. At definite time intervals before the spectrofluorometric measurements were started the lipids were added to the cell suspension. Unless otherwise noted, the incubation of cells with lipids was for 1 min on ice. Finally, the endocytic activity of bulk flow endocytosis was monitored as described in 3.2.4.

3.2.3 Biotinylation and FITC Labelling

All further steps were performed on ice using ice cold buffers and solutions. In order to unspecifically biotinylate the cell surface proteins, a final concentration of either 45 μg, as recommended by Perbio Science, or 240 μg, as applied by Farge et al. (1999), sulfo-NHS-LC-biotin per 1×10^6 cells was added to the cell suspension followed by an incubation for 30 min on ice. After washing (200×g, 5 min, 4 °C) and resuspending the cells in cold HBSS the biotinylated cells were incubated with a final concentration of either 10 μg/ml, as recommended by Perbio Science, or 15 μg/ml, as applied by Farge et al. (1999), streptavidin-FITC for another 30 min on ice and then again washed with cold HBSS. During all further incubations samples were always kept in the dark to avoid bleaching of the fluorophores. When cells were already incubated with exogenous lipids, as done in the original order, the resulting pellet of FITC labelled cells was finally resuspended in a volume of 350 μl cold HBSS and the activity of bulk endocytosis was measured as defined in 3.2.4. In the order following the improved assay, FITC labelled cells were resuspended in HBSS to a final concentration of 1×10^6 cells/ml and incubated with exogenous lipids as described in 3.2.2.

3.2.4 Spectrofluorometric Measurements

BFEA of FITC labelled cells, incubated with or without (control) exogenous lipids, could be monitored by spectrofluorimetry due to the pH sensitivity of FITC. Acidification of the early endocytic vesicles led to a decrease of the FITC signal as a function of time. All experiments were carried out using a SLM-AMINCO Series 2 fluorescence spectrometer (AMINCO-Bowman, Urbana, IL, USA) or a FluoroMax-4 spectrofluorometer (Horiba, Kyoto, Japan). FITC labelled cell suspension (350 μl on ice) was given to a spectrofluorometer cuvette, which was thermostated to 30 °C or 37 °C. At the same time 1 ml of HBSS at 45 °C or 60 °C was added dropwise within 20 s to reach a final temperature of the mixture of 30 °C or 37 °C. As soon as the suspension was tempered, the time based measurement was started with an excitation wavelength of 488 nm and every second the emission was recorded at 508 nm during the entire measurement, typically lasting 12 min. Some of the applied exogenous lipids were labelled with a NBD-group, which is also excitated at the wavelength of 488 nm. Thus, the intensity of cells incubated with the respective NBD-lipid but not labelled with FITC was monitored as a function of time and substracted from the kinetics recorded in the subsequent measurement with FITC labelled cells.

3.2.5 Quantification of Endocytic Activity

The decrease of the FITC signal as a function of time was monitored separately for every cell sample in the absence (control) or presence of different amounts of various exogenous lipids. Due to the high variation of the activity of bulk flow endocytosis in different experimental setups, at least one control sample was prepared for every setup and all measurements within this setup were related to the activity of the control sample. To be able to compare the endocytic activity of different measurements with each other, the decrease of the FITC signal was standardised using a nonlinear least square fit with the following function for a general exponential decrease: $f(t) = ae^{-t/\tau} + b$, where a is the scale, b the offset, and τ the time constant. The goodness of fit was specified by calculating the coefficient of determination R^2, which is a measure of how well the regression line approximates the real data points. Measurements with $R^2 < 0.5$ were not evaluated. Measurements were then presented as an standardised increase of the FITC signal by calculating BFEA at time t with $f(0) - f(t)$, where $f(t)$ was the fluorescence intensity at time t and $f(0)$ was taken from the fit. For the exact quantification of the

change of BFEA with the percentage of added exogenous lipids, the values of BFEA after 2, 6, and/or 10 min were related to the respective activities of the control samples that were set as 100 %.

During the improvement of this assay it was ascertained that the cell samples lost part of their activity with time they were stored on ice after FITC labelling. To rigorously quantify this *loss of fitness*, control samples were prepared and the resulting FITC signal was recorded exactly every 15 min after starting the first measurement ($t = 0$ min). The maximum extent of BFEA for each measurement was taken from the nonlinear least square fit and related to the respective extent of the first measurement that set as 100 %. The resulting decrease with the time on ice was again fitted with a function for general exponential decrease to obtain a calibration curve for the loss of fitness. Subsequent measurements in the presence of exogenous lipids were performed as described above but recorded at certain time intervals after cell labelling. The resulting BFEA was calculated and corrected with a fitness factor taken from the calibration curve.

3.3 Spectrofluorometry of Clathrin-Endocytosis

This assay for the investigation of the activity of clathrin-mediated endocytosis was mainly done according to the assay for bulk flow endocytosis (see clause 3.2), but instead of labelling the cell surface proteins with sulfo-NHS-LC-biotin and streptavidin-FITC, the transferrin receptor was labelled by the addition of transferrin conjugated to FITC (Tf-FITC) to specifically follow the clathrin-mediated pathway. After the preparation of cells (see 3.3.1) and the subsequent labelling with Tf-FITC (see 3.3.2) the cells were incubated with exogenous lipids as described in 3.2.2 in the improved order. Also the spectrofluorometric measurements and the quantification of endocytic activity were done as detailed for bulk flow endocytosis (see 3.2.4 and 3.2.5), but here clathrin-mediated endocytic activity (CMEA) was analysed.

3.3.1 Preparation of Cells

K562 cells were cultured in suspension to a density of 1×10^6 cells/ml. The desired volume of cell suspension was withdrawn, centrifuged (200×g, 5 min, 37 °C) and resuspended in the same volume of internalisation buffer (IB: RPMI 1640, 0.1 % BSA, 10 mM Hepes, pH 7.4). When BHKasc cells, still undergoing clathrin-mediated endocytosis, were analysed all media and buffers were supplemented with 20 μg/ml TET (BHKasc$^+$). For

induction of clathrin heavy chain antisense RNA expression, TET was removed from growth medium 18 to 20 h before starting of the experiment and all media and buffers were lacking TET (BHKasc$^-$). Adherent BHKasc cells were cultured to 80 % confluency and the growth medium was exchanged to internalisation buffer (IB: DMEM, 0.1 % BSA, 10 mM Hepes, +/-TET, pH 7.4). Cells were then incubated for 30 min at 37 °C and 5 % CO_2 to release the receptors from unlabelled transferrin. Subsequently, BHKasc cells were washed with DPBS and harvested with DPBS$^-$ supplemented with 2 mM EDTA followed by a washing step with DPBS (200×g, 5 min, 4 °C). K562 cells were also washed (200×g, 5 min, 4 °C) and cell pellets of both cell lines were resuspended in ice cold HBSS to prevent any endocytic activity.

3.3.2 FITC Labelling

The following steps were all performed on ice using ice cold buffers. Tf-FITC was added to the cell suspension to a final concentration of 42 μg/ml and 40 μg per 4×10^5 cells. During all further incubations, samples were always kept in the dark to avoid bleaching of the fluorophores. Following an incubation for 15 min on ice, labelled cells were incubated with or without (control) exogenous lipids as specified in 3.2.2 in the improved order.

3.4 Flow Cytometry for Receptor-Endocytosis

Flow cytometry, also known as fluorescence activated cell sorting (FACS), is a method that measures defined characteristics of cells in flow. Cells in suspension are passed as a continuous stream through a cabin where they scatter light of a laser beam and light is emitted by the fluorophores of labelled cells. The fluorescence intensity is recorded according to cell properties such as size and granulation. This method allows detection of fluorescent dye staining, which is coupled to cell size and granularity determinations. Thereby apoptotic or dead cells can be separated from living cells. In contrast to the spectrofluorometric experiments, where the fluorescence of all cells in a cuvette is monitored, it is not possible to measure fluorescence intensities as a function of time. Therefore, with this method the endocytic uptake of labelled antibodies for specific endocytic pathways into the cell was quantified at definite time points.

3.4.1 Preparation of Cells

Adherent cells were grown to 80 % confluency and passaged to six-well-plates 16 h prior to starting of the experiment (2×10^5 cells per well). When BHKasc$^-$ cells were investigated TET was removed from the medium at this step. Growth medium was exchanged by IB (DMEM$^-$, 0.1 % BSA, 10 mM Hepes, +/- TET, pH 7.4) and wells were incubated for 30 min at 37 °C and 5 % CO_2 to release the receptors from unlabelled antibodies.

3.4.2 Incubation with Antibodies and Exogenous Lipids

Suspensions of exogenous lipids were prepared as defined in 3.2.2 with a final concentration of 8 μM and mixed with antibodies (Tf-A488 or Tf-TMR) to a final concentration of 10 μg per 2×10^5 cells. This mixture was at first added to the well with the longest incubation time. After certain time intervals the mixture of lipids and antibodies was added to the other wells to finally get reading points at 2, 5, 10, 15, and 20 min for the Tf-uptake. For each of theses sets one well without labelled antibodies was carried along to obtain the background signal of cells. Simultaneously, for each experimental setup one set of control samples without exogenous lipids and with the same reading points was prepared to be able to relate the endocytic activity of lipid treated samples. During this procedure six-well-plates were kept at 37 °C and 5 % CO_2. Reaching the last time point, plates were directly transferred to 0 °C to stop the uptake of antibodies. The cells were then washed with cold IB and antibodies were detached from the cell surface by an acidic wash with acid buffer (AB: DMEM$^-$, 0.1 % BSA, 20 mM NaAc, pH 2.5) for 3 min. Immediately after this wash, the pH was returned to neutral by the addition of basic buffer (BB: DMEM$^-$, 0.1 % BSA, 30 mM Hepes, pH >11).

In order to control the effectual detachment of antibodies from the cell surface and to obtain the remaining fluorophor signal, the following samples were prepared: two samples per set were cooled down on ice, labelled antibodies together with or without lipids were added and samples were incubated on ice for 1 h. One sample was then treated with an acidic wash as described above while the other one was only washed with cold DPBS. Afterwards all samples were washed with cold DPBS and subsequently cold DPBS$^-$ supplemented with 2 mM EDTA was added. Then cells were scraped, transferred into FACS tubes already containing 2 ml of cold DPBS and centrifuged (200 x g, 5 min, 4 °C). The resulting cell pellet was resuspended in 200 μl cold HBSS and analysed by flow cytometry.

3.4.3 Analysis and Quantification

Cytometric analysis was performed using a FACScan (Becton Dickinson, San Jose, USA) and the software WinMDI (TSRI, San Diego, USA). The FACScan is equipped with a laser at 488 nm and can collect three fluorescent and two scatter properties simultaneously. The intensity of the fluorophor A488 was detected in the FL-1 channel with a filter at 530/30 nm and the TMR signal in the FL-2 channel with a 585/42 nm-filter. Additionally to the fluorescence intensities of cells two scatter properties were recorded. Light scattered in a small angle of 3 ° to 10 ° is called forward scatter (FCS) and correlates with the size of cells. Light reflected to 90 ° is referred to as side scatter (SSC) and is a dimension for the surface structure and granulation of cells. FCS- and SSC-signals were monitored with linear, fluorescence intensities with logarithmical amplification.

Apoptotic and dead cells show different FCS and SSC from living cells. A gate was drawn selecting the population of living cells using a density plot of FCS and SSC. Data were collected for 10,000 cells per sample within this gate and analysed by the software WinMDI. Histograms of the fluorophor corresponding channel were plotted and gated for the same population of living cells. Medians from the histogram statistics were taken as fluorescence intensities of the samples. The background intensity of cells (sample without antibodies) and the intensity of remaining label (sample without acidic wash) were substracted from the intensity of samples at the certain reading points. The change of clathrin-mediated endocytic activity in the presence of exogenous lipids was exactly quantified by relating the activities to the respective activity of the simultaneously prepared control sample that was set as 100 %. This was done for the samples corresponding to time points at 2 min and 20 min, respectively.

3.5 Microscopy

In order to visibly examine the uptake of endocytic tracers into cells or the distribution of exogenous lipids in cell membranes, microscopic images of fluorescently labelled cells were taken as described in the following clauses.

3.5.1 Preparation and Labelling of Cells

Adherent cells were grown to 80 % confluency and passaged to 35 mm culture dishes with glass bottom (MatTek, Ashland, MA, USA) 16 h prior to starting of the experi-

ment (5×10^4 cells per dish). When BHKasc$^-$ cells were investigated TET was removed from the medium at this step. K562 cells were cultured in suspension to a density of 1×10^6 cells/ml. The desired volume of cell suspension was withdrawn and centrifuged (200×g, 5 min, 4 °C/37 °C). For control pictures of detached cells, cells were adherently cultured to 80 % confluency and washed with DPBS. After detaching by the addition of DPBS$^-$ containing 2 mM EDTA, cell suspensions were centrifuged (200 x g, 5 min, 4 °C/37 °C). Cell pellets were then resuspended in the desired buffer for subsequent labelling.

Labelling with Transferrin (Clathrin-Mediated Endocytosis)

To visualise the uptake of labelled transferrin into cells, the medium of adherent cells was exchanged to the same volume of IB (DMEM$^-$, 0.1 % BSA, +/- TET, 10 mM Hepes, pH 7.4) and cell pellets of suspended or detached cells were resuspended in IB (DMEM$^-$/ RPMI 1640$^-$, 0.1 % BSA, 10 mM Hepes, +/- TET, pH 7.4). After an incubation for 30 min at 37 °C and 5 % CO_2 to release the receptors from unlabelled transferrin, either Tf-FITC or Tf-TMR was added to the cells yielding a final concentration of 2 μg per 5×10^4 cells. After incubating for certain times at 37 °C and 5 % CO_2 cells were transferred to ice to stop the uptake of the tracer.

Labelling with NBD-Lipids (Intracellular Lipid Distribution)

The distribution of exogenously added lipids in cell membranes was observed by adding NBD-labelled lipids to the cells. NBD-lipid solutions were prepared as described in 3.2.2. The medium of adherent cells was exchanged to HBSS and cell pellets of suspended or detached cells were resuspended in HBSS. After the addition of lipid solution, cells were incubated with the desired concentration of lipids for different times either on ice or at 37 °C.

Cells labelled to visualise endocytic uptake were washed and resuspended in cold HBSS, cells incubated with NBD-lipids were not washed and immediately imaged. Suspended or detached cells were transferred to 35 mm culture dishes with glass bottom (5×10^4 cells per dish). The uptake of labelled transferrin or NDB-lipids was then observed by microscopy as described in the following clause.

3.5.2 Fluorescence Microscopy

Labelled cells were analysed using an inverse standard microscope equipped with a Plan-Neofluar 100×/1.3 numerical aperture objective, a standard fluorescein filter set (BP 450 to 490 nm excitation filter, FT 510 nm dichroic mirror, and LP 515 nm emission filter), and a standard rhodamine filter set (BP 546 nm excitation filter, FT 580 nm dichroic mirror, and LP 590 nm emission filter) (Carl Zeiss, Oberkochen, Germany). Confocal microscopy was performed using an inverted IX81 fluorescence microscope equipped with a Fluoview 1000 scanhead (Olympus, Hamburg, Germany) and a 60×/1.35 numerical aperture oil immersion objective. The fluorophores were excited with a diode laser at 468 nm and emission was recorded using a 540/40 nm bandpass filter.

CHAPTER 4

Results

4.1 Improvement of the Spectrofluorometric Assay

In order to investigate the influence of monolayer area asymmetry on endocytic activity, the first aim of the present study was to reinvestigate the results of Farge et al. (1999) with diverse exogenous lipids and to distinctly quantify the change of bulk flow endocytic activity (BFEA) of K562 cells with the percentage of lipids added to the outer or inner leaflet of the plasma membrane. In doing so, the spectrofluorometric assay for bulk flow endocytosis was exactly performed as described in the publication of Farge et al. (1999): K562 cells were first incubated with various exogenous lipids for 30 minutes at 37 °C followed by the labelling of cell surface proteins with FITC (see clause 3.2; original order). Since FITC is sensitive to pH, the BFEA of cells could then be monitored by a decrease of the FITC signal with time due to the acidification of the early endosomes. The recorded kinetics were standardised by calculating the BFEA at time t with $f(0) - f(t)$, where $f(t)$ was the fluorescence intensity at time t and $f(0)$ was taken from a nonlinear least square fit.

As shown by Farge, in the present study the addition of exogenous lipids to K562 cells led to an alteration of BFEA compared to the activity of control cells, which were not treated with exogenous lipids. In contrast to the results of Farge, the differences in BFEA did not exclusively correspond to the theoretical expectations. Phosphatidylcholine with one short and one long chain (C_6-PC), that is known to remain in the outer layer of

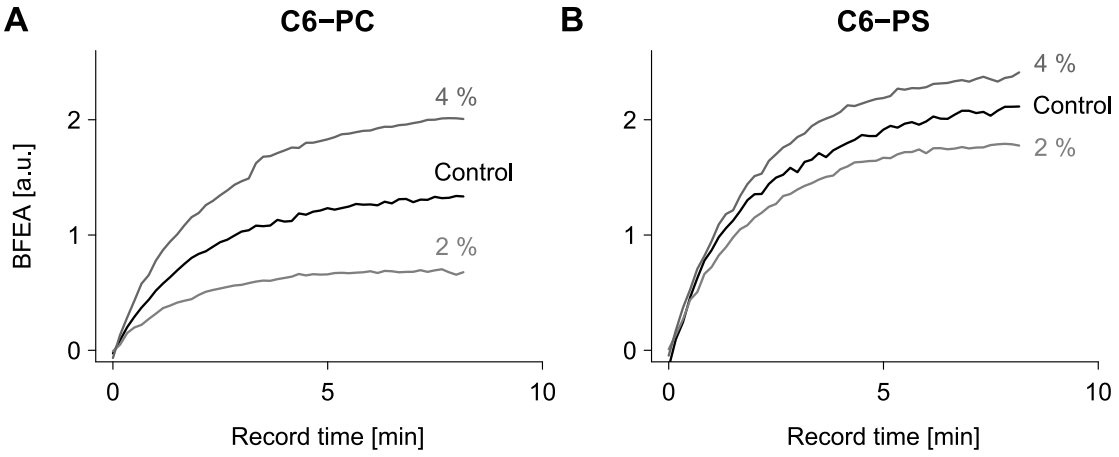

Figure 4.1: Typical kinetics of bulk flow endocytic activity (BFEA) of K562 cells preincubated with exogenous lipids at 37 °C. Cells were incubated with different amounts of C_6-PC or C_6-PS for 30 min at 37 °C before cell surface proteins were labelled with FITC. Standardised measurements of FITC intensities as a function of time illustrate typical kinetics, the varying influence of C_6-PC (A) or C_6-PS (B) on BFEA, and the highly unequal extend of BFEA of control samples obtained in different experimental setups.

the plasma membrane (Cribier et al., 1993; Farge et al., 1999), could enhance as well as decrease BFEA. The same was observed for phosphatidylserine with one long and one short chain (C_6-PS), which was shown to be translocated to the inner leaflet of the plasma membrane of K562 cells (Cribier et al., 1993; Farge et al., 1999). In Figure 4.1 typical kinetics illustrate the varying influence of the exogenous lipids C_6-PC (Fig. 4.1 A) and C_6-PS (Fig. 4.1 B) as well as the highly unequal extent of BFEA of control samples in different experimental setups. In these exemplary measurements, the standardised BFEA activity of control samples of the same cell line increased to about 1.3 as well as to about 2.1 (Fig. 4.1 A and B, respectively) after 8 minutes of measuring the FITC signal.

In order to be able to compare measurements performed in different experimental setups with each other and to precisely quantify the influence of exogenous lipids on BFEA, the change of BFEA was calculated as follows: the values of BFEA after 6 minutes of recording the FITC signal were related to the respective activities of control samples, which were not incubated with exogenous lipids, and set as 100 % activity. In Figure 4.2 standard box and whisker plots are shown for experiments with $n \geq 5$, where n is the number of independent experiments. The boxes describe median and upper and lower

quartiles, whereas the whiskers are defined by the maximum observation within the 1.5 times interquartile range (IQR), which is equal to the difference between the third and first quartile. Outliers beyond the range of the whiskers are marked separately ($\diamond$). For experiments with $n < 5$ the percentage of BFEA of each measurement is plotted in one dimensional scatter plots (x). The change in BFEA was tested for significance with an one sample t-test. Evaluated BFEA was considered as significantly different from the activity of control samples, which was set to 100 % activity, at the 0.05 level and is marked in the plots (*). For all performed experiments, the means of obtained BFEA, standard error of the mean (SEM), and p-values of significant changes are summarised in Table 4.1.

Since C_6-PC remains on the outer leaflet, its addition was expected to cause an inhibition of BFEA, but for nearly all applied lipid concentrations, 2 %, 4 %, and 8 % C_6-PC, and both incubations of cells with lipids, 15 and 30 minutes at 37 °C, the resulting means either varied around 100 % activity or showed an increased activity with a very high variation (see Fig. 4.2 A). At 15 minutes incubation time, mean and SEM highly increased with the percentage of added lipids. When cells were incubated with exogenous C_6-PC for 30 minutes at 37 °C, the resulting BFEA values at 2 and 8 % C_6-PC again varied around 100 % activity. Only at 4 % of C_6-PC for 30 minutes, BFEA were higher than in the respective control samples in both independent experiments, but this change in BFEA was not significant.

The second applied lipid, C_6-PS, is thought to be translocated to the inner layer (Cribier et al., 1993; Farge et al., 1999) and was therefore expected to enhance the activity. Also here, the resulting BFEA ranged around 100 % for all but one applied lipid concentration, 2 %, 4 %, 6 %, or 8 % C_6-PS, and incubation of cells with lipids, 15 or 30 minutes at 37 °C (see Fig. 4.2 B). Only when 6 % of C_6-PS were added for 30 minutes, the BFEA of all three experiments is slightly higher than the BFEA of controls, leading to an significantly increased change in BFEA to 116 ± 4 % (mean $\pm$ SEM).

Thus, neither the expected inhibition of BFEA by exogenous C_6-PC nor a clear enhancement of BFEA by exogenous C_6-PS, as shown by Farge et al. (1999), could be obtained in these experiments. Performing the assay in the original order including the incubation of cells with exogenous lipids at 37 °C before cell surface proteins were labelled with FITC, the addition of exogenous lipids had no distinct influence on BFEA of K562 cells.

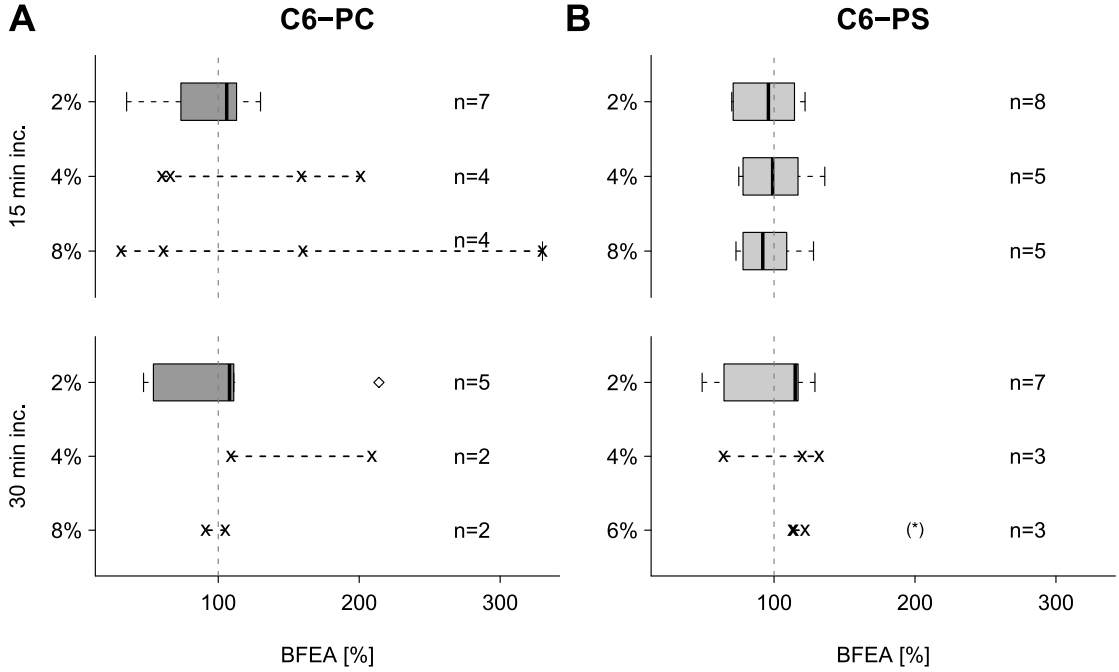

Figure 4.2: Bulk flow endocytic activity (BFEA) of K562 cells preincubated with exogenous lipids at 37 °C. Cells were incubated with different amounts of C_6-PC or C_6-PS for 15 or 30 min at 37 °C before cell surface proteins were labelled with FITC. Values of BFEA after 6 min of recording were related to the respective activity of control samples, which was set as 100 %. For $n \geq 5$, where n is the number of independent experiments, standard box and whisker plots describe median and upper and lower quartiles as well as smallest and largest observations or 1.5×IQR and outliers ($\diamond$), respectively. For $n < 5$ the percentage of BFEA is plotted for each measurement (x). Changes were tested for significance with an one sample t-test ($*$, $p \leq 0.05$).

Table 4.1: Values of bulk flow endocytic activity (BFEA) of K562 cells preincubated with exogenous lipids at 37 °C. BFEA was determined as explained in the description of Figure 4.2. The table presents resulting means and SEM of BFEA in percent [%]. When changes were significantly different from 100 % activity at the 0.05 level, also p-values obtained with an one sample t-test are written in parentheses.

	C_6-PC		C_6-PS	
	15 min inc.	30 min inc.	15 min inc.	30 min inc.
2 %	92 ± 31	107 ± 60	94 ± 21	94 ± 31
4 %	122 ± 60	159 ± 50	101 ± 23	105 ± 30
6 %	-	-	-	116 ± 4 (0.029)
8 %	146 ± 117	98 ± 7	96 ± 20	-

4.1.1 Loss of Fitness

A single measurement including the sample preparation and the 12-minutes-read-out took on average 15 minutes. During this time the other samples were kept on ice. To clarify, whether the endocytic activity of cells is affected by the time treated and FITC labelled cell samples are stored on ice prior to spectrofluorometric measurements, controls without exogenous lipids were prepared as follows: K562 cells were washed, incubated in HBSS without exogenous lipids at 37 °C for 30 minutes and subsequently labelled with FITC. Then, BFEA of labelled cells was determined after various incubation times on ice as done before. The successively analysed controls exhibited a decrease of activity with time cells were stored on ice. In Figure 4.3 A the standardised kinetics are plotted with their order of analysis, 1^{st} to 6^{th}. This *loss of fitness* led to an activity decrease of more than 50 % after an one-hour incubation on ice corresponding to the recording of four samples.

To be able to compare BFEA values of successively monitored samples in further experiments, the loss of fitness with time on ice was precisely quantified as follows. Experiments with control cells were repeated for several times recording the FITC signal exactly every 15 minutes after starting the first measurement at t = 0 minutes. After the nonlinear least square fit of the kinetics with $f(t) = ae^{-t/\tau} + b$, the maximum extent of BFEA of each measurement was taken from the exponential fit, which is represented by scale a, and related to the respective maximum extent of the first sample, which was set as 100 %. Here, the maximum extent and not the values after definite time intervalls served for comparison in order to avoid errors by the trend of the kinetics. As a control, also the values after 2 and 10 minutes were compared leading to the same result (data not shown). Figure 4.3 B gives standard box and whisker plots for experiments with $n \geq 5$ and one dimensional scatter plots for $n < 5$ as explained in clause 4.1. It confirmes the decrease of activity with time samples were stored on ice. After 45 minutes on ice the activity of control cells was reduced to 51 ± 16 % and after 90 minutes to 35 ± 13 %. The individual measurements of BFEA against the time on ice were then fitted with three different functions: a linear, a mono-exponential, as well as a bi-exponential decrease. Based on the higher coefficient of determination R^2 of the mono-exponential fit (linear $R^2 = 0.807$; mono-exponential $R^2 = 0.836$; bi-exponential $R^2 = 0.000$) as well as the distribution of residuals, the mono-exponential fit was chosen for further analysis. The obtained calibration curve was used to calculate a factor for the correction of BFEA

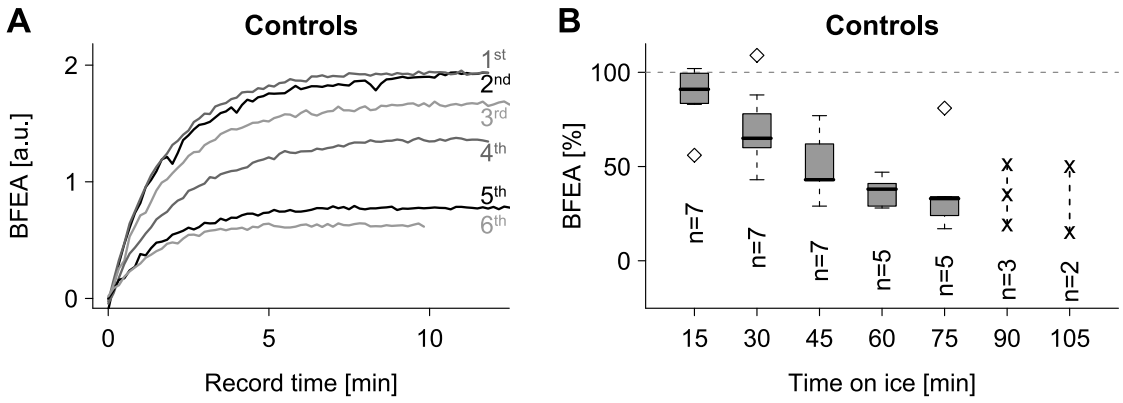

Figure 4.3: *Loss of fitness* with the storage of cell samples on ice. Control samples without exogenous lipids were analysed as before, but monitoring the FITC signal exactly every 15 min. **A:** Standardised kinetics in the order of analysis, 1^{st} to 6^{th}, demonstrate the decrease of activity with time control cells were stored on ice. **B:** Maximum extents of bulk flow endocytic activity (BFEA), which are taken from the exponential fit, were related to the respective extent of the first sample, which was set as 100 %. Standard box and whisker plots with outliers ($\diamond$) are given for experiments with $n \geq 5$ and one dimensional scatter plots (x) for $n < 5$ (see Fig. 4.2 for an explanation of the plots).

values of further experiments in the presence of exogenous lipids, which will be referred to as *fitness factor*. By that, it was now possible to compare measurements with each other that were recorded in definite time intervals of 15 minutes after the first measurement was started at $t = 0$ minutes.

In order to assess the influence of exogenous lipids on bulk flow endocytosis of K562 cells, experiments were repeated including the correction of values in subsequent analysis of BFEA. Cell samples were incubated with different exogenous lipids at 37 °C and, following FITC labelling of cell surface proteins, FITC intensity was recorded as before, but measurements were started every 15 minutes and the amount of BFEA after 10 minutes of measuring was corrected by the fitness factor calculated as explained above. The influence of short chain PS incubated with K562 cells for either 15 or 30 minutes at 37 °C is shown in Figure 4.4 A and B, respectively. One dimensional scatter plots picture the distribution of BFEA after 10 minutes of recording corrected by the fitness factor and with n given in the respective line. When cells were incubated with C_6-PS for 15 minutes, means of BFEA were reduced to 85 ± 12 % at 2 % C_6-PS, 79 ± 8 % at 4 % C_6-PS, and 82 ± 11 % at 8 % C_6-PS, but none of the changes was significantly different from control activity. Compared to that, means of BFEA were increased when cells were incubated

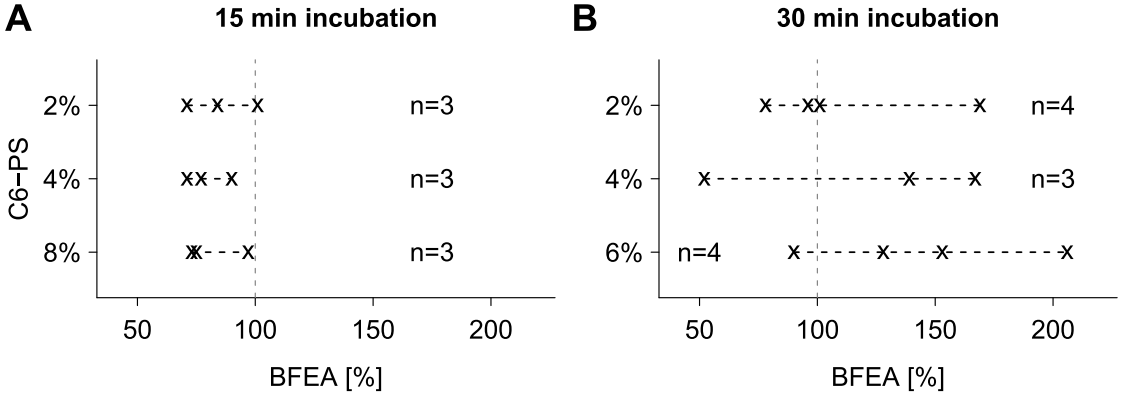

Figure 4.4: Bulk flow endocytic activity (BFEA) of K562 cells preincubated with exogenous C_6-PS at 37 °C and corrected by a fitness factor. Cells were incubated with different amounts of C_6-PS for 15 min (A) or 30 min (B) at 37 °C before cell surface proteins were labelled with FITC. Values of BFEA after 10 min of recording were related to the respective activity of control samples (100 %) and corrected by a previously calculated *fitness factor*. The percentage of BFEA of each measurement is plotted in one dimensional scatter plots and n is given in the respective line. Results were tested for significance at the 0.05 level, but none of the changes was significantly different from 100 % activity.

with exogenous C_6-PS for 30 minutes at 37 °C. The addition of 2 % C_6-PS resulted in an activity of 111 ± 35 %, 4 % in 119 ± 49 %, and 6 % in 144 ± 42 %. However, the variation was relatively high and also these changes were not significantly different from 100 % activity. This shows that the distinct enhancing influence of exogenous C_6-PS on BFEA of K562 cells as obtained by Farge et al. (1999) could again not be reproduced performing the assay in the original order and this time considering the loss of fitness with time samples were stored on ice by correcting the values by a fitness factor.

4.1.2 Influence of Label Concentration

It arose from discussions with Emmanuel Farge (Curie Institute, Paris), who introduced the spectrofluorometric assay to measure activity of bulk flow endocytosis, that he used higher label concentrations in his experiments. To control a potential influence of the FITC concentration linked to cell surface proteins, the experiments were repeated with higher concentrations of sulfo-NHS-LC-biotin and streptavidin-FITC. The company Perbio Science recommends a final biotin concentration of 1 mg/ml and 45 μg sulfo-NHS-LC-biotin per 1 million cells and a final concentration of streptavidin-FITC of 10 μg/ml. Emmanuel Farge applied higher concentrations: a final biotin concentration of 4 mg/ml

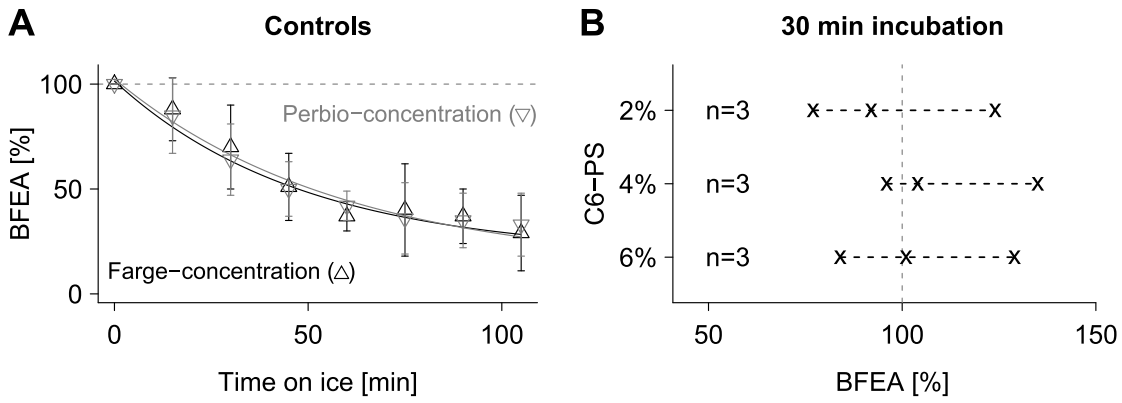

Figure 4.5: A: Comparison of activity reduction with time on ice. Control samples were labelled with two different concentrations of sulfo-NHS-LC-biotin and streptavidin-FITC as recommended by the company Perbio and applied by Farge et al. (1999), respectively. Bulk flow endocytic activity (BFEA) of controls was monitored every 15 min and values of BFEA after 10 min were related to the respective value of the first measurement, which was taken as 100 %. Plotted is the mono-exponential fit of the BFEA values against time samples were stored on ice and means with their standard error of the means for both concentrations. **B: BFEA of K562 cells preincubated with C_6-PS and corrected by a fitness factor when cells were labelled with higher biotin and FITC concentrations.** Cells were incubated with short chain PS for 30 min at 37 °C and labelled with higher label concentrations as used by Farge et al. (1999). Resulting BFEA after 10 min were corrected by the fitness factor and are shown for each measurement in one dimensional scatter plots with n in the respective line. Results were tested for significance, but none of the changes was significantly different from 100 % ($p \leq 0.05$).

resulting in 240 μg sulfo-NHS-LC-biotin per 1 million cells and a final streptavidin-FITC concentration of 15 μg/ml (Farge et al., 1999; Rauch and Farge, 2000). Further experiments were carried out with higher concentrations as used by Farge. First of all, the loss of fitness of controls was determined as in the previous experiments with lower concentrations: control cells without exogenous lipids were labelled using the higher concentrations of sulfo-NHS-LC-biotin and streptavidin-FITC. The activity of control samples was then successively monitored every 15 minutes and the maximum extent of BFEA was related to the extent of the measurement at $t = 0$ minutes, which was set as 100 %. As before, the activities demonstrated an exponential decay with time samples were stored on ice. They were again mono-exponentially fitted and are drawn in Figure 4.5 A in comparison to the decay obtained with the lower Perbio concentrations. Alongside with the exponential fits, means with their SEM are also plotted. Compared to the reduction of BFEA in former experiments with concentrations recommended by Perbio, the measurements using concentrations as established by Farge et al. (1999) pre-

sented a nearly equal decrease of fitness with time samples were incubated on ice. At shorter incubations on ice, the reduction was slightly faster when concentrations as used by Farge were applied, for instance 64 % instead of 67 % after 30 minutes.

Subsequently, experiments in the presence of short chain PS were repeated using the concentrations applied by Farge and analysed as before. Again either 2 %, 4 %, or 6 % of exogenous C_6-PS were added to the cells followed by an incubation for 30 minutes at 37 °C. The resulting BFEA after 10 minutes of recording was related to the value of the respective control and corrected by the fitness factor. The results of three independent experiments for each lipid concentration are shown in Figure 4.5 B in one dimensional scatter plots. Also using the higher label concentrations as applied by Farge, the incubation with exogenous C_6-PS had no consistent influence on BFEA of K562 cells. The addition of 2 % C_6-PS resulted in an activity of 99 ± 19 %, 4 % C_6-PS in 112 ± 17 % BFEA, and 6 % C_6-PS in 105 ± 19 % BFEA. Thus, also using label concentrations as applied by Farge, BFEA values varied again around 100 % and it could again not been shown that the addition of exogenous C_6-PS significantly effects BFEA of K562 cells.

Summarising the results up to here, the influence of exogenous lipids on BFEA of K562 cells as obtained by Farge et al. (1999) could not be reproduced, even following exactly the protocol as described by Farge. It was found that FITC labelled K562 cells exhibit a loss of fitness with time cell samples are stored on ice, but even the precise quantification of this loss and the correction of BFEA values by a fitness factor did not result in a distinct influence of exogenous lipids on BFEA of K562 cells. Likewise, the verification of the influence of label concentrations for the unspecific labelling of cell surface proteins with FITC did neither show an alteration of the fitness decrease nor demonstrate a change in the lacking influence of exogenous C_6-PS on BFEA. Therefore, the protocol of this assay was modified as explained in the following clause.

4.1.3 Change of Lipid Incubation and Temperature

Following the protocol of Farge, the cells were incubated with exogenous lipids for at least 15 minutes at 37 °C to allow the lipids to be incorporated into and, depending on the lipid species, translocated across the plasma membrane. Subsequently, cell surface proteins were labelled with FITC while keeping the cell suspension on ice to prevent any endocytic activity. All together, the labelling required about 75 minutes. In summary, the cells were incubated with lipids for at least 90 minutes, 15 or 30 minutes at 37 °C followed by

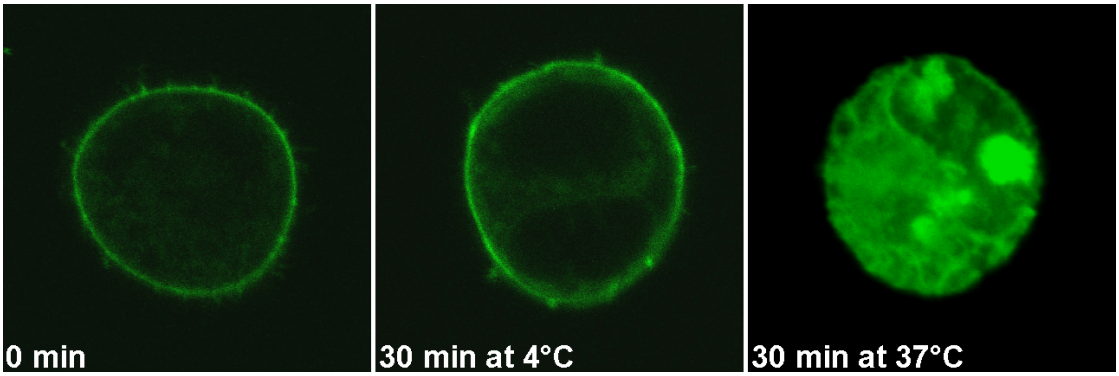

Figure 4.6: Distribution of C_6-NBD-PS in K562 cells after incubation at different temperatures. 4 % of C_6-NBD-PS were added to K562 cells and confocal microscopic pictures were taken immediately after the addition of lipids and after 30 min when cells were incubated with NBD-lipids either at 4 °C or at 37 °C. As presented in the left and middle image, immediately after the addition and after 30 min at 4 °C the main part of C_6-NBD-PS was still in the plasma membrane, whereas after 30 min at 37 °C, shown in the right image, the lipids were dispersed in the whole cell and staining of the plasma membrane was strongly reduced.

about 75 minutes on ice, before starting the measurements. In order to determine the distribution of exogenous lipids in cells after certain times, 4 % of NBD-labelled PS were added to K562 cells and confocal microscopic images were taken immediately after the addition of lipids to the cells and after 30 minutes of incubation at either 4 °C or 37 °C. As shown in Figure 4.6 in the left image, immediately after the addition C_6-NBD-lipids were only present in the plasma membrane. After 30 minutes at 4 °C, the main part was still in the plasma membrane and only a slight dying of intracellular structures could be observed (Fig. 4.6; middle). After 30 minutes at 37 °C, the label was dispersed in the whole cell and seemed to accumulate in inner cell compartments (Fig. 4.6; right). Staining of the plasma membrane was strongly reduced in comparison to 30 minutes at 4 °C. This shows that after an incubation of 30 minutes at 37 °C, the main part of exogenously added NBD-lipids was not present in the plasma membrane anymore and could therefore not account for a difference in the monolayer area asymmetry.

To avoid rather long incubation times, the protocol was adapted as specified in 3.2.2: the sequence of cell incubation with lipids and labelling with FITC was inverted. Cell surface proteins were first labelled with FITC while keeping the cells on ice and afterwards exogenous lipids were added at different time intervals before the measurements

were started. When no other times are indicated, the addition of lipids was carried out exactly 1 minute before starting the respective measurement.

Additionally to the shorter incubation time, the effect of a lower temperature during the measurements was assayed. Under the previous conditions, the detection of endocytic activity could be at its maximum level and therefore differences could be hardly observable. According to the improved protocol, all measurements including the investigation of the loss of fitness and the addition of different exogenous lipids were iterated at 30 °C. Results of bulk flow endocytosis for both temperatures, 30 °C and 37 °C, as well as for different cell lines are shown in the following clause.

4.2 Influence of Exogenous Lipids on Endocytosis

4.2.1 Bulk Flow Endocytosis

K562 Cells

The change in bulk flow endocytic activity (BFEA) of K562 cells in the presence of exogenous lipids was investigated following the improved protocol of the spectrofluorometric assay. Considering the loss of fitness with time on ice, the higher label concentrations, and the shorter lipid incubation for 1 minute on ice unless otherwise stated, the experiments were repeated with various exogenous lipids. The results of measurements performed at 37 °C are shown in Figure 4.7 demonstrating BFEA values after 2 and 10 minutes of recording the FITC signal for different amounts of exogenous lipids. For experiments with $n \geq 5$ standard box and whisker plots illustrate median and upper and lower quartiles as well as smallest and largest observations or 1.5×IQR and outliers ($\diamond$), respectively. For experiments with $n < 5$ the percentage of BFEA of each measurement is presented in one dimensional scatter plots (x). Changes in BFEA were tested with an one sample t-test and considered as significant at the 0.05 level (*).

Following the improved protocol with shorter incubations of cells with exogenous lipids, the addition of C_6-PS, which is known to be translocated to the inner leaflet of the plasma membrane, led to an enhancement of bulk flow endocytic activity that was, at some concentrations of C_6-PS, significantly different to the activity of control samples. The means increased with raising concentrations of exogenous C_6-PS from 133 ± 25 % BFEA at 1 % C_6-PS to 137 ± 32 % BFEA at 4 % C_6-PS after 2 minutes and from 115 ± 23 % to 152 ± 71 % after 10 minutes of recording. At higher concen-

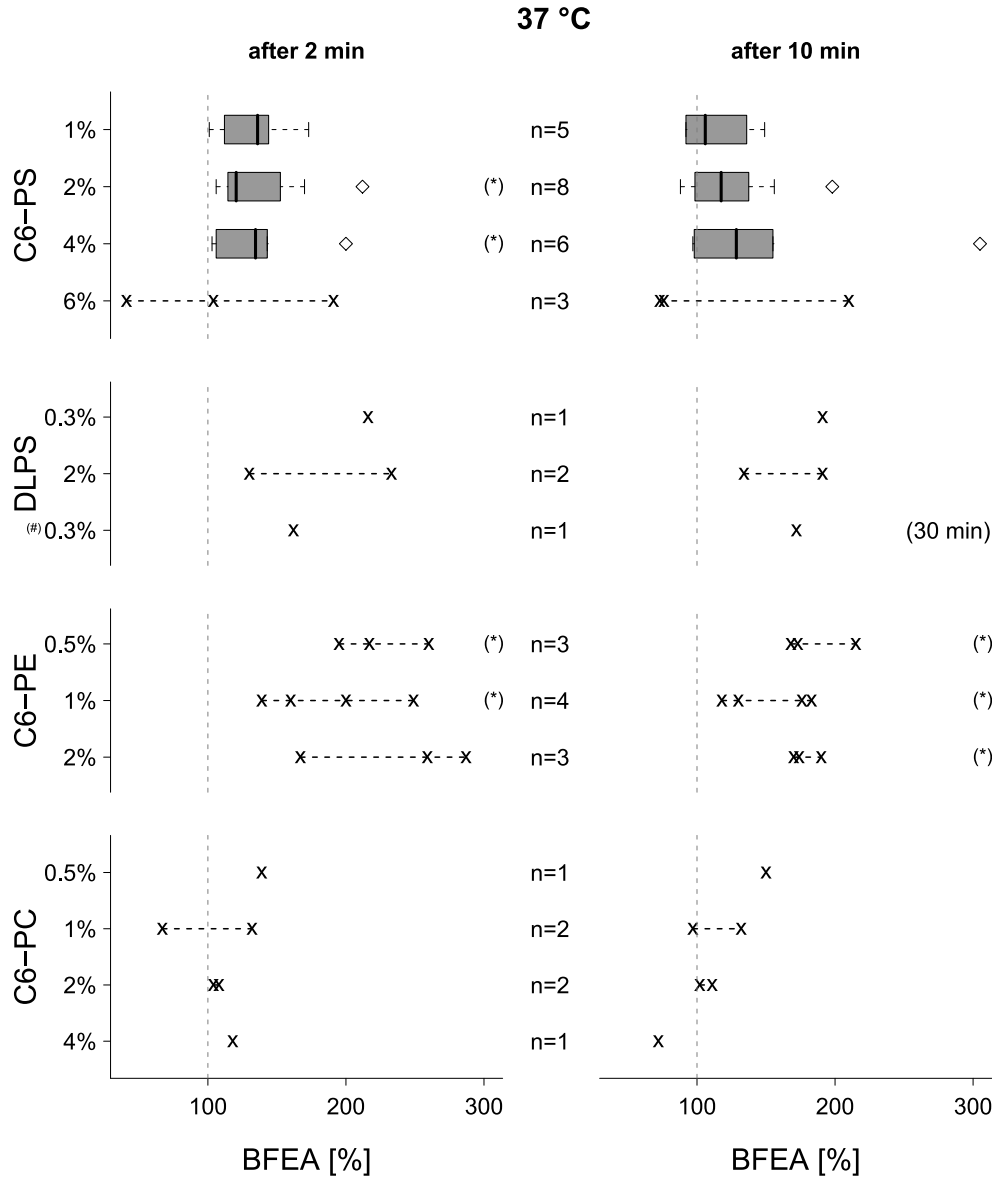

Figure 4.7: Bulk flow endocytic activity (BFEA) of K562 cells at 37 °C. FITC labelled cells were incubated with various exogenous lipids and resulting BFEA after 2 and 10 min of recording was related to the respective activity of controls (100 %) and corrected with a fitness factor. For $n \geq 5$ standard box and whisker plots describe median and upper and lower quartiles as well as smallest and largest observations or 1.5×IQR and outliers ($\diamond$), respectively. For $n < 5$ the percentage of BFEA is plotted for each measurement (x). Changes were tested for significance with an one sample t-test ($*$, $p \leq 0.05$). $^{(\#)}$ Indicated time (30 min) corresponds to incubation of cells with lipids on ice before starting the respective measurement. When no times are given, incubation was 1 min on ice.

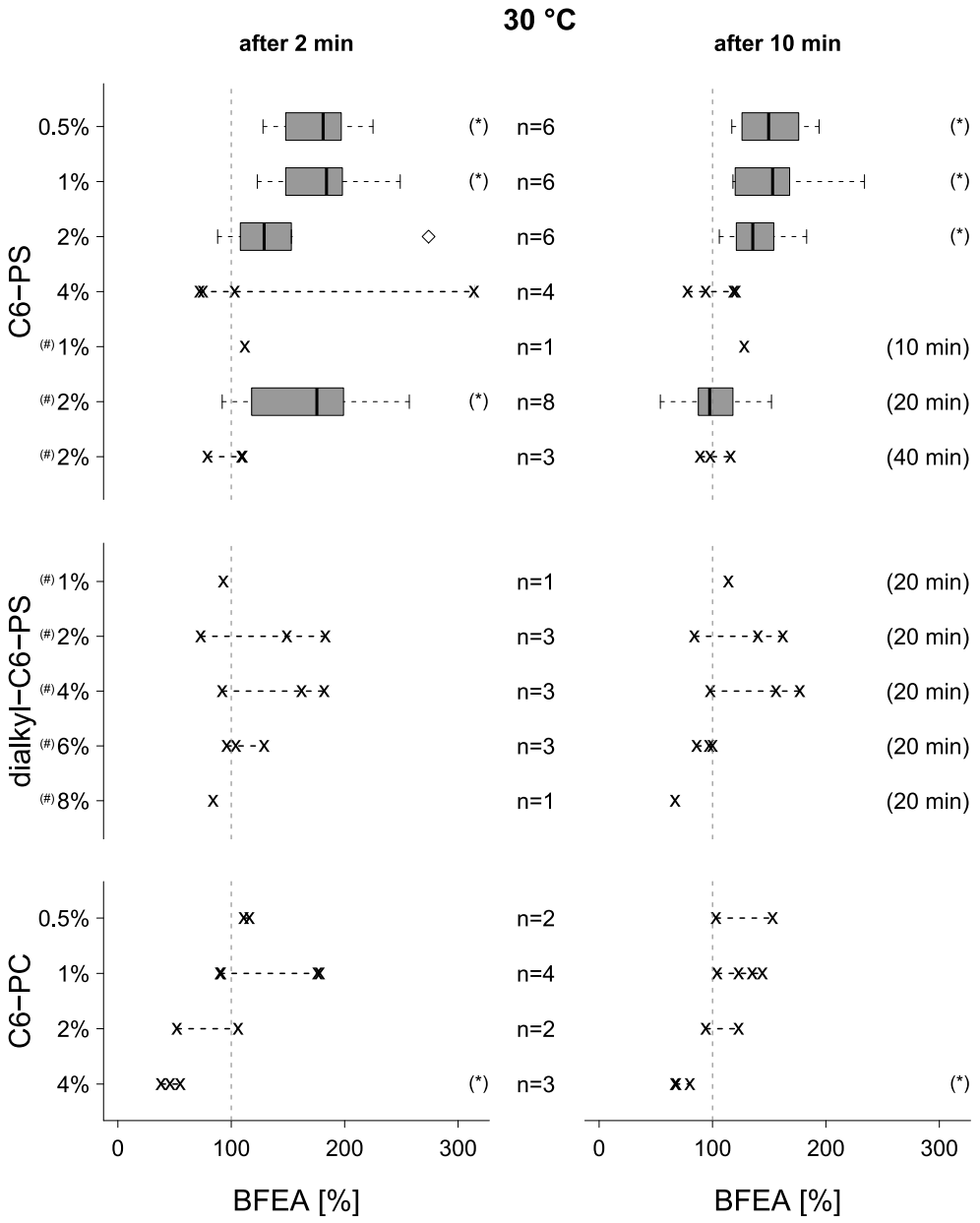

Figure 4.8: Bulk flow endocytic activity (BFEA) of K562 cells at 30 °C. See Figure 4.7 for a key to the plots. Changes were tested for significance with an one sample t-test ($*$, $p \leq 0.05$). (#) Indicated times (e.g. 10 min) correspond to incubation of cells with lipids on ice before starting the respective measurement. When no times are given, incubation was 1 min on ice.

trations, namely at 6 % C_6-PS, means dropped to 112 ± 61 % BFEA after 2 minutes and to 120 ± 64 % BFEA after 10 minutes. Changes in BFEA were significantly different from 100 % activity after 2 minutes of recording when 2 % or 4 % of C_6-PS were applied with p-values of 0.025 and 0.050, respectively. In both time intervals, 2 and 10 minutes after recording, SEM increased with the percentage of added lipids. Overall, the stimulation of BFEA was slightly stronger after 2 than after 10 minutes of recording the FITC signal.

K562 cells were additionally incubated with DLPS, a phospholipid comprising two medium length fatty acid chains with 12 C atoms, which is also translocated to the inner layer of the plasma membrane. The resulting BFEA was remarkably higher than in control samples. The highest stimulation of 216 % was obtained in the presence of 0.3 % DLPS after 2 minutes. For comparison, when the same amount of DLPS was preincubated with cells for 30 minutes on ice instead of 1 minute, the resulting BFEA was with 162 % after 2 minutes lower. Likewise, at 2 % DLPS means of BFEA were lower than at 0.3 % DLPS incubated for 1 minute, but still presented a clear stimulating influence. The overall enhancement was again higher after 2 minutes of measuring. Although the number of experiments is not sufficient for statistical analysis, the fact that a stimulation of BFEA was obtained in all experiments performed with DLPS supports the finding of an enhancing influence of exogenous DLPS. Taking the four obtained BFEA values together, the change in BFEA to 185 ± 41 % after 2 minutes and to 172 ± 23 % after 10 minutes was significant with p-values of 0.037 and 0.013, respectively.

As a third exogenous lipid, that is translocated to the cytoplasmic layer, C_6-PE was investigated. Addition of this lipid resulted equally in high stimulations of BFEA, which were significantly different from 100 % activity at each but one applied lipid concentration. Here, the highest stimulation of 238 ± 51 % was observed after 2 minutes in the presence of 2 % C_6-PE, which was the highest applied lipid amount, but this change was not significant. After 2 minutes of recording, means dropped from 224 ± 27 % at 0.5 % C_6-PE to 187 ± 42 % at 1 % C_6-PE and changes were significant with p-values of 0.023 and 0.037, respectively. The values after 10 minutes showed a similar distribution, BFEA dropped from 185 ± 21 % with $p = 0.029$ at 0.5 % C_6-PE to 152 ± 28 % with $p = 0.050$ at 1 % C_6-PE and increased again to 178 ± 9 % at 2 % C_6-PE. Although the latter value was not maximum, it was with $p = 0.006$ the most significant change due to a very low variation.

In addition to lipids that were expected to stimulate endocytic activity, the influence of short chain PC, that remains on the outer layer, was also tested. The resulting values

of BFEA varied around 100 % activity for 1 % and 2 % of C_6-PC after both recording times. After 2 minutes, BFEA was 100 ± 33 % at 1 % C_6-PC as well as 106 ± 2 % at 2 % C_6-PC and after 10 minutes BFEA dropped from 115 ± 18 % at 1 % C_6-PC to 107 ± 5 % at 2 % C_6-PC. The number of independent experiments with definite concentrations of C_6-PC was not sufficient for statistical analysis and obviously there was no significant inhibition, even taking all experiments together. However, after 10 minutes of recording and taking all of the six independent measurements into account, a downward drift could be observed with ascending amount of added C_6-PC.

Along with shorter incubation times of exogenous lipids, a lower temperature during the measurements was inspected. Following the improved protocol, all measurements including the loss of fitness and the addition of different exogenous lipids were repeated at 30 °C. The loss of fitness was quantified as described in 4.1.1. At this lower temperature, it was distinctly slower: after 1 hour on ice BFEA of controls was down to 59 % and after 1.5 hours to 45 % compared to activities of 43 % and 31 % at 37 °C, respectively.

The results for the changes in BFEA at 30 °C in the presence of various exogenous lipids are shown in Figure 4.8. Compared to the results obtained for 37 °C, the stimulation by C_6-PS was stronger and changes were significant for 0.5 % and 1 % of exogenous C_6-PS. The highest activity of 181 ± 40 % was obtained at 1 % C_6-PS after 2 minutes of recording and was significantly different with $p = 0.006$. After both recording times, resulting BFEA was about the same at 0.5 % and 1 % C_6-PS, roughly 180 % after 2 minutes and 155 % after 10 minutes, and decreased at 2 % of C_6-PS to around 145 %. When 4 % C_6-PS were applied, the values of BFEA varied around 100 % activity after both recording times with a huge variation after 2 minutes. Also here, the overall stimulation was higher after 2 minutes of measuring the FITC signal. In order to investigate a potential influence of longer incubations of cells with lipids and, hence, a longer time for the incorporation and subsequent translocation of exogenous lipids, the cells had been incubated with either 1 % or 2 % C_6-PS for 10, 20, or 40 minutes on ice before the respective measurement was started. With the longer incubation times, the resulting values of BFEA varied around 100 % for all tested lipid concentrations and incubation times aside from one exception: after 2 minutes of recording, when cells were incubated with 2 % C_6-PS for 20 minutes, the activity was with 167 ± 51 % and a p-value of 0.011 significantly higher than the activity of control samples, but had a large variation.

Further to the influence of short chain diacyl-PS, dialkyl-C_6-PS was also investigated, because it is not hydrolysed when incubated with cells. Since it is incorporated and

Table 4.2: Values of bulk flow endocytic activity (BFEA) of K562 cells. BFEA was determined as explained in the description of Figure 4.7. Presented are times of incubations of cells with lipids on ice in minutes (inc. [min]) as well as resulting means and SEM of BFEA in percent [%]. When changes were significantly different from 100 % activity, also p-values obtained with an one sample t-test are written in parentheses ($p \leq 0.05$).

		inc.	30 °C		37 °C	
		[min]	2 min	10 min	2 min	10 min
C_6-PS	0.5 %	1	177 ± 32 (0.003)	152 ± 27 (0.007)	-	-
	1 %	1	181 ± 40 (0.006)	158 ± 39 (0.021)	133 ± 25	115 ± 23
	2 %	1	147 ± 60	139 ± 25 (0.017)	137 ± 34 (0.025)	124 ± 34
	4 %	1	141 ± 99	103 ± 18	137 ± 32 (0.050)	152 ± 71
	6 %	1	-	-	112 ± 61	120 ± 64
	1 %	10	112	128	-	-
	2 %	20	167 ± 51 (0.011)	102 ± 28	-	-
	2 %	40	99 ± 14	101 ± 11	-	-
dialkyl-C_6-PS	1 %	20	93	114	-	-
	2 %	20	135 ± 46	129 ± 33	-	-
	4 %	20	145 ± 39	144 ± 33	-	-
	6 %	20	110 ± 14	94 ± 6	-	-
	8 %	20	84	67	-	-
DLPS	0.3 %	1	-	-	216	191
	2 %	1	-	-	181 ± 51	163 ± 29
	0.3 %	30	-	-	162	172
C_6-PE	0.5 %	1	-	-	224 ± 27 (0.023)	185 ± 21 (0.029)
	1 %	1	-	-	187 ± 42 (0.037)	152 ± 28 (0.050)
	2 %	1	-	-	238 ± 51	178 ± 9 (0.006)
C_6-PC	0.5 %	1	114 ± 3	128 ± 25	139	150
	1 %	1	134 ± 43	127 ± 15	100 ± 33	115 ± 18
	2 %	1	79 ± 27	109 ± 15	106 ± 2	107 ± 5
	4 %	1	46 ± 7 (0.008)	74 ± 7 (0.021)	118	72

translocated to the inner leaflet of the plasma membrane more slowly than diacyl-PS (Fellmann et al., 2000), K562 cells were preincubated with the lipids for 20 minutes on ice for all applied lipid concentrations. From 1 % to 4 % dialkyl-C_6-PS the resulting means of BFEA increased with the lipid concentration from 93 % to 145 ± 39 % after 2 minutes of recording and from 114 % to 144 ± 33 % after 10 minutes. Although at 2 % and 4 % dialkyl-C_6-PS most values were above 100 % activity and presented an upward drift with increasing lipid concentration, changes were not significantly different from 100 % activity. Since the number of independent experiments was relatively small for

statistical analysis, all values at 2 % and 4 % dialkyl-C_6-PS were combined, resulting in a significant change to a mean of 138 ± 39 % BFEA with $p = 0.007$. At higher lipid concentrations, BFEA diminished again, at 6 % dialkyl-C_6-PS the values varied around 100 % activity and at 8 % of exogenous dialkyl-C_6-PS activities were even decreased.

As for 37 °C, the influence of exogenous lipids, which were expected to decrease endocytic activity, was examined at 30 °C by applying C_6-PC to the cells. For 0.5 % and 1 % of C_6-PC, the obtained values of BFEA were higher than 100 % control activity, but when higher concentrations of C_6-PC were added to the cells, four out of five values were lower than 100 %. At 4 % C_6-PC, the activities were significantly inhibited to a mean of 46 ± 7 % with $p = 0.008$ after 2 minutes and to 74 ± 7 % with $p = 0.021$ after 10 minutes of recording. All together, the values of BFEA showed a downward drift with increasing percentage of added C_6-PC for both recording times and the influence of C_6-PC was stronger after 2 minutes of measuring. For all performed experiments, the means of obtained BFEA, SEM, and p-values are summarised in Table 4.2.

Additionally to the qualitative alteration of bulk flow endocytosis by different exogenous lipids, Farge et al. (1999) found an average linear dependence of the initial slope of BFEA kinetics on the percentage of added PS (Farge et al., 1999, Fig. 3B). The incline of this dependence was estimated to be $1.1 \pm 0.4\,\% \cdot (\mathrm{min} \cdot \%\mathrm{PS})^{-1}$ at 37 °C, where %PS is the amount of exogenously added PS. This was declared to correspond to an increase of a factor of about five in the bulk flow endocytosis kinetics for an addition of 4 % C_6-PS. To be able to compare this factor, the measurements were analysed as described by Farge. Relative fluorescence quenching at time t was calculated with $1 - F_t/F_0$, where F_0 was derived from the exponential fit and F_t was the fluorescence intensity at time t. Then the first 60 seconds of these kinetics were fitted with a function for a general linear increase. At first, the dependence of the initial slope on the time, in which samples were stored on ice, was investigated. The initial slope appeared to be also dependent on the time cells were incubated on ice. Hence, the calculated slopes of the kinetics in the presence of exogenous lipids were corrected with a fitness factor obtained by a calibration curve for the initial slope calculated as outlined before. The corrected values of individual experiments were again fitted with a linear function giving the linear dependence of the initial slope relative to the lipid concentrations as shown by Farge et al. (1999).

Estimated values for the inclines and SEM are presented in Table 4.3 reflecting the standardised linear increase or decrease of the initial slope per percent of the respec-

Table 4.3: Inclines of initial slopes of bulk flow endocytic activity (BFEA) of K562 cells. Inclines were standardised and estimated relative to the percentage of exogenously added lipids (%EL) as presented by Farge et al. (1999). See text for an explanation of the calculation.

	Initial Slope Inclines of BFEA [% ·(min·%EL)$^{-1}$]	
	30 °C	37 °C
C_6-PS	-0.013 ± 0.006	0.003 ± 0.010
dialkyl-C_6-PS	0.000 ± 0.002	-
C_6-PE	-	0.007 ± 0.020
C_6-PC	-0.003 ± 0.006	-0.015 ± 0.014

tive exogenously added lipid (%EL) and per minute of measuring the initial slope. Even though only the kinetics with lower amounts of C_6-PS were accounted for the calculation, because of the diminishment of BFEA at concentrations higher than 2 % at 30 °C and higher than 4 % at 37 °C (see Fig. 4.7 and 4.8), the incline of the measurements performed at 30 °C was negative and only slightly positive at 37 °C. For comparison, the value for exogenous C_6-PS at 37 °C was estimated to be 0.003 ± 0.010 % ·(min·%EL)$^{-1}$, whereas Farge obtained a value of 1.1 ± 0.4 % ·(min·%PS)$^{-1}$. Also for dialkyl-C_6-PS only kinetics with lipid concentrations lower than 6 % were accounted, but the initial slopes did not depend on the lipid concentration. The highest positive incline of 0.007 ± 0.020 % ·(min·%EL)$^{-1}$ was observed for C_6-PE at 37 °C, in which all kinetics from 0.5 % to 2 % C_6-PE were taken into account. For C_6-PC, a lipid that was expected to inhibit endocytosis, the calculation presented a decline for both temperatures, but it was at 30 °C lower and at 37 °C only a little steeper than the decline of C_6-PS at 30 °C. Thus, considering the highest estimated incline, an increase in the bulk flow kinetics of a factor of 1.028 was found for an addition of 4 % C_6-PE, whereas Farge estimated an increase of a factor of about five for an addition of 4 % C_6-PS.

BHKasc$^+$ Cells

Up to date, the influence of exogenous lipids on bulk flow endocytosis was only shown for the suspension cell line K562 (Farge et al., 1999). To determine whether the endocytic activity of other cell lines can also be influenced, the experiments were repeated using BHKasc cells. This is a cell line with inducible expression of clathrin heavy chain antisense RNA (Iversen et al., 2001), in which activation of antisense RNA causes an

inhibition of clathrin heavy chain expression and, hence, clathrin-mediated endocytosis. For the investigation of BFEA in this cell line, only BHKasc$^+$ cells still undergoing clathrin-mediated endocytosis were used.

First of all, it was tested whether these cells also show a loss of BFEA when they are incubated on ice. Experiments to quantify the loss of fitness were performed as described in 4.1.1. Also for this cell line, a loss of fitness with the incubation on ice was found that was evaluated for the calculation of a calibration curve as described above. The decrease of activity with time on ice, which also showed a mono-exponential correlation, was at 30 °C higher than for K562 cells at 30 °C, but similar to the decrease found for K562 cells at 37 °C. For instance, after 45 minutes the activity of BHKasc$^+$ cells was down to 51 % and the activity of K562 cells was reduced to 52 % at 37 °C and 68 % at 30 °C.

Subsequently, measurements including the addition of exogenous lipids were performed at 30 °C. Figure 4.9 demonstrates the results for different amounts of C_6-PS and lyso-PC in one dimensional scatter plots. This time lyso-PC instead of C_6-PC was chosen to represent a lipid species that remains on the outer leaflet of the plasma membrane, because in some cell lines C_6-PC is partially translocated to the inner leaflet (Pomorski et al., 1999). For BHKasc cells it was not known whether C_6-PC is translocated and by applying lyso-PC it was assured that the added lipids remain on the outer layer. Although C_6-PS was known to be translocated to the inner leaflet and, hence, was expected to stimulate endocytosis, all but one value of BFEA at all applied lipid concentrations were lower than 100 %. After both recording times, 2 and 10 minutes, means of BFEA were comparable and exhibited a similar trend of a small upward drift with the amount of added C_6-PS, for instance from 75 ± 18 % at 1 % C_6-PS to 90 ± 1 % at 4 % C_6-PS after 10 minutes. At 2 % C_6-PS the changes to 81 ± 7 % BFEA after 2 minutes and to 86 ± 8 % BFEA after 10 minutes were estimated to be significant with p-values of 0.021 and 0.050, respectively.

Accordingly, when cells were incubated with different amounts of lyso-PC, which is known to remain on the outer layer of the plasma membrane, all determined values of BFEA were lower than the activities of control samples. This inhibition of BFEA increased with the amount of added lyso-PC from 86 ± 8 % at 1 % lyso-PC to 74 ± 9% at 4 % lyso-PC after 2 minutes and was significant with $p = 0.015$ at 2 % lyso-PC after 2 minutes and for all applied concentrations after 10 minutes of recording the FITC signal. Means of BFEA, SEM, and p-values for significant changes are summarised in Table 4.4.

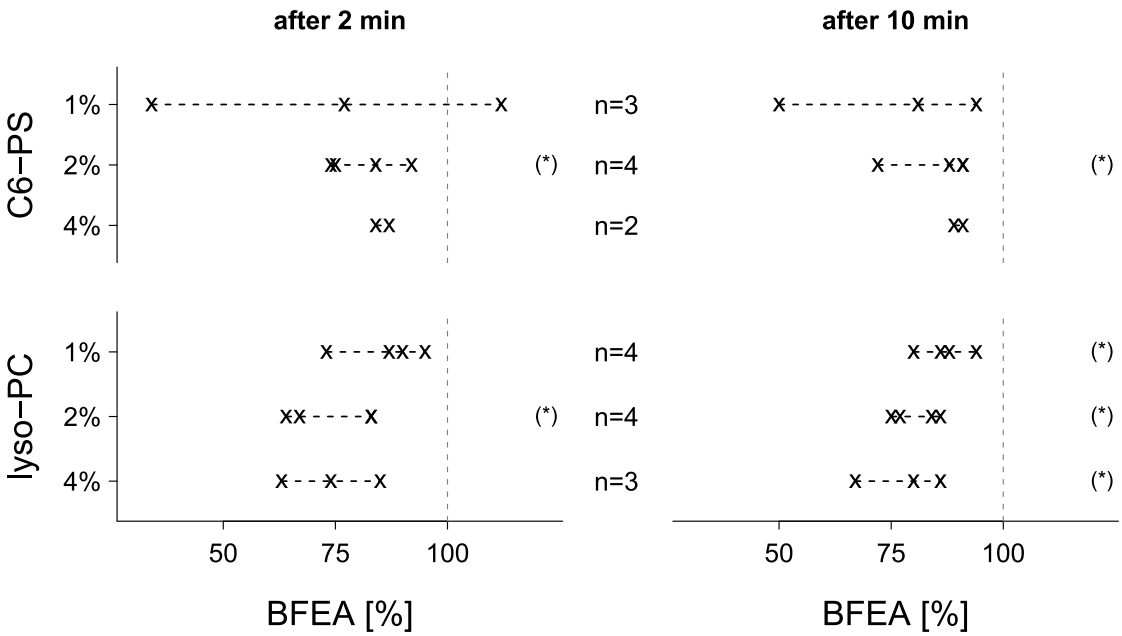

Figure 4.9: Bulk flow endocytic activity (BFEA) of BHKasc$^+$ cells at 30 °C. FITC labelled cells were incubated with various exogenous lipids for 1 min on ice and resulting BFEA after 2 and 10 min of recording was related to control activities (100 %) and corrected with a fitness factor. The percentage of BFEA of each measurement is illustrated in one dimensional scatter plots with n in the respective line. Changes were tested for significance with an one sample t-test ($*$, $p \leq 0.05$).

Table 4.4: Values of bulk flow endocytic activity (BFEA) of BHKasc$^+$ cells. FITC labelled cells were incubated with either C_6-PS or lyso-PC for 1 min on ice and BFEA was measured at 30 °C. The table presents resulting means and SEM of BFEA in percent [%]. When changes were significantly different from 100 % activity, also p-values obtained with an one sample t-test are included in parentheses ($p \leq 0.05$).

	C_6-PS		lyso-PC	
	2 min	10 min	2 min	10 min
1 %	74 ± 32	75 ± 18	86 ± 8	87 ± 5 (0.020)
2 %	81 ± 7 (0.021)	86 ± 8 (0.050)	74 ± 9 (0.015)	81 ± 5 (0.005)
4 %	86 ± 2	90 ± 1	74 ± 9	78 ± 8 (0.049)

Summarising the influence of exogenous lipids on bulk flow endocytic activity of K562 and BHKasc$^+$ cells investigated following the improved protocol, it could be shown that BFEA of K562 cells was significantly stimulated by lipids that are known to be translocated to the inner leaflet of the plasma membrane. In the presence of C_6-PS, this stimulation was higher and significant at more applied lipid concentrations when measurements were performed at 30 °C instead of 37 °C. A significant enhancement of BFEA of K562 cells could also be shown for the exogenous lipids DLPS and C_6-PE, whereas dialkyl-C_6-PS seemed to have no influence on the activity under the chosen conditions. Also an inhibition by lipids known to remain on the outer leaflet of the plasma membrane was observed, but this significant decrease of BFEA by C_6-PC could only be shown when 4 % C_6-PC were applied and measurements were performed at 30 °C. At lower lipid concentrations, C_6-PC had no distinct influence on BFEA.

Additionally, it could also be shown for BHKasc$^+$ cells that BFEA is effected by exogenous lipids. In contrast to the results for K562 cells, C_6-PS had no stimulating but an inhibiting influence, which was significant when 2 % C_6-PS were present. BFEA was likewise decreased when lyso-PC was applied. This partial inhibition was significant for all applied lipid concentrations after 10 minutes of measuring the activity and increased with the amount of added lipids.

Thus, in addition to the reproduced influence of exogenous C_6-PS and C_6-PE on BFEA of K562 cells, which was already presented by Farge et al. (1999), it was observed that BFEA of K562 cells is also effected by other exogenous lipids, namely DLPS and C_6-PC, and that this influence was significant at certain lipid concentrations. Moreover, the influence of exogenous lipids on BFEA was supplementary shown for a second cell line. BFEA of BHKasc$^+$ cells was significantly inhibited in the presence of C_6-PS and lyso-PC.

4.2.2 Clathrin-Independent Bulk Flow Endocytosis

In addition to the influence of exogenous lipids on bulk flow endocytosis of K562 and BHKasc$^+$ cells, the effect on clathrin-independent bulk flow endocytosis in different cell lines was also examined. Clathrin-independent bulk flow endocytic activity (CI-BFEA) implies the unspecific uptake of cell surface proteins into acidic compartments via all endocytic pathways aside from the clathrin-mediated pathway. The experiments were again performed with the spectrofluorometric assay following the improved protocol,

but for these examinations clathrin-mediated endocytosis of the different cell lines was inhibited as explained below.

K562 Cells

To inhibit clathrin-mediated endocytosis in K562 cells, cells were treated with chlorpromazine (CPZ) before and while performing the assay. The cationic amphiphilic drug CPZ abolishes the formation of clathrin-coated endocytic vesicles by interfering with the interaction between the adapter protein AP-2 and the clathrin-coated pit lattice (Wang et al., 1993). Before relieving the cells from growth medium, CPZ was added to a final concentration of 56 μM CPZ followed by an incubation for 30 minutes at 37 °C and 5 % CO_2. Then the spectrofluorometric assay was executed as before (see clause 3.2; improved order) but with 56 μM CPZ present in all media and buffers. The inhibition of the clathrin-mediated endocytic pathway by chlorpromazine differs from cell line to cell line in a dose dependent manner (Colin et al., 2005). The CPZ concentration of 56 μM was chosen according to previous studies showing a reduction in the number of LDL receptors on the cell surface to about 30 % (Wang et al., 1993) and a complete block of equine arteritis virus entry into BHK-21 cells via clathrin-dependent endocytosis (Nitschke et al., 2008). Furthermore, at this concentration LDL receptors begin to disappear from the cell surface immediately after cells are exposed to CPZ and the maximum loss of receptors occurs after an incubation of 30 minutes (Wang et al., 1993). Therefore, cells were preincubated with CPZ for 30 minutes to ensure the effectual inhibition of clathrin-mediated endocytosis before labelling the cells with FITC and performing the subsequent measurements to investigate CI-BFEA of K562 cells.

First of all, the loss of fitness with time cells were stored on ice was estimated as explained before (see 4.1.1). The obtained calibration curve showed a mono-exponential loss of fitness which was slightly faster than the fitness decline of untreated cells. For example, the activity of cells treated with CPZ was decreased to 60 % after 45 minutes on ice measured at 30 °C, whereas the activity of untreated cells was 68 % under the same conditions. The following values of CI-BFEA were all corrected with a fitness factor obtained by the calibration curve of the loss of fitness of cells treated with CPZ.

In order to test the effect of chlorpromazine on the endocytic activity of K562 cells, untreated cell samples (without CPZ) and cell samples treated with CPZ were prepared at the same time and the endocytic activity was recorded with the spectrofluorometric assay. This procedure allowed to verify the reduction of bulk flow endocytic activity

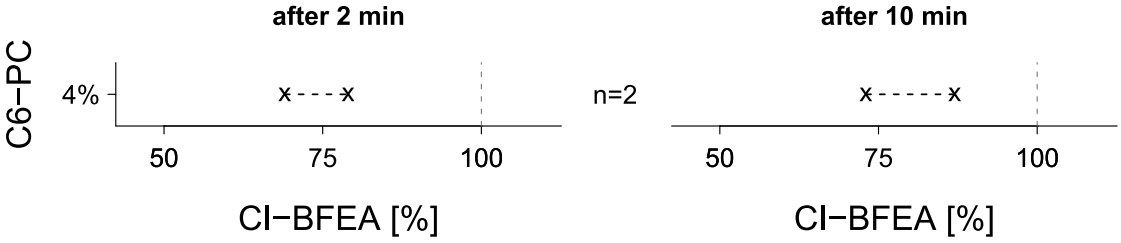

Figure 4.10: Clathrin-independent BFEA (CI-BFEA) of K562 cells at 30 °C. To inhibit the clathrin-mediated pathway, cells were treated with chlorpromazine and analysed as before. FITC labelled cells were incubated with exogenous C_6-PC for 1 min on ice and the resulting CI-BFEA after 2 and 10 min of recording at 30 °C was related to the respective activity of controls (100 %), which were also treated with chlorpromazine but not incubated with lipids, and subsequently corrected with the fitness factor. Activities are shown in one dimensional scatter plots with n given in the respective line. Changes were tested for significance with an one sample t-test, but inhibitions were not significantly different from 100 % activity ($p \leq 0.05$).

when the clathrin-mediated pathway was inhibited. Compared to the activity of untreated cells, the endocytic activity of cells treated with CPZ was significantly reduced to 71 ± 7 % with $p = 0.026$ after 2 minutes and down to 68 ± 20 % after 10 minutes of recording, which was measured in three independent experiments.

As illustrated in Figure 4.10, the influence of exogenous lipids on the activity of CI-BFEA was studied by the addition of C_6-PC. The experiments were performed as before and resulting activities were related to the respective activities of controls, which were not incubated with exogenous lipids but also treated with CPZ. The addition of 4 % C_6-PC resulted in a distinct decrease of CI-BFEA. This could be shown in two independent setups and the same amount of lipids led to a relatively equal inhibition in both experiments: 69 % and 79 % after 2 minutes as well as 73 % and 87 % after 10 minutes of recording. This indicates an inhibition of CI-BFEA of K562 cells by C_6-PC, which seems to be stronger after 2 than after 10 minutes of measuring endocytic activity. Compared to the results of BFEA of the same cell line not treated with CPZ, thus still undergoing clathrin-endocytosis, and determined with the same technique, the inhibition by 4 % of C_6-PC was lower: 46 ± 7 % BFEA ($n = 3$) compared to 74 ± 5 % CI-BFEA ($n = 2$), both evaluated after 2 minutes. Although the number of independent experiments is very low for the investigation of CI-BFEA in K562 cells, the low variation of the obtained activities suggest some confidence of this result, which indicates a distinct inhibition of CI-BFEA of K562 cells by exogenous C_6-PC, which was lower than the inhibition of BFEA of K562 cells at the same amount of exogenous C_6-PC.

BHKasc$^-$ Cells

The influence of exogenous lipids on clathrin-independent bulk flow endocytosis was verified with BHKasc cells, this time using BHKasc$^-$ cells. In BHKasc cells the expression of clathrin heavy chain antisense RNA can be induced by removing tetracycline (TET) from the growth medium leading to the inhibition of clathrin-mediated endocytosis (Iversen et al., 2001; Ter-Avetisyan et al., 2009). After 18 hours of induction of this expression, the internalisation of transferrin was shown to be inhibited by about 90 % (Iversen et al., 2003). Thus, TET was removed from growth medium 18 to 20 hours before experiments were started and CI-BFEA of BHKasc$^-$ cells expressing clathrin heavy chain antisense RNA and, hence, not undergoing clathrin-mediated endocytosis was analysed as before, but lacking tetracycline in all applied media and buffers.

Also BHKasc$^-$ cells showed a loss of fitness with time cells were incubated on ice, which was faster than the fitness reduction of BHKasc$^+$ cells, which are still undergoing clathrin-mediated endocytosis. For instance, after 30 minutes on ice, endocytic activity of BHKasc$^-$ cells was reduced to 55 %, whereas the activity of BHKasc$^+$ cells was still at 65 % of control activity when measurements were executed at 30 °C.

To be able to compare the bulk flow endocytic activity of BHKasc cells either still undergoing clathrin-mediated endocytosis, namely BHKasc$^+$ cells, or lacking the clathrin-mediated pathway, i.e. BHKasc$^-$ cells, the same passage of BHKasc$^+$ cells was seeded out into two different culture flasks. Then, TET had been removed from one of the two flasks 18 to 20 hours before the experiment was started. Following, both forms of BHKasc cells, BHKasc$^+$ and BHKasc$^-$ cells, were biotinylated and labelled in the same experimental setup, but all media and buffers comprising and lacking TET, respectively. After measuring BFEA of BHKasc$^+$ cells and CI-BFEA of BHKasc$^-$ cells as previously described, the values of activity were corrected with the fitness factor obtained for the respective form of BHKasc cells. Then, BFEA values of BHKasc$^+$ cells were related to CI-BFEA values of BHKasc$^-$ cells, resulting in 98 ± 22 % after 2 minutes of measuring. This was obtained in 10 independent experiments, indicating that the amount of unspecifically internalised FITC into acidified endocytic vesicles was not significantly different in BHKasc$^+$ cells, which were undergoing clathrin-mediated endocytosis, and in BHKasc$^-$ cells, in which clathrin-mediated endocytosis was inhibited.

Subsequently, the influence of exogenous lipids on CI-BFEA of BHKasc$^-$ cells was quantified as explained before and is illustrated in Figure 4.11 presenting the percentage

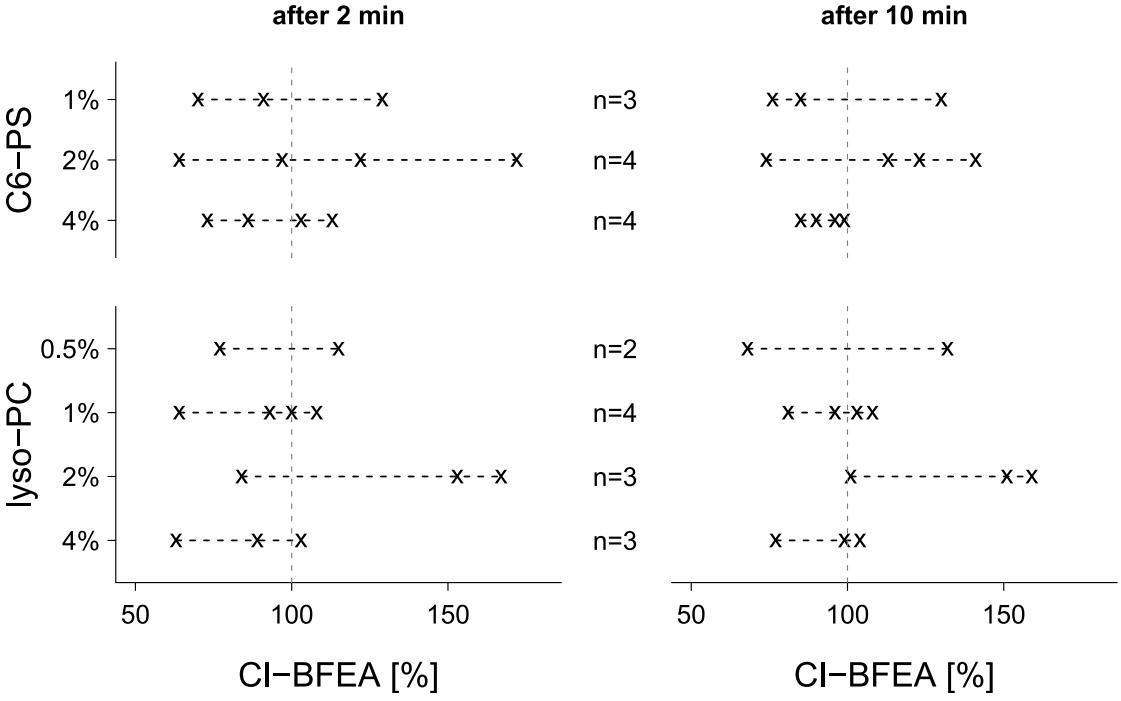

Figure 4.11: Activity of clathrin-independent bulk flow endocytosis (CI-BFEA) of BHKasc$^-$ cells at 30 °C. FITC labelled cells were incubated with different amounts of either C_6-PS or lyso-PC for 1 min on ice, the resulting CI-BFEA after 2 and 10 min of recording at 30 °C was related to the respective activity of controls (100 %) and subsequently corrected with the fitness factor. The percentage of CI-BFEA is plotted for each measurement in one dimensional scatter plots with the number of independent experiments n in the respective line. Changes were tested for significance with an one sample t-test, but none of the changes was significantly different from 100 % activity ($p \leq 0.05$).

of CI-BFEA for each measurement in one dimensional scatter plots. When cells were incubated with different amounts of C_6-PS, the resulting values of CI-BFEA varied around 100 % activity. Although there was a slight upward trend from 97 ± 24 % to 114 ± 39 % CI-BFEA after 2 minutes of recording, when cells were incubated with 1 % and 2 % of C_6-PS, respectively, the changes were not significant and the variation was increasing with the amount of added lipids. When 4 % C_6-PS were applied, the activity diminished to a mean of 94 ± 15 % after 2 minutes of recording. All together, the means of CI-BFEA were very similar after 2 and 10 minutes of recording the FITC signal.

In contrast to the clear and mainly significant inhibition of BFEA in BHKasc$^+$ cells by lyso-PC, CI-BFEA in BHKasc$^-$ cells was not inhibited by the addition of lyso-PC. The

Table 4.5: Values of clathrin-independent bulk flow endocytic activity (CI-BFEA) of BHKasc$^-$ cells. FITC labelled cells were incubated with either C_6-PS or lyso-PC for 1 min on ice and CI-BFEA was determined at 30 °C. The table shows resulting means and SEM of CI-BFEA in percent [%]. Changes were tested for significance at the 0.05 level with an one sample t-test, but none of the changes was significantly different from 100 %.

	C_6-PS		lyso-PC	
	2 min	10 min	2 min	10 min
0.5 %	-	-	96 ± 19	100 ± 32
1 %	97 ± 24	97 ± 24	91 ± 17	97 ± 10
2 %	114 ± 39	113 ± 25	135 ± 36	137 ± 26
4 %	94 ± 15	93 ± 5	85 ± 17	93 ± 12

determined values of CI-BFEA varied around 100 % for each but one applied concentration of exogenous lyso-PC. Surprisingly, at a concentration of 2 % lyso-PC the activities increased to means around 135 % after both recording times, although at lower and higher concentrations of lyso-PC the means were somewhat less than 100 %. Clathrin-independent bulk flow endocytic activity of BHKasc$^-$ cells in the presence of exogenous C_6-PS and lyso-PC is summarised in Table 4.5 giving means and SEM. These results indicate that, contrary to the observations for BFEA of BHKasc$^+$ cells and CI-BFEA of K562 cells, CI-BFEA of BHKasc$^-$ cells is most likely not influenced by the applied exogenous lipids.

Summarising the results of the influence of exogenous lipids on CI-BFEA of the two investigated cell lines, it could be shown that also CI-BFEA of K562 cells is influenced by exogenous lipids. It is decreased in the presence of exogenous C_6-PC and this inhibition was lower than the inhibition of BFEA of K562 cells by the same exogenous lipid at the same concentration. Contrary to the results for BFEA of BHKasc$^+$ cells, CI-BFEA of BHKasc$^-$ cells is most likely not influenced by the exogenous lipids C_6-PS and lyso-PC.

4.2.3 Clathrin-Mediated Endocytosis

As clathrin-mediated endocytosis is the best characterised endocytic pathway and many proteins involved and able to induce membrane curvature are known, it was of particular interest to check the influence of exogenous lipids on this pathway. For the examination, the spectrofluorometric assay was slightly changed as defined in clause 3.3. Briefly, instead of unspecifically labelling cell surface proteins with FITC, transferrin conjugated

to FITC was used to specifically follow the uptake via clathrin-mediated endocytosis based on the pH sensitivity of FITC and the acidification of early endosomes. Incubation with exogenous lipids, spectrofluorometric measurements of the FITC signal, and analyses of the clathrin-mediated endocytic activity (CMEA) were performed as before following the improved protocol.

K562 Cells

At first, the influence of exogenous lipid on CMEA was investigated in K562 cells. For the standardisation and to be able to compare different measurements with each other, the fitness reduction of CMEA with time samples were stored on ice was quantified. Here, the resulting mono-exponential decay with time was slower than in the measurements of bulk flow endocytosis. When CMEA was recorded at 30 °C, the activity after 60 minutes was still 94 % for clathrin-mediated endocytosis, whereas it was only 59 % for bulk flow endocytosis after the same time and at the same temperature.

Subsequently, the change in CMEA in the presence of exogenous lipids was quantified as before, including the correction of CMEA values by a fitness factor, and is illustrated in Figure 4.12, which presents the percentage of CMEA for each measurement in one dimensional scatter plots with the number of independent experiments n in the respective line. The addition of short chain PC caused a significant inhibition after 2 minutes of recording the FITC signal at both applied lipid concentrations, 2 % as well as 4 % C_6-PC. At 2 % C_6-PC the mean of CMEA after 2 minutes was 82 ± 1 % with a p-value of

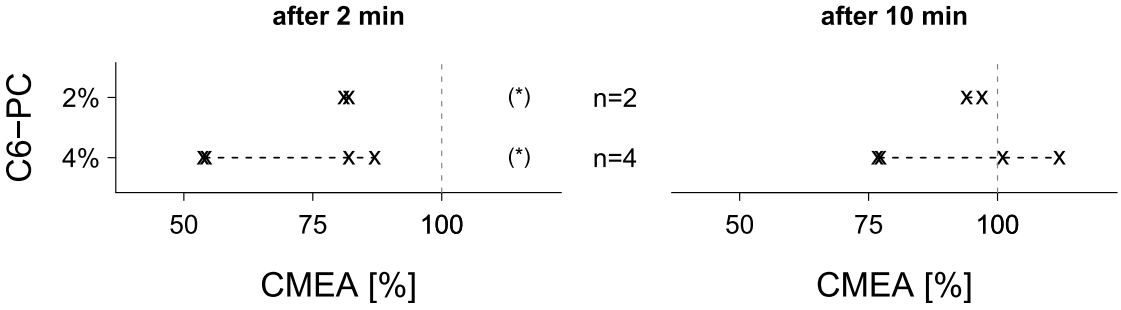

Figure 4.12: Clathrin-mediated endocytic activity (CMEA) of K562 cells at 30 °C. Cells were labelled with transferrin-FITC, incubated with exogenous C_6-PC for 1 min on ice, and CMEA was spectrofluorometrically analysed. The percentage of CMEA of each measurement is presented in one dimensional scatter plots with n in the respective line. Changes were tested for significance with an one sample t-test ($*$, $p \leq 0.05$).

0.017 and at 4 % C_6-PC the mean was 69 ± 15 % with a p-value of 0.040, suggesting an increasing inhibition of CMEA with the amount of added C_6-PC. After 10 minutes of recording, the inhibition was smaller and not significant, but the means were also decreasing with the amount of added lipids: 96 ± 2 % at 2 % C_6-PC and 92 ± 15 % at 4 % C_6-PC. This was shown in two independent experiments for 2 % C_6-PC and in four experiments for 4 % C_6-PC. Thus, these results showed an inhibiting influence of exogenous C_6-PC on CMEA of K562 cells. As for BFEA of K562 cells, the obtained values showed the following trend: an increasing inhibition of activity with the amount of added exogenous lipids, which is distinctly stronger after 2 minutes than after 10 minutes of measuring the fluorescence signal.

BHKasc Cells

To underline the results for the influence of exogenous lipids on clathrin-mediated endocytosis in K562 cells, the effect of exogenous lipids on CMEA of a second cell line was tested. This time BHKasc$^+$ cells, still undergoing clathrin-mediated endocytosis, as well as BHKasc$^-$ cells, in which clathrin-mediated endocytosis is inhibited, were used. By using both, BHKasc$^+$ and BHKasc$^-$ cells, the effectual inhibition of clathrin-mediated endocytosis in BHKasc$^-$ cells could additionally be determined. As before, at first the influence of the time cell samples were stored on ice on the activity of control samples was determined. For this purpose, BHKasc$^+$ as well as BHKasc$^-$ cells from the same cell passage were prepared in the same experimental setup (see 4.2.2), incubated with transferrin-FITC, and clathrin-mediated activity was measured by spectrofluorometry in the absence of exogenous lipids.

Surprisingly, quantification showed that BHKasc$^-$ cells had about the same extent of CMEA as obtained for BHKasc$^+$ cells. Therefore, the effectual inhibition of clathrin-mediated endocytosis in BHKasc$^-$ cells was visually tested by fluorescence microscopy. BHKasc$^+$ and BHKasc$^-$ cells were incubated with transferrin conjugated to tetramethyl-6-rhodamine (Tf-TMR) for 20 minutes at 37 °C and 5 % CO_2 and then rapidly transferred to ice to stop the uptake of tracers. After washing the labelled cells, microscopic images were taken to visualise the uptake of Tf-TMR. Since BHKasc cells grow in adherent layers and need to be detached for measurements with the spectrofluorometric assay, the visualisation of transferrin uptake was performed not only for adherent but also for detached BHKasc cells. The images of BHKasc$^+$ and BHKasc$^-$ cells labelled with Tf-TMR in either adherent culture or in suspension are shown in Figure 4.13. When

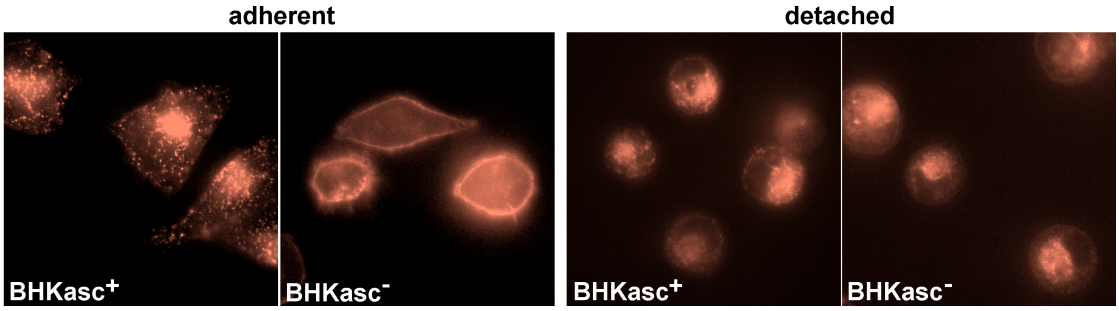

Figure 4.13: Transferrin uptake of adherent and detached BHKasc cells. BHKasc$^+$ and BHKasc$^-$ were grown either in adherent culture or in suspension and incubated with transferrin conjugated to TMR for 20 min at 37 °C and 5 % CO_2. When adherent cells were examined, labelled transferrin was taken up into the cell in BHKasc$^+$ cells but remained attached to the plasma membrane in BHKasc$^-$ cells, what clearly showed the inhibition of clathrin-mediated endocytosis in BHKasc$^-$ cells. In contrast, when cells were detached before incubated with transferrin, tracers were taken up in BHKasc$^+$ as well as in BHKasc$^-$ cells.

adherent cells were incubated with Tf-TMR, inner compartments of BHKasc$^+$ cells were labelled, whereas in BHKasc$^-$ cells TMR-labelled transferrin remained attached to the plasma membrane and was not taken up into cells. This showed clearly the clathrin-mediated uptake of Tf-TMR into BHKasc$^+$ cells and the inhibition of clathrin-mediated endocytosis in BHKasc$^-$ cells when cells were grown in adherent cultures. In contrast to these observations in adherently growing cells, the inhibition of clathrin-mediated endocytosis in BHKasc$^-$ cells did not work when cells were detached before incubated with Tf-TMR as done for the spectrofluorometric assay. When cells were in suspension, inner compartments of cells were labelled by Tf-TMR in BHKasc$^+$ as well as in BHKasc$^-$ cells and no visual difference of transferrin uptake between BHKasc$^+$ and BHKasc$^-$ cells could be observed.

As discussed in the introduction, cells most likely adapt the extent of specific endocytic pathways to their cellular and environmental conditions. The microscopic images of detached BHKasc cells illustrated that the inhibition of clathrin-mediated endocytosis in BHKasc$^-$ cells is not assured when adherently growing cells were detached for the measurements in the spectrofluorometric assay. To avoid the investigation of specific receptor-mediated pathways in cells that may have adapted the regulation of endocytic pathways due to their treatment, another technique was chosen to analyse clathrin-mediated endocytosis in BHKasc cells. For flow cytometric analyses the cells can be kept in adherent cultures during the incubation with labelled transferrin to specifically

follow clathrin-mediated endocytosis and need to be detached for the cytometric measurements only at the very end of the assay. At this time point, the quantitative uptake of transferrin is already stopped by transferring the samples on ice. Subsequently, the remaining transferrin is detached from the cell surface before the detachment of cells, which assures that labelled transferrin cannot be taken up due to altered endocytic activities (for detailed description see clause 3.4).

For this flow cytometric assay, it was first tested whether different samples could be compared with each other. Therefore, several control samples without the addition of exogenous lipids were prepared in the same experimental setup as follows: labelled transferrin was added to cell samples followed by an incubation for definite intervals at 37 °C and 5 % CO_2. After the incubation, remaining label on the cell surface was detached by an acidic wash and clathrin-mediated endocytic activity at different time points was analysed by flow cytometric quantification of intracellular fluorescence intensities. Figure 4.14 A demonstrates typical kinetics of intracellular fluorescence intensities as a measure of CMEA plotted against time of label incubation at 37 °C. Illustrated is one out of four independent experiments with BHKasc$^+$ cells giving an example for the very low variation and good reproducibility of control samples. The same was obtained for BHKasc$^-$ cells in two independent experiments. Taken together, the relation of CMEA of control samples to each other, in which the activity of the first sample was set as 100 %, resulted in a variation of controls of 100 ± 2 % after 2 minutes, 100 ± 3 % after 5 minutes, 100 ± 3 % after 10 minutes, 100 ± 2 % after 20 minutes, and 100 ± 3 % after 30 minutes of cell incubation with labelled transferrin. This assured that different samples, prepared in the same experimental setup, were remarkable well comparable without considering, for instance, a loss of fitness with time samples are stored on ice.

As a next step, the inhibition of clathrin-mediated endocytosis in BHKasc$^-$ cells was verified by relating the activity of BHKasc$^-$ control samples to the activity of BHKasc$^+$ control samples prepared in the same setup. It could be shown that CMEA of BHKasc$^-$ cells was significantly reduced to a mean of 55 ± 11 % with $p = 0.031$ after 2 minutes and to 87 ± 1 % with $p = 0.004$ after 20 minutes when BHKasc$^-$ cells were cultured in the absence of tetracycline for 18 hours. This was evaluated in three independent experiments. In other studies, the transferrin internalisation of this cell line was shown to be inhibited by 90 % after 18 hours of antisense RNA expression (Iversen et al., 2003). Compared to that, the inhibition of clathrin-mediated endocytosis in BHKasc$^-$ cells determined in the actual study was, although significant, distinctly lower.

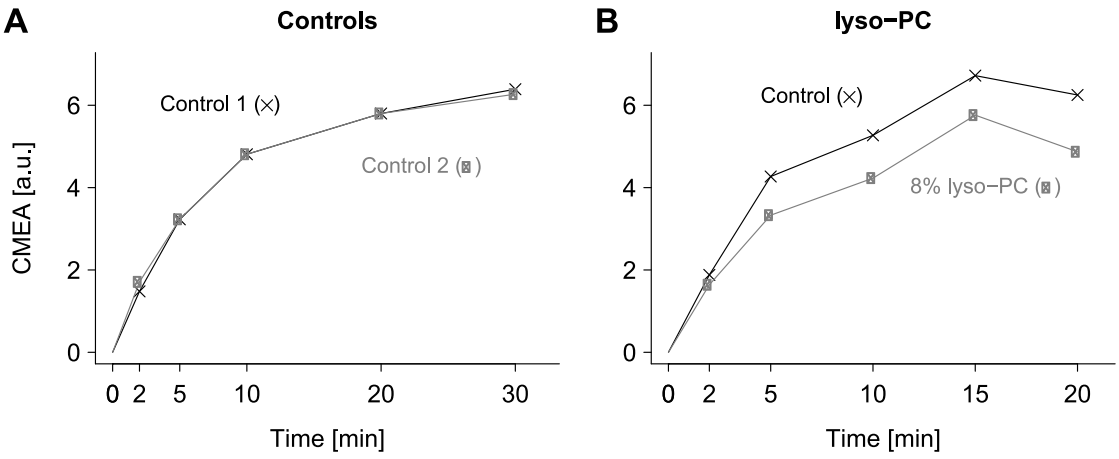

Figure 4.14: Typical kinetics of clathrin-mediated endocytic activity (CMEA) of BHKasc$^+$ cells obtained in flow cytometric measurements. BHKasc$^+$ cells were incubated with either only labelled transferrin (controls) or a mixture of labelled transferrin and exogenous lipids for definite times at 37 °C. After the detachment of remaining transferrin from the cell surface, endocytosed transferrin was quantified by flow cytometry. Intracellular fluorescence intensities as a measure of CMEA are plotted against time of label incubation at 37 °C. **A:** The comparison of two kinetics of controls prepared in the same experimental setup exemplarily illustrates the very low variation and good reproducibility of samples. **B:** Typical kinetics are giving examples for the influence of exogenous lipids, in this case lyso-PC, on CMEA of BHKasc$^+$ cells. For complete results see Fig. 4.15.

Subsequently, the influence of exogenous lipids on clathrin-mediated endocytosis in BHKasc$^+$ as well as in BHKasc$^-$ cells was quantified by the incubation of cells with exogenous lipids. Different amounts of either C_6-PS, C_6-PC, or lyso-PC were added to the cell samples together with labelled transferrin, incubated for definite intervals at 37 °C, and intracellular fluorescence intensities were quantified by flow cytometry. In each independent experimental setup, a control sample was prepared together with samples containing exogenous lipids and, for subsequent analysis, intensities of samples incubated with lipids were related to intensities of control samples which were set as 100 %. In Figure 4.14 B kinetics of a control sample and a sample incubated with exogenous lipids, in this case lyso-PC, which were prepared in the same experimental setup, illustrate the influence of exogenous lyso-PC on CMEA of BHKasc$^+$ cells. This single experiment shows that lyso-PC inhibited CMEA at all evaluated time points. Statistical analysis of further experiments with different exogenous lipids is presented in Figure 4.15 in one dimensional scatter plots with the number of independent experiments n in the respective line. Here, values of time points after 2 minutes and 10 minutes incubation represent

the influence of the specific exogenous lipid on values of CMEA at all investigated time points.

In the presence of 4 % C_6-PS, which is thought to be translocated to the inner leaflet of the plasma membrane, the resulting CMEA of BHKasc$^+$ cells was decreased to 52 % after 2 minutes and down to 93 % after 10 minutes. This was consistent with the observation for the influence of C_6-PS on bulk flow endocytic activity in BHKasc$^+$ cells. BFEA of BHKasc$^+$ cells was as well decreased by the addition of C_6-PS and this inhibition was significantly different from 100 % activity when 2 % C_6-PS were applied (see Fig. 4.9). Although the decrease of CMEA in BHKasc$^+$ cells could be shown in only one experiment, this finding can be confirmed by comparing the result with the influence of C_6-PS on BFEA of the same cells, which also showed an inhibiting influence of C_6-PS on the respective endocytic activity.

In a like manner, at the same amount of C_6-PS, CMEA of BHKasc$^-$ cells was reduced to 76 % after 2 minutes and to 86 % after 10 minutes. Interestingly, a lower amount of C_6-PS, namely 1 %, added to the cells 10 minutes before labelled transferrin was applied, caused a lower inhibition: 83 % after 2 minutes and 88 % after 10 minutes. Although the number of experiments was again not sufficient for statistical analysis, the finding of an inhibition in two independent experiments and the very low variation of this assay suggest that an inhibition of CMEA of BHKasc$^-$ cells by exogenous C_6-PS is very likely. This inhibitory effect of C_6-PS on CMEA of BHKasc$^-$ cells was not in accordance with the results for CI-BFEA in BHKasc$^-$ cells. The influence of C_6-PS on CI-BFEA was fluctuating between stimulation and inhibition of activity and showed a high variation (see Fig. 4.11). Here, it must be pointed out that measurements for CI-BFEA were performed with detached cells whereas the experiments for CMEA were carried out with adherent BHKasc$^-$ cells. Thus, the results are in all likelihood not comparable due to differing endocytic activities of adherent and detached BHKasc$^-$ cells.

Since C_6-PC was shown to be partially translocated to the inner leaflet of some cell lines (Pomorski et al., 1999), it was not known whether C_6-PC remains on the outer monolayer of BHKasc cells, as it is the case for K562 cells, or is either partially or completely translocated to the inner leaflet. However, when 4 % of C_6-PC were added to BHKasc$^+$ cells, the determined activities were reduced to 84 ± 5 % after 2 minutes and to 91 ± 6 % after 10 minutes, which was shown in two independent experiments. This indicates that C_6-PC, which significantly inhibited CMEA of K562 cells (see Fig. 4.12), had also an inhibitory effect on CMEA of BHKasc$^+$ cells.

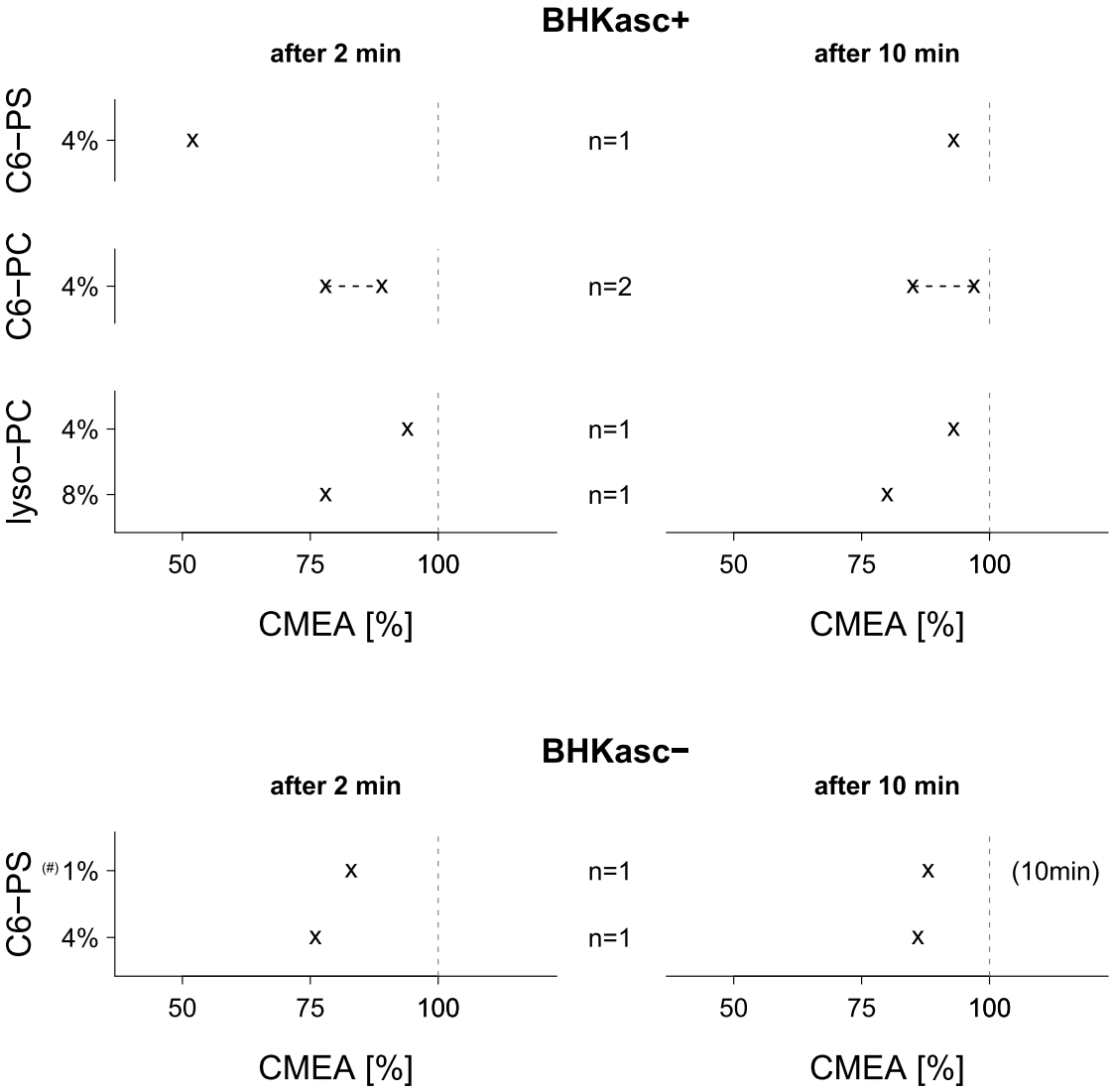

Figure 4.15: Clathrin-mediated endocytic activity (CMEA) of BHKasc cells at 37 °C. BHKasc$^+$ or BHKasc$^-$ cells were incubated with a mixture of labelled transferrin and exogenous lipids and resulting CMEA after 2 and 10 min of incubation with transferrin was analysed by flow cytometry and related to the activity of control samples, which were prepared in the same setup and set as 100 % activity. The percentage of CMEA is plotted for each measurement in one dimensional scatter plots with the number of independent experiments n in the respective line. Changes were tested for significance at the 0.05 level with an one sample t-test, but none of the changes was significantly different from 100 %. $^{(\#)}$ Indicated time (10 min) corresponds to incubation of cells with lipids at 37°C before transferrin was added. When no times are given, lipid and transferrin addition was simultaneous.

Furthermore, in the presence of lyso-PC, a lipid that remains on the outer layer, the resulting CMEA of BHKasc$^+$ cells was decreased at both applied lipid concentrations. At 4 % lyso-PC, CMEA was reduced to 94 % after 2 minutes and to 93 % after 10 minutes, and at 8 % lyso-PC, CMEA was down to 78 % after 2 minutes and to 80 % after 10 minutes. For comparison, in the presence of lyso-PC, BFEA of BHKasc$^+$ cells was also inhibited at all tested lipid concentrations and nearly all changes were significantly different from 100 % activity (see Fig. 4.9). Thus, the finding of an inhibition of CMEA in two independent experiments, the increasing inhibition with higher lipid concentrations, and the low variation of this assay suggest that lyso-PC had an inhibitory effect on CMEA of BHKasc$^+$ cells as it had on BFEA of BHKasc$^+$ cells.

Hep2 Cells

As a third cell line, Hep2 cells were chosen to investigate the influence of exogenous lipids on clathrin-mediated endocytosis. CMEA of this cell line was also quantified by flow cytometry and, at first, the variation of control samples was determined to ensure the comparability of different samples. As for BHKasc cells, control samples without exogenous lipids were prepared in the same experimental setup and obtained CMEA values of different control samples were related to each other. Also here, the variation was found to be very low. After 2 minutes of incubation with labelled transferrin at 37 °C, control samples showed an activity of 98 ± 2 % and, after 20 minutes, control activity was 99 ± 1 %, which was obtained in two independent experiments.

In order to test the influence of exogenous lipids on CMEA of Hep2 cells, different amounts of either C_6-PS or lyso-PC were added to the cell samples and activities were quantified as explained above. Resulting CMEA values are illustrated in Figure 4.16 presenting one dimensional scatter plots with the number of independent experiments n in the respective line. Changes were tested for significance with an one sample t-test at the 0.05 level, but none of the changes was significantly different from 100 %.

When either 4 % or 8 % of C_6-PS, which is thought to be translocated to the inner leaflet of the plasma membrane, were added to the cells, each but one value of CMEA was higher than 100 %. At 4 % of C_6-PS, the activity was with 95 % CMEA after 2 minutes slightly decreased but still in the range of control activity and enhanced to 107 % CMEA after 10 minutes. At 8 % of C_6-PS, resulting means were enhanced to 124 ± 2 % CMEA after 2 minutes and 126 ± 9 % CMEA after 10 minutes. This was obtained in two independent experiments. So far, the influence of exogenous lipids on endocytic activity

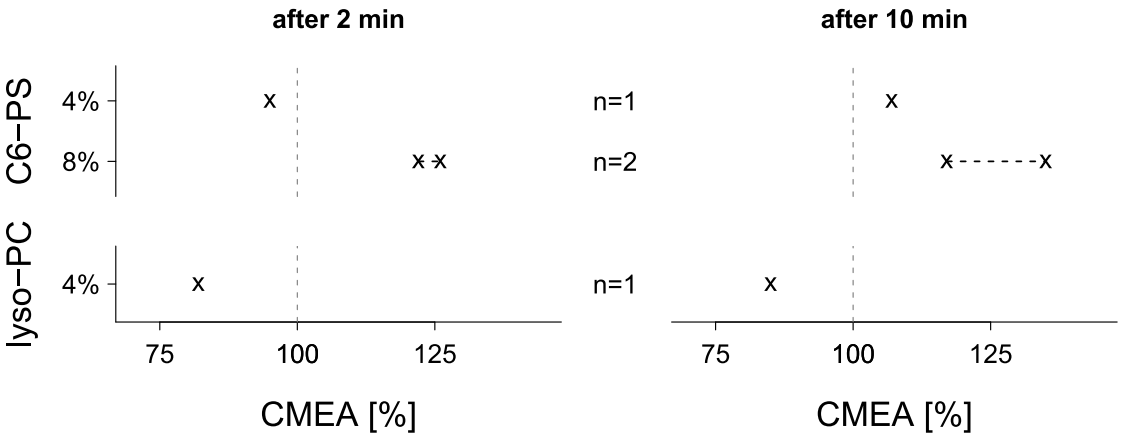

Figure 4.16: Clathrin-mediated endocytic activity (CMEA) of Hep2 cells at 37 °C. Hep2 cells were incubated with a mixture of labelled transferrin and exogenous lipids and resulting CMEA after 2 and 10 min of incubation with transferrin was analysed by flow cytometry and related to the activity of control samples, which were prepared in the same setup and set as 100 %.The percentage of CMEA is plotted for each measurement in one dimensional scatter plots with n in the respective line. Changes were tested for significance at the 0.05 level with an one sample t-test, but none of the changes was significantly different from 100 %.

of Hep2 cells has not been studied, therefore, these preliminary results cannot be compared to other findings, and the number of independent experiments is comparatively small. However, due to the very low variation of the flow cytometric assay and the observation, that CMEA values were increased at each but one reading point and that the enhancement was increasing with the amount of added C_6-PS, these results suggest an enhancement of CMEA of Hep2 cells by exogenous C_6-PS.

As for the investigations of bulk flow endocytic activity of BHKasc$^+$ cells, lyso-PC instead of C_6-PC was chosen to represent a lipid species that remains on the outer leaflet of the plasma membrane, since it was also not known whether C_6-PC remains on the outer monolayer of Hep2 cells or is either partially or completely translocated to the inner leaflet. However, when cells were incubated with 4 % of lyso-PC, CMEA values were lower than 100 % activity at all reading points, for instance 82 % CMEA after 2 minutes and 85 % CMEA after 10 minutes incubation. As above, this result cannot be compared to other findings and the inhibition by lyso-PC was shown in only one experiment. Here again, the very low variation of the used flow cytometric assay and the fact, that the inhibiting influence of lyso-PC was obtained for all of the five reading points, suggest some confidence of this preliminary result.

In conclusion, an influence of exogenous lipids on clathrin-mediated endocytic activity of three different cell lines could be shown using either a spectrofluorometric assay for the investigation of K562 cells or a flow cytometric assay for the measurements with BHKasc$^+$, BHKasc$^-$, and Hep2 cells. K562 cells clearly showed an inhibition of CMEA when exogenous C_6-PC was present, which was stronger after 2 minutes than after 10 minutes of measuring and lower than the inhibition of BFEA of K562 cells at the same concentration of C_6-PC obtained with the same technique. In line with the results for BFEA of BHKasc$^+$ cells, also CMEA of BHKasc$^+$ cells was decreased in the presence of C_6-PS as well as when lyso-PC was applied. Furthermore, CMEA of BHKasc$^+$ cells was also decreased when C_6-PC was added to the cells and this inhibition was slightly stronger than the inhibition by the same amount of lyso-PC. In contrast to the results of CI-BFEA of BHKasc$^-$ cells, the results indicated an inhibition of CMEA of BHKasc$^-$ cells by C_6-PS, but this was obtained with two different techniques. For the investigations of CI-BFEA, BHKasc$^-$ cells were detached before the experiments were started, whereas for the analysis of CMEA BHKasc$^-$ cells were still adherent while taking up the labelled transferrin. The inhibition of CMEA of BHKasc$^-$ cells seemed to be less strong than the inhibition of BHKasc$^+$ cells by the same amount of C_6-PS, which was obtained with the same technique. Also for the third investigated cell line, Hep2 cells, it was shown that CMEA was affected by the addition of exogenous lipids. These preliminary results indicate an enhancing effect of C_6-PS and an inhibiting influence of lyso-PC on CMEA of Hep2 cells.

CHAPTER 5

Discussion

Most studies to elucidate endocytic mechanisms have focused on involved proteins which are thought to be in control of cargo recruitment, pathway regulation, as well as the generation of high local curvature for the formation of endocytic vesicles out of a comparably flat plasma membrane (Mayor and Pagano, 2007; Sandvig et al., 2008; Doherty and McMahon, 2009). Structural properties of the plasma membrane, which needs to be shaped into endocytic invaginations, have been largely pursued with less attention and, hence, the role of membrane lipids composing the bilayer structure of plasma membranes may have been underestimated. In this regard, the present study aimed at investigating the influence of plasma membrane structural properties, which were altered by the addition of exogenous lipids, on the activity of endocytosis in living cells. For this purpose, the activity of bulk flow endocytosis either in- or excluding clathrin-mediated endocytic activity and clathrin-mediated endocytic activity by itself were determined in different cell lines. To be able to rigorously quantify the respective endocytic activity of living cells incubated with exogenously added lipids, activities were either monitored with a spectrofluorometric assay as originally established by Farge et al. (1999) or the internalisation of fluorescently labelled proteins was quantified by flow cytometry.

With the first assay, Farge and collaborators were able to qualitatively show the stimulation of bulk flow endocytosis in K562 cells by the addition of exogenous short chain phosphatidylserine (PS) or -ethanolamine (PE) as well as partially inhibited endocytosis by applying lyso-PS or cholesterol derivatives. Although following exactly the protocol

as described by Farge et al. (1999), the first experiments of the present study did not reproduce the enhancement of bulk flow endocytosis in K562 cells by the addition of exogenous short chain PS as shown by Farge et al. (1999). Thus, in the first part of this work the spectrofluorometric assay was successfully improved as represented in the first part of the previous chapter (see clause 4.1). These results will be discussed in the following clause with an concluding comparison of the two assays used in the present work. Subsequently, the improved spectrofluorometric as well as the flow cytometric assay were used to quantify changes of endocytic activity due to altered structural properties of the plasma membrane. Based on the previously presented results of these examinations (see clause 4.2), the influence of exogenous lipids on endocytic pathways of different cell lines will be discussed in the subsequent clauses of the present chapter.

5.1 Quantification of Endocytosis with the Spectrofluorometric Assay

5.1.1 Cells Loosing Their Fitness While Incubated on Ice

When the activity of bulk flow endocytosis in K562 cells was monitored with the spectrofluorometric assay, the first examinations could not show an enhancement by the addition of exogenous C_6-PS as presented in Farge et al. (1999). Instead, it was found that endocytic activity of cells showed a decrease with time cell samples were stored on ice during spectrofluorometric measurements, which originated a varying influence of exogenous lipids depending on the sequence of analysed samples. In order to achieve comparability of different measurements irrespective of the sequence of analyses, the spectrofluorometric assay was improved as follows: decreases of cell fitness with incubations on ice were exactly quantified gaining a fitness factor for the correction of endocytic activity values. However, also the correction of values by this fitness factor did not result in a consistent enhancement of endocytosis by the addition of C_6-PS (see Fig. 4.4) as shown by Farge et al. (1999).

Farge and coworkers did not take into account this reduction of activity with the incubation of cells on ice, but they always followed a specific sequence of measurements: first the sample of control cells was recorded and afterwards the sample with exogenous lipids (Emmanuel Farge, Curie Institute, Paris; personal communication). Assuming that their experiments held the same decrease of activity during time samples were

stored on ice, the enhancement of endocytic activity, when C_6-PS or C_6-PE were applied, would even be higher than estimated by Farge et al. (1999). In contrast, the inhibition of endocytosis, when lyso-PS or poly(ethylene)$_{50}$-glycol-cholesterol was added, would be lower, because part of the decrease would be due to the reduction of activity with the incubation on ice.

5.1.2 Influence of Label Concentration

Discussing these results with Emmanuel Farge, he suggested another possible explanation for the missing influence of C_6-PS in the present study. In his hands, the concentration of biotin during the biotinylation of cells was essential for the sensitivity in measuring endocytosis. Concentrating biotin too high could lead to a dequenching of fluorophors, which is associated to their dilution, and therefore compensate the pH-depending quenching effect during acidification of early endosomes. Interestingly, the concentrations applied by him (4 mg/ml biotin and 15 μg/ml streptadivin-FITC; Farge et al., 1999) were even higher than the concentrations recommended by the company (1 mg/ml biotin and 10 μg/ml streptadivin-FITC; http://www.perbio.com). However, experiments were then repeated using the higher concentrations as applied by Farge. First, the reduction of endocytic activity with time samples were incubated on ice was again precisely analysed. The resulting exponential decay was comparable to the decrease obtained in experiments using concentrations recommended by the company (see Fig. 4.5 A). Also the absolute extent of endocytic activity was not distinctly different at both concentrations. This indicates that higher label concentrations did not lead to a self-quenching of fluorophors on the cell surface. Subsequently, the measurements of endocytic activity of cells incubated with exogenous lipids were repeated using the higher label concentrations. This again did not result in a stimulating effect on endocytic activity of K562 cells when C_6-PS was added (see Fig. 4.5 B), suggesting that the application of higher label concentrations had, in the range of the applied concentrations, no influence on the determination of bulk flow endocytic activity.

5.1.3 Influence of Lipid Incubation and Temperature

As a further step to improve the assay, the sequence of cell incubation with lipids and cell labelling with FITC was inverted. When the assay was performed as outlined in Farge et al. (1999), the total incubation of cells with exogenously added lipids had

been nearly 2 hours before the first measurement was started: 15 or 30 minutes at 37 °C followed by about 75 minutes on ice. For further samples, it was even longer considering the time samples were stored on ice while the FITC signal of previous samples was recorded. Great care should be taken when cells are incubated with exogenous lipids for such long times. After incubations like this, the majority of exogenously added phospholipids is most likely not present anymore in the plasma membrane but released into other compartments within the cell. For NBD-labelled short chain PS, it could clearly be shown in microscopic studies that, directly after the addition of lipids and after an incubation of 30 minutes at 4 °C, the majority of label was still present in the plasma membrane of K562 cells. However, after an incubation for 30 minutes at 37 °C, the fluorophors were dispersed in the whole cell and staining of the plasma membrane was strongly reduced (see Fig. 4.6).

To bypass long incubations of cells with exogenous lipids, the spectrofluorometric assay was modified by inverting the sequence of cell incubation with lipids and cell labelling with FITC, which resulted in a highly reduced incubation period of cells with lipids at low temperatures. On the one hand, this created the detraction that the incubation of cells with exogenous lipids could only be performed below 10 °C, because above this temperature cells undergo endocytosis (Cribier et al., 1993) and therefore FITC-labelled surface proteins as well as exogenous lipids could be internalised into the cell before measurements were started. On the other hand, this assured that exceeding incubation times could be avoided and the majority of exogenously added lipids was still present in the plasma membrane when measurements were started.

Repeating the experiments with different amounts of various exogenous lipids in the inverted sequence of the assay, a significant influence of exogenous lipids on bulk flow endocytic activity of K562 cells could be obtained, which will be discussed in detail in the following (see 5.3.1).

Compared to the results of Farge et al. (1999), determined when cells were incubated with exogenous C_6-PS for 30 minutes at 37 °C before subsequent labelling on ice, the stimulation or inhibition of endocytic activity obtained in the present study was lower, especially at high concentrations of exogenous C_6-PS. The highest endocytic activity in the presence of C_6-PS was observed when a concentration of 1 % C_6-PS was applied: the resulting endocytic activity was around 1.8 times higher than the activity of control cells. However, the stimulation diminished with increasing amounts of added C_6-PS to 1.4 fold at 4 % C_6-PS. For comparison, Farge et al. (1999) found an equal stimulation

of about 1.7 fold at 1 % C_6-PS, but in his study the stimulation was further increasing with ascending amounts of lipids to about 4 fold at 4 % C_6-PS. This stimulating influence was explained by the changes of surface area relations in the plasma membrane due to the addition of exogenous lipids. As mentioned above, Farge and coworkers did not consider the decrease of activity with time samples were stored on ice. Assuming the same decrease as found in the present study, the stimulation estimated by him would even be higher. In contrast to the interpretation by Farge et al. (1999), it could be shown in the present study that the majority of exogenously added C_6-PS, after an incubation for 30 minutes at 37 °C, is not anymore present in the plasma membrane of K562 cells. This means that the majority of exogenously added lipids, or at least a large amount, cannot account for an increased surface area of one of the two layers, because most likely they are already released into the cell after such a long incubation. Thus, the strong influence of exogenous phospholipids on endocytic activity obtained by Farge et al. (1999) can only partly be explained by an alteration of surface areas of the two monolayers composing the plasma membrane bilayer.

Another possible explanation for a stimulating effect of exogenously added aminophospholipids on endocytosis, which may supplementary enhances endocytosis, is a specific activation of endocytosis due to the modified lipid composition of the plasma membrane. The plasma membrane of mammalian cells consists of about 15 % PS related to the total phospholipid amount of the plasma membrane (van Meer et al., 2008) and an addition of 4 % exogenous C_6-PS increases this amount to nearly 20 %. Moreover, when PS is exogenously added, it first incorporates into the outer leaflet of the plasma membrane. Cells need to avoid the exposure of PS on the cell surface for several reasons, for instance because it acts as a susceptibility signal for phagocytosis (Balasubramanian and Schroit, 2003; Fadok et al., 1992). As outlined in the introduction, cells are able to regulate the activity of endocytic pathways for the adaptation to specific conditions. Thus, it is most likely that the increased amount of PS in both leaflets and especially in the outer layer of the plasma membrane leads to specific mechanisms in order to retrieve a noncritical lipid composition of the plasma membrane. By the internalisation of parts of the plasma membrane and the subsequent sorting and/or degradation of PS, cells can achieve back the normal lipid composition.

Interestingly, data obtained in the present study suggest that the upregulation of bulk flow endocytic activity as a consequence of modified lipid composition takes at least 15 minutes at a temperature of 37 °C. When bulk flow endocytic activity of K562

cells was determined in the unimproved sequence of the assay with a preincubation of cells with lipids at 37 °C, a difference in the change of endocytic activity for different incubation times was obtained. The cells were incubated with lipids either for 15 or 30 minutes at 37 °C and the resulting change of endocytic activity was not significantly different from 100 % control activity for both incubation times (see Fig. 4.4). When cells were incubated with lipids for 15 minutes, all values varied around 80 % activity and the variation was, compared to the values obtained for an incubation of 30 minutes, very low. In contrast, when cells were incubated with C_6-PS for 30 minutes at 37 °C, the variation was very high and with increasing amounts of exogenous lipids most values of bulk flow endocytic activity were higher than 100 % up to more than 200 % in the presence of 6 % C_6-PS. This suggests that the specific mechanisms of cells which are triggered due to high concentrations of C_6-PS in the plasma membrane may include a subsequent upregulation of endocytic activity. However, in order to confirm this preliminary result, further investigations with different incubation times are required.

5.2 Comparison of the Assays: Spectrofluorometry versus Flow Cytometry

Although the spectrofluorometric assay used here is very sensitive to changes in endocytic activity and provides, in contrast to the flow cytometric assay, a continuous signal of endocytic activity, the implementation disclosed some huge drawbacks of this assay. First of all, the variation is very high and therefore a high number of experiments is needed to show significant differences in data sets. Compared to that, endocytic activities obtained with the flow cytometric assay show a very low variation and a very good reproducibility of controls (see Fig. 4.14 A). Furthermore, in flow cytometric measurements, signals of dead or apoptotic cells can be excluded from analyses. In spectrofluorometric measurements the FITC signal of all cells within the fluorescence cuvette is recorded, even the signal of dead or apoptotic cells. In addition to that, the unspecific labelling of cell surface proteins for the spectrofluorometric assay takes a least 1 hour, in which cells are incubated on ice, most likely enlarging the number of dying cells. The technique of using the pH sensitivity of FITC to follow endocytosis has mainly been applied for receptor-mediated endocytosis. For these experiments, the fluorophor is directly bound to an endocytic cargo (e.g. transferrin or epidermal growth factor (EGF); Sorkin et al., 1988; Carraway and Cerione, 1993) and, hence, no long cell incubations

on ice are required. The same applies to the flow cytometric assay. The addition and uptake of fluorescently labelled antibodies for the quantification of endocytic activity as well as the addition of exogenous lipids takes place during the cells are cultured under standard conditions. In contrast to that, for the improved spectrofluorometric assay the incubation of cells with exogenous lipids can only be performed below 10 °C. This creates the detraction of slow lipid translocation when exogenous lipids are added, which are subsequently translocated from the outer to the inner leaflet after their incorporation into the plasma membrane. Another drawback is that adherently growing cells need to be detached for spectrofluorometric measurements, which could induce the adaptation of endocytic activities due to environmental changes. In the flow cytometric assay, cells are detached only for final quantification after actual endocytosis took place.

5.3 Endocytosis of K562 cells

5.3.1 Bulk Flow Endocytic Activity

Using the improved spectrofluorometric assay, in the second part of this study it could be shown that bulk flow endocytic activity (BFEA) of K562 cells was significantly stimulated by lipids that are known to be translocated to the inner leaflet of the plasma membrane as well as significantly reduced by lipids that are known to remain on the outer layer. Since exogenous lipids were proposed to alter endocytic activity by increasing the surface area of the respective leaflet of the plasma membrane, these results are in accordance with the theoretical expectations. An enhancement of bulk flow endocytosis in K562 cells by exogenous PS and PE, each with one short chain (C_6-PS and C_6-PE), was already published by Farge et al. in 1999 using the same spectrofluorometric technique but incubating cells with exogenous lipids for 30 minutes at 37 °C. As discussed before (see 5.1.3), by incubating cells with exogenous lipids for shorter times and at lower temperatures in the present study it was assured that exogenously added lipids were still present in the plasma membrane when measurements were started and, thus, could contribute to altered area relations of the membrane bilayer. In addition to the significant enhancement by the exogenous lipids C_6-PS and C_6-PE, an influence of exogenous dilauroyl-PS (DLPS), di-alkyl PS with one short chain (dialkyl-C_6-PS), and PC with one short chain (C_6-PC) was found (see Fig. 4.7 and 4.8).

The changes in activity were investigated at 30 °C as well as at 37 °C for various concentrations of exogenously added lipids. Comparing the results at these two temperatures, the stimulation of endocytosis by C_6-PS was higher for all but one comparable BFEA value when measurements were performed at 30 °C. In addition to that, in the presence of C_6-PS more BFEA values were significantly increased (one sample t-test, $p \leq 0.05$) at 30 °C than at 37 °C. This higher and more often significant stimulation at 30 °C suggests that BFEA stimulation of K562 cells by exogenous C_6-PS was more distinct at 30 °C than at 37 °C. Since at 37 °C BFEA stimulation by other lipids that are translocated to the inner monolayer, e.g. DLPS and C_6-PE, was explicitly higher than the stimulation by C_6-PS, this more distinct stimulation at 30 °C can not be due to the situation that the detection of endocytic activity is at 37 °C at its maximum level and, therefore, differences in BFEA can hardly be obtained. Thus, the minor changes in BFEA by C_6-PS at 37 °C than at 30 °C are based on other reasons. One possible explanation is the more rapid hydrolysis of C_6-PS at higher temperatures (Pomorski et al., 1996) and the consequent influence of the resulting lyso-PS, which remains on or is transported back to the outer layer, against the stimulating effect of C_6-PS.

In order to test whether the relatively short preincubation of cells with exogenous C_6-PS for 1 minute on ice is sufficient for the incorporation of the lipids into the plasma membrane and the subsequent transport to the inner leaflet, longer preincubations of cells with exogenous C_6-PS were tested resulting in two noticeable observations. First, BFEA values of all measurements were determined after 2 as well as after 10 minutes after the respective measurement had been started. When 2 % exogenous C_6-PS were preincubated with cells for 20 minutes on ice, the obtained BFEA was significantly enhanced after 2 minutes of recording and this stimulation was annihilated after 10 minutes of recording. In general, the finding of a stronger stimulation after 2 minutes than after 10 minutes of recording was obtained for nearly all measurements in the presence of C_6-PS, DLPS, and C_6-PE, all lipids that are proposed to stimulate endocytic activity. A possible explanation for this difference is that the increased inner surface area, which is enlarged by exogenous lipids transported during preincubation, causes stimulated endocytic activity directly after cells start to undergo endocytosis by being tempered to 30 °C or 37 °C and that this stimulating effect of altered area relations is partly depleted after a few minutes of enhanced endocytic activity. Interestingly, the difference of a stronger stimulation after 2 minutes than after 10 minutes of recording for all lipids, that were proposed to stimulate endocytic activity, was converse when C_6-PC, a lipid which re-

mains on the outer leaflet of the plasma membrane, was added to the cells. Here, nearly all BFEA values were lower after 2 than after 10 minutes of measuring the FITC signal. These exogenously added lipids only need to incorporate into the plasma membrane and do not need to be transported. Thus, the reducing effect of an increased outer layer leads to the maximal decrease of BFEA directly after cells start to undergo endocytosis. The remaining influence on BFEA after 10 minutes measuring could be based on lower but not yet completely equalized surface area changes which still cause an decrease of BFEA.

Second, BFEA enhancement by 2 % C_6-PS was not significantly different with respect to the standard deviation of the estimator of the mean when cells were preincubated for 1 minute (147 ± 60 % BFEA) and 20 minutes (167 ± 51 % BFEA), respectively, but it completely vanished after a preincubation of cells with lipids for 40 minutes on ice (99 ± 14 % BFEA; see Fig. 4.8). This single observation does not allow to make a final statement on the question whether the relatively short preincubation for 1 minute on ice is sufficient for the incorporation plus the subsequent transport to the inner leaflet. Further series of measurements with different preincubation times are necessary to proof this finding. However, it indicates that a preincubation of 1 minute on ice is, at least for a lipid concentration of 2 % C_6-PS, sufficient to incorporate the lipids into the plasma membrane and to transport the major part of the exogenously added lipids to the inner layer. Presumably, beyond a certain lipid concentration, an incubation of cells with lipids for 1 minute on ice is not sufficient for the incorporation plus the subsequent transport of all exogenously added lipids. At higher lipid concentrations, parts of the lipids were most likely still in the outer membrane layer when measurements had been started after 1 minute of preincubation, whereas other parts had already been transported and could therefore contribute to an increase of the inner surface area. This resulted in opposite, competing influences on the plasma membrane which partially eliminated each other. In addition to this, exogenous lipids, that had not yet been transported to the inner layer while cells were preincubated with lipids, have most likely been transported during the subsequent measurements at 30 or 37 °C leading to a persisting increase of the inner surface area while endocytic activity was recorded.

The later process of a continuing transport of exogenous lipids to the inner layer during the record of endocytic activity could be a major factor why the stimulation of BFEA by dialkyl-C_6-PS was distinctly smaller than the enhancement by C_6-PS and not significant. Since dialkyl-C_6-PS can not be hydrolysed, it was sampled to avoid

the competing influence of hydrolysed lipids as mentioned above. However, this lipid is incorporated and transported to the inner leaflet of the plasma membrane considerably slower than C_6-PS. Characteristic half-times for the inward redistribution of short chain NBD-PS and short chain NBD-dialkyl-PS in human erythrocytes at 37 °C were found to be 2.3 and 41 minutes, respectively (Fellmann et al., 2000). Therefore, all experiments investigating the influence of dialkyl-C_6-PS were carried out with preincubations of cells with different amounts of dialkyl-C_6-PS for 20 minutes on ice. This preincubation of 20 minutes was most likely not sufficient to allow the major part of exogenous dialkyl-C_6-PS to be transported to the inner layer. Here, the obtained small stimulations of BFEA were nearly equal after 2 and 10 minutes of recording the FITC signal. Thus, before drawing conclusions, further experiments are necessary to investigate the incorporation and transport to the inner leaflet of dialkyl-C_6-PS in K562 cells.

The strongest enhancements of BFEA of K562 cells were found when measurements were performed at 37 °C in the presence of different concentrations of either DLPS or C_6-PE. When the latter lipid was present, the resulting BFEA values ranged from 152 ± 28 % up to 238 ± 51 % BFEA and were significantly different from control activity for all but one BFEA value. Remarkably, the stimulation of BFEA was not increasing with the concentration of exogenous lipids. This could be due to the situation that the detection of endocytic activity is at its maximum at 37 °C and, thus, higher stimulations of BFEA can hardly be obtained. Further experiments with lower concentrations of C_6-PE or at lower temperatures could help to elucidate the reason for this finding. In the presence of DLPS. the second lipid for which the strongest stimulation of BFEA was found, the stimulation was in the same range as for C_6-PE and clearly higher than the stimulations by C_6-PS. Although the number of experiments is not sufficient to show a significant difference to 100 % control activity, the fact that an enhancement of BFEA was obtained in all experiments and that the resulting BFEA values were in the same range supports the idea of an stimulating influence of DLPS on BFEA of K562 cells.

The results show that it is exceedingly difficult to find optimal conditions for the experimental setup for each applied lipid, i.e. the best combination of temperature during measurements and preincubation time of cells with exogenous lipids. Both factors influence the time of exogenously added lipids being incorporated and completely translocated to the inner layer. In addition to that, rates of incorporation, translocation, and hydrolysis differ from lipid to lipid. For instance, PE is translocated and hydrolyzed more slowly than PS, whereas dialkyl-PS can not be hydrolyzed but its translocation to

the inner leaflet is distinctly slower (Cribier et al., 1993; Pomorski et al., 1996; Fellmann et al., 2000). Nevertheless, although the experiments did not allow to distinctly quantify changes in the activity of bulk flow endocytosis with the concentration of exogenously added lipids, it could be shown that BFEA of K562 cells is significantly enhanced by lipids that are known to be transported to the inner leaflet, namely C_6-PS, C_6-PE, and DLPS, and significantly reduced by C_6-PC, a lipid that remains on the outer layer. This influence is dependent on the concentration of added lipids and on the preincubation of cells with exogenous lipids.

5.3.2 Clathrin-Independent Bulk Flow Endocytic Activity

Endocytosis comprises many different endocytic pathways with various associated proteins and a high morphological variability. By monitoring bulk flow endocytic activity with the spectrofluorometric assay, the unspecific internalisation of proteins lacking a sorting signal into acidified inner cell compartments was investigated. Since different endocytic pathways are individually regulated and supported by proteins that can sense or stabilise membrane curvature, they might also differently depend on membrane physical properties and, thus, facilitated generation of curvature for endocytic invaginations. In this regard, also the influence of exogenous lipids on clathrin-independent bulk flow endocytosis, i.e. bulk flow endocytosis lacking the clathrin-mediated pathway, and on clathrin-mediated endocytosis, which is discussed in the following clause (see 5.3.3), were investigated.

For the investigation of clathrin-independent bulk flow endocytic activity (CI-BFEA), K562 cells were examined using again the improved spectrofluorometric assay as before, but clathrin-mediated endocytosis was inhibited by treating K562 cells with chlorpromazine. The cationic amphiphilic drug chlorpromazine abolishes the formation of clathrin-coated endocytic vesicles by interfering with the interaction between the adapter protein AP-2 and the clathrin-coated pit lattice (Wang et al., 1993). CI-BFEA of chlorpromazine treated K562 cells was significantly reduced to about 70 % compared to BFEA of untreated control cells still undergoing clathrin-mediated endocytosis. This dimension of inhibition of clathrin-mediated endocytosis sounds reasonable, although the exact proportion of clathrin-mediated endocytosis in ratio to bulk flow endocytosis in K562 cells is not known. The inhibitory effect of chlorpromazine has been published for several cell lines, for instance, at the chlorpromazine concentration used in the present study, it was

shown that the number of low density lipoprotein (LDL) receptors on the cell surface of human fibroblasts was reduced to about 30 % (Wang et al., 1993), transferrin uptake of RAW 264.7 macrophages was inhibited to 18 % (Feng et al., 2010), and the entry of equine arteritis virus into BHK-21 cells was completely blocked (Nitschke et al., 2008). Based on the reduction to about 70 % found in this study and the results published by Harwood et al. (2008) which qualitatively showed an efficient inhibition of clathrin-mediated endocytosis in chlorpromazine treated K562 cells by confocal microscopy, it can be assumed that the inhibition of clathrin-mediated endocytosis by chlorpromazine is also efficient in K562 cells.

Since chlorpromazine incorporates into the plasma membrane, one could argue that the determined reduction is partly due to the incorporation of chlorpromazine molecules into the outer leaflet of the plasma membrane and the resulting increase of the outer surface area of the plasma membrane. However, it was shown that chlorpromazine binds more avidly to the inner leaflet than to the outer leaflet of the plasma membrane (Elferink, 1977), thus, parts of the inhibition can not be due to surface area changes caused by the incorporation of chlorpromazine. On the contrary, if the more avid binding of chlorpromazine to the inner leaflet caused an increase of the inner surface area resulting in an enhancing influence on CI-BFEA, the absolute reduction of endocytic activity would even be higher.

In order to study the influence of exogenous lipids on CI-BFEA, chlorpromazine treated cells were incubated in the presence of 4 % C_6-PC. The resulting CI-BFEA was reduced to about 75 % compared to controls that were also treated with chlorpromazine. Although the number of experiments was too low for statistical analyses, the fact, that all determined values of CI-BFEA were distinctly smaller than 100 % and in the same range, underlines the finding of a reducing influence of C_6-PC on CI-BFEA of K562 cells. Notably, in the presence of 4 % C_6-PC, BFEA was reduced to about one half whereas CI-BFEA was reduced to about three-fourths of the original activities. These values were obtained with the same technique and, thus, given that further experiments would verify the extent of CI-BFEA reduction by C_6-PC, it could further be inferred that also clathrin-mediated endocytic activity of K562 cells is reduced by exogenously added C_6-PC (cf. 5.3.3).

5.3.3 Clathrin-Mediated Endocytic Activity

Clathrin-mediated endocytosis is still the best characterised endocytic pathway involving many proteins known to induce and/or stabilise membrane curvature. Thus, it was particularly interesting to show a potential implication of physical properties of the membrane in this pathway. For the examination, the spectrofluorometric assay was slightly changed: instead of unspecifically labelling cell surface proteins with FITC, transferrin conjugated to FITC was used to specifically follow the uptake of this receptor via clathrin-mediated endocytosis based on the pH sensitivity of FITC and the acidification of early endosomes. Incubation with exogenous lipids, spectrofluorometric measurements of the FITC signal, and analyses of the clathrin-mediated endocytic activity (CMEA) were performed as aforementioned following the improved protocol.

In the presence of either 2 % or 4 % C_6-PC, CMEA of K562 cells was significantly reduced to 82 % and 69 % after 2 minutes, respectively. This significant reduction was largely abolished after 10 minutes of recording the FITC signal: 96 % CMEA at 2 % C_6-PC and 92 % CMEA at 4 % C_6-PC. This distinct difference after 2 and 10 minutes is most likely based on the relatively fast kinetics of cell entry of transferrin. Its half-maximal internalisation occurred after 3 and 2.5 minutes in HeLa and K562 cells, respectively (Beauchamp and Woodman, 1994), and it was shown to be two times faster than the entry of the cytokine interleukin 2 (Subtil et al., 1994) which is endocytosed via RhoA-regulated and dynamin-dependent endocytosis (Lamaze et al., 2001). This means that, after 10 minutes of monitoring the FITC signal, the maximal decrease of the intensity of FITC due to acidification is probably nearly or already reached and differences in the kinetics cannot be determined anymore. However, it could be shown that not only bulk flow endocytosis but also receptor-mediated endocytosis, i.e. clathrin-mediated endocytosis, of K562 cells is significantly inhibited by the addition of exogenous C_6-PC and that this inhibition is increasing with the amount of added lipids. This result is in line with the findings of the previous clause. The decrease of BFEA in the presence of 4 % C_6-PC was shown to be stronger in K562 cells still undergoing clathrin-mediated endocytosis than in cells in which the clathrin-mediated pathway was inhibited by chlorpromazine. Moreover, the inhibition by the same amount of exogenous C_6-PC was shown to be distinctly smaller for CMEA than for BFEA. This preliminary result indicates that bulk flow endocytic activity could be influenced more strongly by C_6-PC than clathrin-mediated endocytic activity. When further experiments support this finding, the difference in

the influence could suggest a differing involvement of the monolayer area asymmetry in the vesiculation during endocytosis. For the clathrin-dependent pathway it is known that many proteins like clathrin and dynamin are involved. These proteins are able to induce the required local membrane curvature for the formation of small endocytic vesicles. Other pathways, such as macropino- and phagocytosis, are mainly actin dependent (Mayor and Pagano, 2007) and may need more support for the formation of curvature by physical properties of the plasma membrane and are therefore more effected by the addition of exogenous lipids.

5.4 Endocytosis of BHKasc cells

Up to now, the influence of exogenous lipids on bulk flow endocytosis was only shown for the suspension cell line K562 (Farge et al., 1999). In order to show this influence on another cell line, adherently growing BHKasc cells with inducible expression of clathrin heavy chain antisense RNA were employed (Iversen et al., 2001) to investigate the influence of exogenous lipids on bulk flow endocytosis either in- or excluding clathrin-mediated endocytic activity and clathrin-mediated endocytic activity by itself as done for K562 cells. In BHKasc cells, clathrin-mediated endocytosis can easily be inhibited by removing tetracycline from the growth medium leading to the expression of clathrin heavy chain antisense RNA (Iversen et al., 2001). However, during the examinations of clathrin-mediated endocytic activity in BHKasc cells it was found that fluorescently labelled analogues of transferrin, a specific receptor to follow clathrin-mediated endocytosis, are internalised into inner cell compartments by detached BHKasc$^-$ cells in which clathrin-mediated endocytosis was supposed to be inhibited. Control experiments revealed that, when BHKasc cells were adherently cultured, transferrin was taken up into inner cell compartments in BHKasc$^+$ cells undergoing clathrin-mediated endocytosis, whereas it remained attached to the cell surface in BHKasc$^-$ cells expressing clathrin heavy chain antisense RNA. Remarkably, when BHKasc cells were detached before incubated with transferrin, the tracer was internalised in both BHKasc$^+$ as well as in BHKasc$^-$ cells (see Fig. 4.13). This shows that one has to be careful with results for endocytosis obtained with adherently growing cells that were detached for the examinations. As stated in the introduction, special treatments of cells may functionally alter the activity of an endocytic route that is more silent or even not existent under normal conditions (Doherty and McMahon, 2009). For instance, it was shown that modifications

of the population context of cells alter cellular activities, such as virus infection, endocytosis, and membrane lipid composition (Snijder et al., 2009). According to this, the internalisation of transferrin into detached BHKasc$^-$ cells could be mediated by an endocytic pathway that is activated or upregulated on account of the irregular detachment of adherently growing cells.

Interestingly, a distinct difference in the influence of exogenous lipids on bulk flow endocytic activity of detached BHKasc$^+$ and BHKasc$^-$ cells was found in corresponding experiments with the improved spectrofluorometric assay. When the influence of exogenously added C_6-PS and lyso-PC on BHKasc$^+$ cells was examined, both lipid species caused reductions of BFEA. In the presence of C_6-PS, all resulting BFEA values were smaller than 100 % control activity and even significantly reduced at a concentration of 2 % C_6-PS. In a like manner, BFEA of BHKasc$^+$ cells was reduced when lyso-PC was applied and this reduction was significant for most of the obtained values. Moreover, the inhibition of BFEA was increasing with the amount of exogenously added lyso-PC. In contrast, neither the addition of different amounts of C_6-PS nor of lyso-PC had an influence on bulk flow endocytic activity of detached BHKasc$^-$ cells lacking tetracycline, that is CI-BFEA of BHKasc$^-$ cells. All determined values of CI-BFEA varied around 100 % control activity without any tendency towards an enhancing or reducing influence. This finding suggests that the modification of endocytic pathways as mentioned above becomes effective in detached BHKasc$^-$ cells already lacking the most abundant endocytic pathway. It was shown that almost the whole uptake of fluid and plasma membrane via endocytosis in BHK-21 cells can be related to the clathrin-mediated pathway (Marsh and Helenius, 1980).

In addition to the drawback that adherently growing BHKasc cells were detached to perform this assay and, thus, specific adaptations of the cells have to be considered as well, it is not known whether specific lipids are transported to the inner leaflet of this cell line. The determined results for BHKasc$^+$ cells incubated with C_6-PS did not correspond to the theoretical expectations of an enhancing influence due to the translocation of C_6-PS to the inner leaflet and the resulting increase of the inner surface area. For the experiments with K562 cells it is known that C_6-PS is translocated to the inner leaflet and C_6-PC remains on the outer layer (Cribier et al., 1993), but the inward movement of specific lipids differs from cell line to cell line. For instance, in dog kidney MDCK II cells spin-labeled analogues of PC are internalised in a rate similar to that of aminophospholipids analogues, whereas in human colon Caco-2 cells the inward

movement was much slower (Pomorski et al., 1999). On that account, for further analysis, it needs to be tested whether in this cell line exogenously added C_6-PS is not only incorporated into the plasma membrane but also translocated to the inner leaflet. It would be also conceivable that the translocation of C_6-PS is distinctly slower in BHKasc than in K562 cells and, thus, that the preincubation of BHKasc cells with lipids for 1 minute on ice is not sufficient for the incorporation and subsequent translocation of the added lipids.

On account of the reasons mentioned above, further experiments to investigate clathrin-mediated endocytic activity of BHKasc cells were performed using the flow cytometric assay. As discussed in clause 5.2, in this assay adherently growing cells are not detached until the essential uptake of labelled antibodies is accomplished and the variation is very low. Although the results obtained with the flow cytometric assay are most of the time based on single experiments, the very low variation and the comparison with other results obtained for BHKasc cells in the present study allow to suggest an influence of exogenous lipids on endocytic activity of BHKasc cells. Bulk flow endocytic activity of detached BHKasc$^+$ cells as well as clathrin-mediated endocytic activity of adherent BHKasc cells is partly inhibited in the presence of exogenously added C_6-PS, C_6-PC, and lyso-PC. Since clathrin-mediated endocytosis was not completely inhibited in BHKasc$^-$ cells (see 4.2.3), it is not possible to conclude whether only clathrin-mediated or also other endocytic pathways of BHKasc cells are influenced by exogenous lipids.

CHAPTER 6

Conclusions and Future Prospects

The hypothesis of a relationship between the activity of lipid translocators and vesicle formation has been supported in several studies and it seems commonly accepted that in particular aminophospholipid translocases (APLT) are involved in endocytosis (e.g. Muthusamy et al., 2009; Graham and Kozlov, 2010). Upon the translocation of lipids from the exoplasmic leaflet to the cytoplasmic layer of the plasma membrane, APLT would mediate an increase of the inner surface area and thereby support the generation of membrane curvature during endocytosis. In this regard, it could be shown in the present study that exogenously added lipids, which change the surface area relation of the plasma membrane, have an influence on endocytic activity. Bulk flow endocytic activity of K562 cells is enhanced by exogenous phosphatidylserine with one short chain (C_6-PS), phosphatidylserine with two long chains (DLPS), and phosphatidylethanolamine with one short chain (C_6-PE) and is partially inhibited by phosphatidylcholine with one short chain (C_6-PC). In addition to this, both clathrin-independent bulk flow and clathrin-mediated endocytic activity decrease in the presence of exogenous C_6-PC. In two other cell lines, namely BHKasc and Hep2 cells, activities of endocytosis were found to be influenced by exogenous lipids as well. In BHKasc cells, clathrin-mediated endocytic activity is partially inhibited in the presence of exogenously applied C_6-PC and lyso-PC. In Hep2 cells, preliminary results indicate a decrease of clathrin-mediated endocytic activity by exogenous lyso-PC and an increase by exogenous C_6-PS. Thus, the present study clearly shows, albeit not quantitatively, the alteration of bulk flow and clathrin-

mediated endocytosis of different cell lines by various exogenous lipids. Interestingly, not only bulk flow endocytosis but also clathrin-mediated endocytosis is influenced by the addition of exogenous lipids. Many proteins noted for their ability to induce membrane curvature are known to interact either with clathrin or other adaptor proteins implicated in the clathrin-mediated pathway (cf. 1.2.1). Thus, even an endocytic pathway, in which such proteins are definitely implicated and suggested to be primarily responsible for the generation of membrane curvature (Ford et al., 2002; Ungewickell and Hinrichsen, 2007; Rappoport, 2008), is influenced by altered physical properties of the plasma membrane.

Among other modifications, the spectrofluorometric assay as described by Farge et al. (1999) was improved by the distinct reduction of cell incubation with exogenous lipids. This assured that exogenous lipids had still been present in the plasma membrane and not yet relieved into other cell compartments before the measurements were started. Thereby, the exogenous lipids could induce differences in the monolayer area asymmetry of the plasma membrane which, in turn, could generate membrane curvature. However, in this assay, it cannot be distinguished whether altered area relations of the two membrane leaflets or changes of the lipid composition of the plasma membrane caused altered endocytic activities. Besides increasing either the inner or outer surface area of the plasma membrane, exogenously added lipids could influence the number and/or size of lateral microdomains in the plasma membrane as well. These microdomains, so called *rafts* (1.1.2), have convincingly been shown to be implicated in endocytic events (Sharma et al., 2004; Cheng et al., 2006; Sarasij et al., 2007). In general, they are supposed to be enriched in phospholipids as well as glycosphingolipids with long saturated fatty acids and the cytoplasmic layer of rafts was suggested to be enriched in phosphatidylethanolamine and phosphatidylserine (Simons and Ikonen, 1997). In addition to that, some cell surface receptors, like the transferrin receptor, comprise a GPI-anchor (Ikezawa, 2002). GPI-anchored proteins are tightly associated with membrane rafts (Brown and London, 1998; Sharma et al., 2004) and trafficking of GPI-anchored proteins was shown to be influenced by altering levels of cellular proteins, specifically cholesterol and sphingolipids (Mayor et al., 1998; Chatterjee et al., 2001). Thus, the addition of exogenous aminophospholipids could also lead to changes in endocytic activity due to alterations of the lipid composition and/or size of membrane rafts involved in specific endocytic pathways.

In order to unequivocally identify the role of APLT in endocytosis, further studies are indicated to explore whether APLT account for monolayer area asymmetries as an

early step in the formation of endocytic invaginations. As mentioned in the introduction (see 1.1.4), two different groups successfully reconstituted P_4-ATPases into model membranes to provide direct biochemical evidence that P_4-ATPases translocate phospholipids (Zhou and Graham, 2009; Coleman et al., 2009). In a like manner, purified APLT reconstituted into model membranes, e.g. giant unilamellar vesicles, could provide an appropiate model system to demonstrate that APLT mediate monolayer area asymmetry leading to membrane bending. In this model system, effects due to the addition of aminophospholipids could be directly related to altered area relation between both membrane leaflets. Concerning the role of APLT in endocytosis, mutants in which specific lipid translocators are downregulated or inactive provide an attractive tool to experimentally address the correlation between lipid translocators and endocytosis. For instance, using P-type ATPase mutant yeast cells, Pomorski et al. (2003) showed a cold-sensitive defect in the uptake of markers for bulk flow and receptor-mediated endocytosis. Further experiments with eukaryotic cells and different mutants would help to elucidate the role of APLT in endocytosis. Alternatively to the flow cytometric measurements, further experiments could be performed using total internal reflection fluorescence microscopy (TIR-FM). This technique permits to selectively image fluorescently labelled proteins at, or very close to (within 50 nm), the plasma membrane of cells, thereby providing a high signal over background of the fluorophors and minimising the photodamage to the cell (Jaiswal and Simon, 2003; Rappoport and Simon, 2003). Thus, endocytosis can be monitored during the first steps by which the initiation of membrane curvature, the necessary precursor to vesiculation, takes place.

Summarising the role of monolayer area asymmetry in endocytosis, it was shown that both, lipids that remain on the outer layer of the plasma membrane as well as lipids that are translocated to the inner leaflet, influence bulk flow and clathrin-mediated endocytic activity in different cell lines. If this influence on endocytosis is caused by an induced asymmetry of the surface areas of the plasma membrane, by alterations of plasma membrane rafts implicated in endocytosis, or by both mechanisms, remains unclear. However, APLT are thought to account for the translocation of aminophospholipids from the outer to the inner leaflet (e.g. Zhou and Graham, 2009; Coleman et al., 2009), thereby creating an imbalance in the surface areas which leads to bending of the plasma membrane. In addition to this, there is more and more evidence that APLT are involved in endocytosis. In this regard, it has been shown recently that binding of guanine nucleotide exchange factors for ADP-ribosylation factor GTPases (Arf-GEF) and

phosphatidylinositol-4-phosphate (PI(4)P) to the C-terminal tail of the yeast P_4-ATPase Drs2p activates flippase activity (Natarajan et al., 2009). This finding corroborates the previously suggested model how APLT are implicated in endocytosis (see 1.3.2 and Puts and Holthuis, 2009). Interaction between Drs2p and Arf-GEF links the APLT to the endocytic machinery and could trigger the recruitment of endocytic accessory proteins to sites of ATPase-dependent phospholipid translocation. Just recently, Graham and Kozlov (2010) suggested a model how PI(4)P and Arf-GEF integrate the function of curvature generation by activating Drs2p flippase activity and insertion of Arf into the membrane, as well as recruiting the adaptor protein AP-1 and clathrin to stabilise the curvature. Thus, monolayer area asymmetry induced by the translocation of lipids is most likely not the only but one of the forces leading to the generation of membrane curvature necessary for endocytic events. On the basis of the mechanisms described above, it seems very unlikely that membranes are curved only by the force of proteins when other mechanisms could facilitate this procedure.

Bibliography

N. Abe, T. Inoue, T. Galvez, L. Klein, and T. Meyer. Dissecting the role of ptdins(4,5)p2 in endocytosis and recycling of the transferrin receptor. *J Cell Sci*, 121(Pt 9):1488–94, 2008.

L. Abrami, S. Liu, P. Cosson, S. H. Leppla, and F. G. van der Goot. Anthrax toxin triggers endocytosis of its receptor via a lipid raft-mediated clathrin-dependent process. *J Cell Biol*, 160(3):321–8, 2003.

J. Aittoniemi, P. S. Niemela, M. T. Hyvonen, M. Karttunen, and I. Vattulainen. Insight into the putative specific interactions between cholesterol, sphingomyelin, and palmitoyl-oleoyl phosphatidylcholine. *Biophys J*, 92(4):1125–37, 2007.

N. Alder-Baerens, Q. Lisman, L. Luong, T. Pomorski, and J. C. Holthuis. Loss of p4 atpases drs2p and dnf3p disrupts aminophospholipid transport and asymmetry in yeast post-golgi secretory vesicles. *Mol Biol Cell*, 17(4):1632–42, 2006.

P. Aspenstrom. Roles of f-bar/pch proteins in the regulation of membrane dynamics and actin reorganization. *Int Rev Cell Mol Biol*, 272:1–31, 2009.

S. F. Bairstow, K. Ling, X. Su, A. J. Firestone, C. Carbonara, and R. A. Anderson. Type igamma661 phosphatidylinositol phosphate kinase directly interacts with ap2 and regulates endocytosis. *J Biol Chem*, 281(29):20632–42, 2006.

K. Balasubramanian and A. J. Schroit. Aminophospholipid asymmetry: A matter of life and death. *Annu Rev Physiol*, 65:701–34, 2003.

J. R. Beauchamp and P. G. Woodman. Regulation of transferrin receptor recycling by protein phosphorylation. *Biochem J*, 303 (Pt 2):647–55, 1994.

A. Benmerah and C. Lamaze. Clathrin-coated pits: vive la difference? *Traffic*, 8(8):970–82, 2007.

S. Birkle, G. Zeng, L. Gao, R. K. Yu, and J. Aubry. Role of tumor-associated gangliosides in cancer progression. *Biochimie*, 85(3-4):455–63, 2003.

M. S. Bretscher. Asymmetrical lipid bilayer structure for biological membranes. *Nat New Biol*, 236(61):11–2, 1972.

M.S. Bretscher. In: Moscona: The cell surface in development. *Wiley*, pages 17–24, 1974.

T. J. Brett, V. Legendre-Guillemin, P. S. McPherson, and D. H. Fremont. Structural definition of the f-actin-binding thatch domain from hip1r. *Nat Struct Mol Biol*, 13(2):121–30, 2006.

D. A. Brown and E. London. Structure and origin of ordered lipid domains in biological membranes. *J Membr Biol*, 164(2):103–14, 1998.

F. Campelo, H. T. McMahon, and M. M. Kozlov. The hydrophobic insertion mechanism of membrane curvature generation by proteins. *Biophys J*, 95(5):2325–39, 2008.

F. Campelo, G. Fabrikant, H. T. McMahon, and M. M. Kozlov. Modeling membrane shaping by proteins: focus on ehd2 and n-bar domains. *FEBS Lett*, 584(9):1830–9, 2010.

P. B. Canham. The minimum energy of bending as a possible explanation of the biconcave shape of the human red blood cell. *J Theor Biol*, 26(1):61–81, 1970.

3rd Carraway, K. L. and R. A. Cerione. Fluorescent-labeled growth factor molecules serve as probes for receptor binding and endocytosis. *Biochemistry*, 32(45):12039–45, 1993.

R. Chadda, M. T. Howes, S. J. Plowman, J. F. Hancock, R. G. Parton, and S. Mayor. Cholesterol-sensitive cdc42 activation regulates actin polymerization for endocytosis via the geec pathway. *Traffic*, 8(6):702–17, 2007.

S. Chantalat, S. K. Park, Z. Hua, K. Liu, R. Gobin, A. Peyroche, A. Rambourg, T. R. Graham, and C. L. Jackson. The arf activator gea2p and the p-type atpase drs2p interact at the golgi in saccharomyces cerevisiae. *J Cell Sci*, 117(Pt 5):711–22, 2004.

S. Chatterjee, E. R. Smith, K. Hanada, V. L. Stevens, and S. Mayor. Gpi anchoring leads to sphingolipid-dependent retention of endocytosed proteins in the recycling endosomal compartment. *Embo J*, 20(7):1583–92, 2001.

C. Y. Chen, M. F. Ingram, P. H. Rosal, and T. R. Graham. Role for drs2p, a p-type atpase and potential aminophospholipid translocase, in yeast late golgi function. *J Cell Biol*, 147(6): 1223–36, 1999.

Y. J. Chen, P. Zhang, E. H. Egelman, and J. E. Hinshaw. The stalk region of dynamin drives the constriction of dynamin tubes. *Nat Struct Mol Biol*, 11(6):574–5, 2004.

Y. Cheng, W. Boll, T. Kirchhausen, S. C. Harrison, and T. Walz. Cryo-electron tomography of clathrin-coated vesicles: structural implications for coat assembly. *J Mol Biol*, 365(3):892–9, 2007.

Z. J. Cheng, R. D. Singh, D. K. Sharma, E. L. Holicky, K. Hanada, D. L. Marks, and R. E. Pagano. Distinct mechanisms of clathrin-independent endocytosis have unique sphingolipid requirements. *Mol Biol Cell*, 17(7):3197–210, 2006.

J. A. Coleman, M. C. Kwok, and R. S. Molday. Localization, purification, and functional reconstitution of the p4-atpase atp8a2, a phosphatidylserine flippase in photoreceptor disc membranes. *J Biol Chem*, 284(47):32670–9, 2009.

M. Colin, L. Mailly, S. Rogee, and J. C. D'Halluin. Efficient species c hadv infectivity in plasmocytic cell lines using a clathrin-independent lipid raft/caveola endocytic route. *Mol Ther*, 11(2):224–36, 2005.

S. D. Conner and S. L. Schmid. Regulated portals of entry into the cell. *Nature*, 422(6927): 37–44, 2003.

S. Cribier, J. Sainte-Marie, and P. F. Devaux. Quantitative comparison between aminophospholipid translocase activity in human erythrocytes and in k562 cells. *Biochim Biophys Acta*, 1148(1):85–90, 1993.

P. R. Cullis and B. de Kruijff. Lipid polymorphism and the functional roles of lipids in biological membranes. *Biochim Biophys Acta*, 559(4):399–420, 1979.

L. A. Dada, E. Novoa, E. Lecuona, H. Sun, and J. I. Sznajder. Role of the small gtpase rhoa in the hypoxia-induced decrease of plasma membrane na,k-atpase in a549 cells. *J Cell Sci*, 120 (Pt 13):2214–22, 2007.

D. L. Daleke. Phospholipid flippases. *J Biol Chem*, 282(2):821–5, 2007.

D. L. Daleke and W. H. Huestis. Erythrocyte morphology reflects the transbilayer distribution of incorporated phospholipids. *J Cell Biol*, 108(4):1375–85, 1989.

D. L. Daleke and J. V. Lyles. Identification and purification of aminophospholipid flippases. *Biochim Biophys Acta*, 1486(1):108–27, 2000.

H. Damke, T. Baba, A. M. van der Bliek, and S. L. Schmid. Clathrin-independent pinocytosis is induced in cells overexpressing a temperature-sensitive mutant of dynamin. *J Cell Biol*, 131 (1):69–80, 1995.

R. F. de Almeida, A. Fedorov, and M. Prieto. Sphingomyelin/phosphatidylcholine/cholesterol phase diagram: boundaries and composition of lipid rafts. *Biophys J*, 85(4):2406–16, 2003.

H. J. Deuling and W. Helfrich. Red blood cell shapes as explained on the basis of curvature elasticity. *Biophys J*, 16(8):861–8, 1976.

P. F. Devaux. Static and dynamic lipid asymmetry in cell membranes. *Biochemistry*, 30(5): 1163–73, 1991.

P. F. Devaux. Is lipid translocation involved during endo- and exocytosis? *Biochimie*, 82(5): 497–509, 2000.

P. F. Devaux and R. Morris. Transmembrane asymmetry and lateral domains in biological membranes. *Traffic*, 5(4):241–6, 2004.

P. F. Devaux and M. Seigneuret. Specificity of lipid-protein interactions as determined by spectroscopic techniques. *Biochim Biophys Acta*, 822(1):63–125, 1985.

P. F. Devaux, I. Lopez-Montero, and S. Bryde. Proteins involved in lipid translocation in eukaryotic cells. *Chem Phys Lipids*, 141(1-2):119–32, 2006.

P. F. Devaux, A. Herrmann, N. Ohlwein, and M. M. Kozlov. How lipid flippases can modulate membrane structure. *Biochim Biophys Acta*, 1778(7-8):1591–600, 2008.

G. J. Doherty and H. T. McMahon. Mechanisms of endocytosis. *Annu Rev Biochem*, 78:857–902, 2009.

J. G. Donaldson. Arfs and membrane lipids: sensing, generating and responding to membrane curvature. *Biochem J*, 414(2):e1–2, 2008.

S. J. Doxsey, F. M. Brodsky, G. S. Blank, and A. Helenius. Inhibition of endocytosis by anti-clathrin antibodies. *Cell*, 50(3):453–63, 1987.

G. Drin and B. Antonny. Amphipathic helices and membrane curvature. *FEBS Lett*, 584(9): 1840–7, 2009.

J. G. Elferink. The asymmetric distribution of chlorpromazine and its quaternary analogue over the erythrocyte membrane. *Biochem Pharmacol*, 26(24):2411–6, 1977.

D. M. Engelman. Membranes are more mosaic than fluid. *Nature*, 438(7068):578–80, 2005.

V. A. Fadok, D. R. Voelker, P. A. Campbell, J. J. Cohen, D. L. Bratton, and P. M. Henson. Exposure of phosphatidylserine on the surface of apoptotic lymphocytes triggers specific recognition and removal by macrophages. *J Immunol*, 148(7):2207–16, 1992.

E. Fahy, S. Subramaniam, H. A. Brown, C. K. Glass, Jr. Merrill, A. H., R. C. Murphy, C. R. Raetz, D. W. Russell, Y. Seyama, W. Shaw, T. Shimizu, F. Spener, G. van Meer, M. S. VanNieuwenhze, S. H. White, J. L. Witztum, and E. A. Dennis. A comprehensive classification system for lipids. *J Lipid Res*, 46(5):839–61, 2005.

E. Farge and P. F. Devaux. Shape changes of giant liposomes induced by an asymmetric transmembrane distribution of phospholipids. *Biophys J*, 61(2):347–57, 1992.

E. Farge, D. M. Ojcius, A. Subtil, and A. Dautry-Varsat. Enhancement of endocytosis due to aminophospholipid transport across the plasma membrane of living cells. *Am J Physiol*, 276 (3 Pt 1):C725–33, 1999.

P. Fellmann, A. Zachowski, and P. F. Devaux. Synthesis and use of spin-labeled lipids for studies of the transmembrane movement of phospholipids. *Methods Mol Biol*, 27:161–75, 1994.

P. Fellmann, P. Herve, T. Pomorski, P. Muller, D. Geldwerth, A. Herrmann, and P. F. Devaux. Transmembrane movement of diether phospholipids in human erythrocytes and human fibroblasts. *Biochemistry*, 39(17):4994–5003, 2000.

D. Feng, W. L. Zhao, Y. Y. Ye, X. C. Bai, R. Q. Liu, L. F. Chang, Q. Zhou, and S. F. Sui. Cellular internalization of exosomes occurs through phagocytosis. *Traffic*, 11(5):675–87, 2010.

F. Fernandes, L. M. Loura, F. J. Chichon, J. L. Carrascosa, A. Fedorov, and M. Prieto. Role of helix 0 of the n-bar domain in membrane curvature generation. *Biophys J*, 94(8):3065–73, 2008.

D. E. Folmer, R. P. Elferink, and C. C. Paulusma. P4 atpases - lipid flippases and their role in disease. *Biochim Biophys Acta*, 1791(7):628–35, 2009.

M. G. Ford, I. G. Mills, B. J. Peter, Y. Vallis, G. J. Praefcke, P. R. Evans, and H. T. McMahon. Curvature of clathrin-coated pits driven by epsin. *Nature*, 419(6905):361–6, 2002.

A. Frost, V. M. Unger, and P. De Camilli. The bar domain superfamily: membrane-molding macromolecules. *Cell*, 137(2):191–6, 2009.

J. L. Gallop and H. T. McMahon. Bar domains and membrane curvature: bringing your curves to the bar. *Biochem Soc Symp*, (72):223–31, 2005.

R.B. Gennis. Biomembranes. *Springer Verlag*, 1989.

H. Girao, M. I. Geli, and F. Z. Idrissi. Actin in the endocytic pathway: from yeast to mammals. *FEBS Lett*, 582(14):2112–9, 2008.

Q. Gong, M. Weide, C. Huntsman, Z. Xu, L. Y. Jan, and D. Ma. Identification and characterization of a new class of trafficking motifs for controlling clathrin-independent internalization and recycling. *J Biol Chem*, 282(17):13087–97, 2007.

T. R. Graham. Flippases and vesicle-mediated protein transport. *Trends Cell Biol*, 14(12):670–7, 2004.

T. R. Graham and M. M. Kozlov. Interplay of proteins and lipids in generating membrane curvature. *Curr Opin Cell Biol*, 22(4):430–6, 2010.

J. F. Hancock. Lipid rafts: contentious only from simplistic standpoints. *Nat Rev Mol Cell Biol*, 7(6):456–62, 2006.

C. G. Hansen and B. J. Nichols. Molecular mechanisms of clathrin-independent endocytosis. *J Cell Sci*, 122(Pt 11):1713–21, 2009.

L. J. Harwood, H. Gerber, F. Sobrino, A. Summerfield, and K. C. McCullough. Dendritic cell internalization of foot-and-mouth disease virus: influence of heparan sulfate binding on virus uptake and induction of the immune response. *J Virol*, 82(13):6379–94, 2008.

V. Haucke. Phosphoinositide regulation of clathrin-mediated endocytosis. *Biochem Soc Trans*, 33(Pt 6):1285–9, 2005.

L. Hinrichsen, A. Meyerholz, S. Groos, and E. J. Ungewickell. Bending a membrane: how clathrin affects budding. *Proc Natl Acad Sci U S A*, 103(23):8715–20, 2006.

S. Honing, D. Ricotta, M. Krauss, K. Spate, B. Spolaore, A. Motley, M. Robinson, C. Robinson, V. Haucke, and D. J. Owen. Phosphatidylinositol-(4,5)-bisphosphate regulates sorting signal recognition by the clathrin-associated adaptor complex ap2. *Mol Cell*, 18(5):519–31, 2005.

C. A. Horvath, D. Vanden Broeck, G. A. Boulet, J. Bogers, and M. J. De Wolf. Epsin: inducing membrane curvature. *Int J Biochem Cell Biol*, 39(10):1765–70, 2007.

T. Houndolo, P. L. Boulay, and A. Claing. G protein-coupled receptor endocytosis in adp-ribosylation factor 6-depleted cells. *J Biol Chem*, 280(7):5598–604, 2005.

Z. Hua, P. Fatheddin, and T. R. Graham. An essential subfamily of drs2p-related p-type atpases is required for protein trafficking between golgi complex and endosomal/vacuolar system. *Mol Biol Cell*, 13(9):3162–77, 2002.

H. Ikezawa. Glycosylphosphatidylinositol (gpi)-anchored proteins. *Biol Pharm Bull*, 25(4):409–17, 2002.

E. Ikonen. Roles of lipid rafts in membrane transport. *Curr Opin Cell Biol*, 13(4):470–7, 2001.

T. G. Iversen, G. Skretting, A. Llorente, P. Nicoziani, B. van Deurs, and K. Sandvig. Endosome to golgi transport of ricin is independent of clathrin and of the rab9- and rab11-gtpases. *Mol Biol Cell*, 12(7):2099–107, 2001.

T. G. Iversen, G. Skretting, B. van Deurs, and K. Sandvig. Clathrin-coated pits with long, dynamin-wrapped necks upon expression of a clathrin antisense rna. *Proc Natl Acad Sci U S A*, 100(9):5175–80, 2003.

K. Jacobson, O. G. Mouritsen, and R. G. Anderson. Lipid rafts: at a crossroad between cell biology and physics. *Nat Cell Biol*, 9(1):7–14, 2007.

J. K. Jaiswal and S. M. Simon. Total internal reflection fluorescence microscopy for high-resolution imaging of cell-surface events. *Curr Protoc Cell Biol*, Chapter 4:Unit 4 12, 2003.

J. Joseph, C. C. Shih, and C. S. Lai. Synthesis of the spin-labeled derivative of an ether-linked phospholipid possessing high antineoplastic activity. *Chem Phys Lipids*, 58(1-2):19–26, 1991.

M. Kalia, S. Kumari, R. Chadda, M. M. Hill, R. G. Parton, and S. Mayor. Arf6-independent gpi-anchored protein-enriched early endosomal compartments fuse with sorting endosomes via a rab5/phosphatidylinositol-3'-kinase-dependent machinery. *Mol Biol Cell*, 17(8):3689–704, 2006.

M. Kirkham and R. G. Parton. Clathrin-independent endocytosis: new insights into caveolae and non-caveolar lipid raft carriers. *Biochim Biophys Acta*, 1746(3):349–63, 2005.

R. W. Klemm, C. S. Ejsing, M. A. Surma, H. J. Kaiser, M. J. Gerl, J. L. Sampaio, Q. de Robillard, C. Ferguson, T. J. Proszynski, A. Shevchenko, and K. Simons. Segregation of sphingolipids and sterols during formation of secretory vesicles at the trans-golgi network. *J Cell Biol*, 185 (4):601–12, 2009.

M. M. Kozlov. Biophysics: Joint effort bends membrane. *Nature*, 463(7280):439–40, 2010.

D. Lai, J. R. Springstead, and H. G. Monbouquette. Effect of growth temperature on ether lipid biochemistry in archaeoglobus fulgidus. *Extremophiles*, 12(2):271–8, 2008.

C. Lamaze, A. Dujeancourt, T. Baba, C. G. Lo, A. Benmerah, and A. Dautry-Varsat. Interleukin 2 receptors and detergent-resistant membrane domains define a clathrin-independent endocytic pathway. *Mol Cell*, 7(3):661–71, 2001.

Y. Lange and J. M. Slayton. Interaction of cholesterol and lysophosphatidylcholine in determining red cell shape. *J Lipid Res*, 23(8):1121–7, 1982.

D. Lichtenberg, F. M. Goni, and H. Heerklotz. Detergent-resistant membranes should not be identified with membrane rafts. *Trends Biochem Sci*, 30(8):430–6, 2005.

J. Liu, M. Kaksonen, D. G. Drubin, and G. Oster. Endocytic vesicle scission by lipid phase boundary forces. *Proc Natl Acad Sci U S A*, 103(27):10277–82, 2006.

K. Liu, K. Surendhran, S. F. Nothwehr, and T. R. Graham. P4-atpase requirement for ap-1/clathrin function in protein transport from the trans-golgi network and early endosomes. *Mol Biol Cell*, 19(8):3526–35, 2008.

I. Lopez-Montero, N. Rodriguez, S. Cribier, A. Pohl, M. Velez, and P. F. Devaux. Rapid transbilayer movement of ceramides in phospholipid vesicles and in human erythrocytes. *J Biol Chem*, 280(27):25811–9, 2005.

R. Lundmark and S. R. Carlsson. Sorting nexin 9 participates in clathrin-mediated endocytosis through interactions with the core components. *J Biol Chem*, 278(47):46772–81, 2003.

R. Lundmark and S. R. Carlsson. Driving membrane curvature in clathrin-dependent and clathrin-independent endocytosis. *Semin Cell Dev Biol*, 21(4):363–70, 2010.

R. Lundmark, G. J. Doherty, M. T. Howes, K. Cortese, Y. Vallis, R. G. Parton, and H. T. McMahon. The gtpase-activating protein graf1 regulates the clic/geec endocytic pathway. *Curr Biol*, 18(22):1802–8, 2008a.

R. Lundmark, G. J. Doherty, Y. Vallis, B. J. Peter, and H. T. McMahon. Arf family gtp loading is activated by, and generates, positive membrane curvature. *Biochem J*, 414(2):189–94, 2008b.

E. Macia, M. Ehrlich, R. Massol, E. Boucrot, C. Brunner, and T. Kirchhausen. Dynasore, a cell-permeable inhibitor of dynamin. *Dev Cell*, 10(6):839–50, 2006.

A. Maeda, M. Amano, Y. Fukata, and K. Kaibuchi. Translocation of na(+),k(+)-atpase is induced by rho small gtpase in renal epithelial cells. *Biochem Biophys Res Commun*, 297(5): 1231–7, 2002.

D. Marsh and I. C. Smith. An interacting spin label study of the fluidizing and condensing effects of cholesterol on lecithin bilayers. *Biochim Biophys Acta*, 298(2):133–44, 1973.

M. Marsh and A. Helenius. Adsorptive endocytosis of semliki forest virus. *J Mol Biol*, 142(3): 439–54, 1980.

M. Marsh and A. Helenius. Virus entry: open sesame. *Cell*, 124(4):729–40, 2006.

S. Mayor and R. E. Pagano. Pathways of clathrin-independent endocytosis. *Nat Rev Mol Cell Biol*, 8(8):603–12, 2007.

S. Mayor, S. Sabharanjak, and F. R. Maxfield. Cholesterol-dependent retention of gpi-anchored proteins in endosomes. *Embo J*, 17(16):4626–38, 1998.

H. T. McMahon and J. L. Gallop. Membrane curvature and mechanisms of dynamic cell membrane remodelling. *Nature*, 438(7068):590–6, 2005.

C. J. Merrifield, M. E. Feldman, L. Wan, and W. Almers. Imaging actin and dynamin recruitment during invagination of single clathrin-coated pits. *Nat Cell Biol*, 4(9):691–8, 2002.

R. D. Minshall, C. Tiruppathi, S. M. Vogel, and A. B. Malik. Vesicle formation and trafficking in endothelial cells and regulation of endothelial barrier function. *Histochem Cell Biol*, 117 (2):105–12, 2002.

S. Monier, D. J. Dietzen, W. R. Hastings, D. M. Lublin, and T. V. Kurzchalia. Oligomerization of vip21-caveolin in vitro is stabilized by long chain fatty acylation or cholesterol. *FEBS Lett*, 388(2-3):143–9, 1996.

A. Motley, N. A. Bright, M. N. Seaman, and M. S. Robinson. Clathrin-mediated endocytosis in ap-2-depleted cells. *J Cell Biol*, 162(5):909–18, 2003.

P. Muller and A. Herrmann. Rapid transbilayer movement of spin-labeled steroids in human erythrocytes and in liposomes. *Biophys J*, 82(3):1418–28, 2002.

P. Muller, T. Pomorski, and A. Herrmann. Incorporation of phospholipid analogues into the plasma membrane affects atp-induced vesiculation of human erythrocyte ghosts. *Biochem Biophys Res Commun*, 199(2):881–7, 1994.

S. Munro. Lipid rafts: elusive or illusive? *Cell*, 115(4):377–88, 2003.

B. P. Muthusamy, P. Natarajan, X. Zhou, and T. R. Graham. Linking phospholipid flippases to vesicle-mediated protein transport. *Biochim Biophys Acta*, 1791(7):612–9, 2009.

P. Natarajan, K. Liu, D. V. Patil, V. A. Sciorra, C. L. Jackson, and T. R. Graham. Regulation of a golgi flippase by phosphoinositides and an arfgef. *Nat Cell Biol*, 11(12):1421–6, 2009.

K. Nishi and K. Saigo. Cellular internalization of green fluorescent protein fused with herpes simplex virus protein vp22 via a lipid raft-mediated endocytic pathway independent of caveolae and rho family gtpases but dependent on dynamin and arf6. *J Biol Chem*, 282(37):27503–17, 2007.

M. Nitschke, T. Korte, C. Tielesch, G. Ter-Avetisyan, G. Tunnemann, M. C. Cardoso, M. Veit, and A. Herrmann. Equine arteritis virus is delivered to an acidic compartment of host cells via clathrin-dependent endocytosis. *Virology*, 377(2):248–54, 2008.

R. J. North. Cellular kinetics associated with the development of acquired cellular resistance. *J Exp Med*, 130(2):299–314, 1969.

R. Nossal. Energetics of clathrin basket assembly. *Traffic*, 2(2):138–47, 2001.

A. Papadopulos, S. Vehring, I. Lopez-Montero, L. Kutschenko, M. Stockl, P. F. Devaux, M. Kozlov, T. Pomorski, and A. Herrmann. Flippase activity detected with unlabeled lipids by shape changes of giant unilamellar vesicles. *J Biol Chem*, 282(21):15559–68, 2007.

R. G. Parton and K. Simons. The multiple faces of caveolae. *Nat Rev Mol Cell Biol*, 8(3):185–94, 2007.

R. G. Parton, M. Hanzal-Bayer, and J. F. Hancock. Biogenesis of caveolae: a structural model for caveolin-induced domain formation. *J Cell Sci*, 119(Pt 5):787–96, 2006.

C. C. Paulusma and R. P. Oude Elferink. The type 4 subfamily of p-type atpases, putative aminophospholipid translocases with a role in human disease. *Biochim Biophys Acta*, 1741 (1-2):11–24, 2005.

C. C. Paulusma and R. P. Oude Elferink. Diseases of intramembranous lipid transport. *FEBS Lett*, 580(23):5500–9, 2006.

L. Pelkmans and M. Zerial. Kinase-regulated quantal assemblies and kiss-and-run recycling of caveolae. *Nature*, 436(7047):128–33, 2005.

M. M. Perry and A. B. Gilbert. Yolk transport in the ovarian follicle of the hen (gallus domesticus): lipoprotein-like particles at the periphery of the oocyte in the rapid growth phase. *J Cell Sci*, 39:257–72, 1979.

V. A. Petit and M. Edidin. Lateral phase separation of lipids in plasma membranes: effect of temperature on the mobility of membrane antigens. *Science*, 184(142):1183–5, 1974.

L. J. Pike. Rafts defined: a report on the keystone symposium on lipid rafts and cell function. *J Lipid Res*, 47(7):1597–8, 2006.

A. Pohl, P. F. Devaux, and A. Herrmann. Function of prokaryotic and eukaryotic abc proteins in lipid transport. *Biochim Biophys Acta*, 1733(1):29–52, 2005.

T. Pomorski and A. K. Menon. Lipid flippases and their biological functions. *Cell Mol Life Sci*, 63(24):2908–21, 2006.

T. Pomorski, P. Muller, B. Zimmermann, K. Burger, P. F. Devaux, and A. Herrmann. Transbilayer movement of fluorescent and spin-labeled phospholipids in the plasma membrane of human fibroblasts: a quantitative approach. *J Cell Sci*, 109 (Pt 3):687–98, 1996.

T. Pomorski, A. Herrmann, P. Muller, G. van Meer, and K. Burger. Protein-mediated inward translocation of phospholipids occurs in both the apical and basolateral plasma membrane domains of epithelial cells. *Biochemistry*, 38(1):142–50, 1999.

T. Pomorski, S. Hrafnsdottir, P. F. Devaux, and G. van Meer. Lipid distribution and transport across cellular membranes. *Semin Cell Dev Biol*, 12(2):139–48, 2001.

T. Pomorski, R. Lombardi, H. Riezman, P. F. Devaux, G. van Meer, and J. C. Holthuis. Drs2p-related p-type atpases dnf1p and dnf2p are required for phospholipid translocation across the yeast plasma membrane and serve a role in endocytosis. *Mol Biol Cell*, 14(3):1240–54, 2003.

L. R. Poulsen, R. L. Lopez-Marques, S. C. McDowell, J. Okkeri, D. Licht, A. Schulz, T. Pomorski, J. F. Harper, and M. G. Palmgren. The arabidopsis p4-atpase ala3 localizes to the golgi and requires a beta-subunit to function in lipid translocation and secretory vesicle formation. *Plant Cell*, 20(3):658–76, 2008.

M. E. Poupart, D. Fessart, M. Cotton, S. A. Laporte, and A. Claing. Arf6 regulates angiotensin ii type 1 receptor endocytosis by controlling the recruitment of ap-2 and clathrin. *Cell Signal*, 19(11):2370–8, 2007.

K. Powell. Cell biology: ahead of the curve. *Nature*, 460(7253):318–20, 2009.

C. F. Puts and J. C. Holthuis. Mechanism and significance of p(4) atpase-catalyzed lipid transport: Lessons from a na(+)/k(+)-pump. *Biochim Biophys Acta*, 1791(7):603–11, 2009.

C. F. Puts, G. Lenoir, J. Krijgsveld, P. Williamson, and J. C. Holthuis. A p4-atpase protein interaction network reveals a link between aminophospholipid transport and phosphoinositide metabolism. *J Proteome Res*, 9(2):833–42, 2010.

L. Rajendran and K. Simons. Lipid rafts and membrane dynamics. *J Cell Sci*, 118(Pt 6): 1099–102, 2005.

R. Ramachandran, T. J. Pucadyil, Y. W. Liu, S. Acharya, M. Leonard, V. Lukiyanchuk, and S. L. Schmid. Membrane insertion of the pleckstrin homology domain variable loop 1 is critical for dynamin-catalyzed vesicle scission. *Mol Biol Cell*, 20(22):4630–9, 2009.

J. Z. Rappoport. Focusing on clathrin-mediated endocytosis. *Biochem J*, 412(3):415–23, 2008.

J. Z. Rappoport and S. M. Simon. Real-time analysis of clathrin-mediated endocytosis during cell migration. *J Cell Sci*, 116(Pt 5):847–55, 2003.

C. Rauch and E. Farge. Endocytosis switch controlled by transmembrane osmotic pressure and phospholipid number asymmetry. *Biophys J*, 78(6):3036–47, 2000.

W. R. Riekhof, J. Wu, M. A. Gijon, S. Zarini, R. C. Murphy, and D. R. Voelker. Lysophosphatidylcholine metabolism in saccharomyces cerevisiae: the role of p-type atpases in transport and a broad specificity acyltransferase in acylation. *J Biol Chem*, 282(51):36853–61, 2007.

T. F. Roth and K. R. Porter. Yolk protein uptake in the oocyte of the mosquito aedes aegypti. l. *J Cell Biol*, 20:313–32, 1964.

K. G. Rothberg, J. E. Heuser, W. C. Donzell, Y. S. Ying, J. R. Glenney, and R. G. Anderson. Caveolin, a protein component of caveolae membrane coats. *Cell*, 68(4):673–82, 1992.

A. Roux, D. Cuvelier, P. Nassoy, J. Prost, P. Bassereau, and B. Goud. Role of curvature and phase transition in lipid sorting and fission of membrane tubules. *Embo J*, 24(8):1537–45, 2005.

A. F. Ruaud, L. Nilsson, F. Richard, M. K. Larsen, J. L. Bessereau, and S. Tuck. The c. elegans p4-atpase tat-1 regulates lysosome biogenesis and endocytosis. *Traffic*, 10(1):88–100, 2009.

S. Sabharanjak, P. Sharma, R. G. Parton, and S. Mayor. Gpi-anchored proteins are delivered to recycling endosomes via a distinct cdc42-regulated, clathrin-independent pinocytic pathway. *Dev Cell*, 2(4):411–23, 2002.

E. Sackmann, H. P. Duwe, and H. Engelhardt. Membrane bending elasticity and its role for shape fluctuations and shape transformations of cells and vesicles. *Faraday Discuss Chem Soc*, (81):281–90, 1986.

K. Sandvig, M. L. Torgersen, H. A. Raa, and B. van Deurs. Clathrin-independent endocytosis: from nonexisting to an extreme degree of complexity. *Histochem Cell Biol*, 129(3):267–76, 2008.

R. C. Sarasij, S. Mayor, and M. Rao. Chirality-induced budding: a raft-mediated mechanism for endocytosis and morphology of caveolae? *Biophys J*, 92(9):3140–58, 2007.

M. Sargiacomo, P. E. Scherer, Z. Tang, E. Kubler, K. S. Song, M. C. Sanders, and M. P. Lisanti. Oligomeric structure of caveolin: implications for caveolae membrane organization. *Proc Natl Acad Sci U S A*, 92(20):9407–11, 1995.

S. B. Sato, T. Taguchi, S. Yamashina, and S. Toyama. Wortmannin and li+ specifically inhibit clathrin-independent endocytic internalization of bulk fluid. *J Biochem*, 119(5):887–97, 1996.

F. Schroeder, G. Nemecz, W. G. Wood, C. Joiner, G. Morrot, M. Ayraut-Jarrier, and P. F. Devaux. Transmembrane distribution of sterol in the human erythrocyte. *Biochim Biophys Acta*, 1066(2):183–92, 1991.

U. Seifert, K. Berndl, and R. Lipowsky. Shape transformations of vesicles: Phase diagram for spontaneous- curvature and bilayer-coupling models. *Phys Rev A*, 44(2):1182–1202, 1991.

M. Seigneuret and P. F. Devaux. Atp-dependent asymmetric distribution of spin-labeled phospholipids in the erythrocyte membrane: relation to shape changes. *Proc Natl Acad Sci U S A*, 81(12):3751–5, 1984.

P. Sengupta, D. Holowka, and B. Baird. Fluorescence resonance energy transfer between lipid probes detects nanoscopic heterogeneity in the plasma membrane of live cells. *Biophys J*, 92 (10):3564–74, 2007.

Y. Shao, W. Akmentin, J. J. Toledo-Aral, J. Rosenbaum, G. Valdez, J. B. Cabot, B. S. Hilbush, and S. Halegoua. Pincher, a pinocytic chaperone for nerve growth factor/trka signaling endosomes. *J Cell Biol*, 157(4):679–91, 2002.

P. Sharma, R. Varma, R. C. Sarasij, Ira, K. Gousset, G. Krishnamoorthy, M. Rao, and S. Mayor. Nanoscale organization of multiple gpi-anchored proteins in living cell membranes. *Cell*, 116 (4):577–89, 2004.

M. P. Sheetz and S. J. Singer. Biological membranes as bilayer couples. a molecular mechanism of drug-erythrocyte interactions. *Proc Natl Acad Sci U S A*, 71(11):4457–61, 1974.

S. Sigismund, T. Woelk, C. Puri, E. Maspero, C. Tacchetti, P. Transidico, P. P. Di Fiore, and S. Polo. Clathrin-independent endocytosis of ubiquitinated cargos. *Proc Natl Acad Sci U S A*, 102(8):2760–5, 2005.

S. Sigismund, E. Argenzio, D. Tosoni, E. Cavallaro, S. Polo, and P. P. Di Fiore. Clathrin-mediated internalization is essential for sustained egfr signaling but dispensable for degradation. *Dev Cell*, 15(2):209–19, 2008.

J. R. Silvius and I. R. Nabi. Fluorescence-quenching and resonance energy transfer studies of lipid microdomains in model and biological membranes. *Mol Membr Biol*, 23(1):5–16, 2006.

K. Simons and E. Ikonen. Functional rafts in cell membranes. *Nature*, 387(6633):569–72, 1997.

S. J. Singer and G. L. Nicolson. The fluid mosaic model of the structure of cell membranes. *Science*, 175(23):720–31, 1972.

R. D. Singh, Y. Liu, C. L. Wheatley, E. L. Holicky, A. Makino, D. L. Marks, T. Kobayashi, G. Subramaniam, R. Bittman, and R. E. Pagano. Caveolar endocytosis and microdomain association of a glycosphingolipid analog is dependent on its sphingosine stereochemistry. *J Biol Chem*, 281(41):30660–8, 2006.

B. Snijder, R. Sacher, P. Ramo, E. M. Damm, P. Liberali, and L. Pelkmans. Population context determines cell-to-cell variability in endocytosis and virus infection. *Nature*, 461(7263):520–3, 2009.

A. Sorkin. Cargo recognition during clathrin-mediated endocytosis: a team effort. *Curr Opin Cell Biol*, 16(4):392–9, 2004.

A. D. Sorkin, L. V. Teslenko, and N. N. Nikolsky. The endocytosis of epidermal growth factor in a431 cells: a ph of microenvironment and the dynamics of receptor complex dissociation. *Exp Cell Res*, 175(1):192–205, 1988.

H. Sprong, P. van der Sluijs, and G. van Meer. How proteins move lipids and lipids move proteins. *Nat Rev Mol Cell Biol*, 2(7):504–13, 2001.

J. M. Stapelbroek, T. A. Peters, D. H. van Beurden, J. H. Curfs, A. Joosten, A. J. Beynon, B. M. van Leeuwen, L. M. van der Velden, L. Bull, R. P. Oude Elferink, B. A. van Zanten, L. W. Klomp, and R. H. Houwen. Atp8b1 is essential for maintaining normal hearing. *Proc Natl Acad Sci U S A*, 106(24):9709–14, 2009.

A. Subtil, A. Hemar, and A. Dautry-Varsat. Rapid endocytosis of interleukin 2 receptors when clathrin-coated pit endocytosis is inhibited. *J Cell Sci*, 107 (Pt 12):3461–8, 1994.

A. Sune and A. Bienvenue. Relationship between the transverse distribution of phospholipids in plasma membrane and shape change of human platelets. *Biochemistry*, 27(18):6794–800, 1988.

A. Tagawa, A. Mezzacasa, A. Hayer, A. Longatti, L. Pelkmans, and A. Helenius. Assembly and trafficking of caveolar domains in the cell: caveolae as stable, cargo-triggered, vesicular transporters. *J Cell Biol*, 170(5):769–79, 2005.

X. Tang, M. S. Halleck, R. A. Schlegel, and P. Williamson. A subfamily of p-type atpases with aminophospholipid transporting activity. *Science*, 272(5267):1495–7, 1996.

G. Ter-Avetisyan, G. Tunnemann, D. Nowak, M. Nitschke, A. Herrmann, M. Drab, and M. C. Cardoso. Cell entry of arginine-rich peptides is independent of endocytosis. *J Biol Chem*, 284 (6):3370–8, 2009.

A. Toker. The synthesis and cellular roles of phosphatidylinositol 4,5-bisphosphate. *Curr Opin Cell Biol*, 10(2):254–61, 1998.

D. Tosoni, C. Puri, S. Confalonieri, A. E. Salcini, P. De Camilli, C. Tacchetti, and P. P. Di Fiore. Ttp specifically regulates the internalization of the transferrin receptor. *Cell*, 123(5):875–88, 2005.

K. Trajkovic, C. Hsu, S. Chiantia, L. Rajendran, D. Wenzel, F. Wieland, P. Schwille, B. Brugger, and M. Simons. Ceramide triggers budding of exosome vesicles into multivesicular endosomes. *Science*, 319(5867):1244–7, 2008.

E. J. Ungewickell and L. Hinrichsen. Endocytosis: clathrin-mediated membrane budding. *Curr Opin Cell Biol*, 19(4):417–25, 2007.

T. Utsugi, A. J. Schroit, J. Connor, C. D. Bucana, and I. J. Fidler. Elevated expression of phosphatidylserine in the outer membrane leaflet of human tumor cells and recognition by activated human blood monocytes. *Cancer Res*, 51(11):3062–6, 1991.

G. van Meer, D. Halter, H. Sprong, P. Somerharju, and M. R. Egmond. Abc lipid transporters: extruders, flippases, or flopless activators? *FEBS Lett*, 580(4):1171–7, 2006.

G. van Meer, D. R. Voelker, and G. W. Feigenson. Membrane lipids: where they are and how they behave. *Nat Rev Mol Cell Biol*, 9(2):112–24, 2008.

P. Verkade, T. Harder, F. Lafont, and K. Simons. Induction of caveolae in the apical plasma membrane of madin-darby canine kidney cells. *J Cell Biol*, 148(4):727–39, 2000.

L. H. Wang, K. G. Rothberg, and R. G. Anderson. Mis-assembly of clathrin lattices on endosomes reveals a regulatory switch for coated pit formation. *J Cell Biol*, 123(5):1107–17, 1993.

S. Wicky, H. Schwarz, and B. Singer-Kruger. Molecular interactions of yeast neo1p, an essential member of the drs2 family of aminophospholipid translocases, and its role in membrane trafficking within the endomembrane system. *Mol Cell Biol*, 24(17):7402–18, 2004.

P. Xu, J. Okkeri, S. Hanisch, R. Y. Hu, Q. Xu, T. G. Pomorski, and X. Y. Ding. Identification of a novel mouse p4-atpase family member highly expressed during spermatogenesis. *J Cell Sci*, 122(Pt 16):2866–76, 2009.

Y. Yoon, J. Tong, P. J. Lee, A. Albanese, N. Bhardwaj, M. Kallberg, M. A. Digman, H. Lu, E. Gratton, Y. K. Shin, and W. Cho. Molecular basis of the potent membrane-remodeling activity of the epsin 1 n-terminal homology domain. *J Biol Chem*, 285(1):531–40, 2009.

A. Zachowski. Phospholipids in animal eukaryotic membranes: transverse asymmetry and movement. *Biochem J*, 294 (Pt 1):1–14, 1993.

X. Zha, L. M. Pierini, P. L. Leopold, P. J. Skiba, I. Tabas, and F. R. Maxfield. Sphingomyelinase treatment induces atp-independent endocytosis. *J Cell Biol*, 140(1):39–47, 1998.

X. Zhou and T. R. Graham. Reconstitution of phospholipid translocase activity with purified drs2p, a type-iv p-type atpase from budding yeast. *Proc Natl Acad Sci U S A*, 106(39): 16586–91, 2009.

J. Zimmerberg and M. M. Kozlov. How proteins produce cellular membrane curvature. *Nat Rev Mol Cell Biol*, 7(1):9–19, 2006.

Acknowledgements

The present work has been carried out in a cooperation of the Institut de Biologie Physico-Chimique, Paris, in the workgroup “Biologie Physico-Chimique des Protéines Membranaires” and the Humboldt-Universität zu Berlin in the workgroup “Molekulare Biophysik” under the supervision of Professor Dr Philippe Devaux and Professor Dr Andreas Herrmann. This work would not have been possible without the support of a number of people, to whom I want to express my special thanks.

First and foremost, I would like to thank my supervisors Professor Dr Philippe Devaux and Professor Dr Andreas Herrmann for all their support and assistance with my thesis and for the offer of Philippe to work on this very challenging topic. Thanks for all the motivation and support, not only related to scientific issues.

Next, I want to express my thanks to my colleagues in Paris and Berlin. Dr Nathalie Sauvonnet from the Institut Pasteur introduced me into the secrets of cell culture as well as flow cytometry and generously shared transfected cell lines. Besides providing me with ether lipid analogues, Dr Fabrice Giusti taught me how to play petanque the right way and got never tired of distracting me from failed experiments. Dr Sophie Cribier in Paris and Dr Thomas Korte in Berlin were always prepared to help me with any problems in microscopy. I am much obliged to Dr Peter Müller and Professor Dr Thomas Pomorski for helpful discussions about experimental setups as well as very helpful suggestions and comments. All remaining members of the groups are acknowledged for providing me with a nice and helpful atmosphere and the warm feeling that there is always someone who listens to never ending problems with living samples.

A special word of thanks is well earned by Professor Dr John Findlay and the entire Marie Curie “BIOMEM” consortium. I had such a great time, and really enjoyed the excellent conferences and workshops organised by the members of the consortium. Because a large part of the fun I had during these meetings was caused by my fellow Marie

Curie students, I want to thank my *scientific family* for being such good company.

Apart from science, special thanks go to the many people that supported me during my time in Paris and Berlin. This includes (in no particular order) Paola for every single of our stair-breaks, Steffi for being best company in discovering leisure activities in Paris, and my little sister for our summer 2006.

And finally, but importantly, I want to thank my personal statistician who patiently discovered all non-normally distributed data and all to often had to put my head back into place.

List of Publications

Journal Articles

Devaux, P.F., Herrmann, A., Ohlwein, N., Kozlov, M.M. (2008). How lipid flippases can modulate membrane structure. *Biochim Biophys Acta*, 1778(7-8): 1591-1600.

Ludwig, K., Schade, B., Böttcher, C., Korte, T., Ohlwein, N., Baljinnyam, B., Veit, M., Herrmann, A. (2008). Electron cryomicroscopy reveals different F1+F2 protein States in intact parainfluenza virions. *J Virol*, 82(7): 3775-3781.

Book Chapter

Ohlwein, N., Herrmann, A., Devaux, P.F. (2011). Endocytosis and Lipid Asymmetry. *Wiley Series in Protein and Peptide*: Membrane Asymmetry And Transmembrane Motion Of Lipids. Chapter V - Biological Functions Associated with Lipid Asymmetry. ISBN: 0470388455.

Talks

BIOMEM Annual Assembly, Madrid, Spain (October 2008). *Influence of Exogenous Lipids on Endocytosis in BHKasc and K562 Cells.*

BIOMEM Annual Assembly, Berlin, Germany (September 2007). *Endocytosis controlled by Monolayer Area Asymmetry of the Plasma Membrane.*

FLIPPASES Annual Assembly, Granada, Spain (March 2007). *Endocytosis controlled by Monolayer Area Asymmetry of the Plasma Membrane.*

BIOMEM Annual Assembly, Utrecht, The Netherlands (June 2006). *Endocytosis and Phospholipid Flippase Activity*

Posters

FEBS Meeting: New concepts in Lipidology, Noordwijkerhout, The Netherlands (October 2006). *Endocytosis controlled by the Asymmetry of Phospholipids in the Plasma Membrane.*

International DFG Symposium: Formation and stability of β-sheets, Berlin, Germany (October 2004). *Influence of Ataxin-3 on p97/VCP Induced Membrane Fusion.*

Selbständigkeitserklärung

Ich versichere hiermit, die vorliegende Arbeit selbständig, ausschließlich unter Verwendung der angegebenen Mittel und ohne unerlaubte Hilfen angefertigt zu haben.

Ich besitze keinen entsprechenden Doktorgrad und habe mich anderwärts nicht um einen Doktorgrad beworben.

Die dem Promotionsverfahren zugrunde liegende Promotionsordnung ist mir bekannt.

Nina Ohlwein